SUZLON BLADE TECHNOLOGY
Composite Material Process Deparment

UNIVERSIDAD CARLOS III DE MADRID
Materials Science Engineering and Chemical Engineering Department

PROYECTO FIN DE CARRERA

Analisys of the effects of variation the Resin Mixing Ratio on Mechanical Properties of composite materials.

Leganés, October 2012

Author: David Bo Lu Sun

Suzlon Supervisor: Frank Saarloos
University Carlos III tutor: Jose Manuel Torralba Castello

ACKNOWLEDGEMENTS

I would like to take this opportunity to thank all those who in one way or another have made possible the realization of this Thesis, and therefore the completion of this stage of my life as a student.

First, thank the Department of Materials Engineering and Chemical Engineering, for allowing me to make this project in its area, despite belonging to another specialty. Especially to the professor Jose Manuel Torralba, for their dedication and unconditional support throughout this project.

I would also like to thank and dedicate this project to my family, for always being there, showing me their support and confidence, for driving me to keep going and believing in me all these years of career.

Thanks to all of you, a bit of this are yours.

RESUMEN

Suzlon Blade Technology es una empresa que se dedica a la manufactura de palas de aerogeneradores además de investigar en el ámbito de los materiales. Una de las muchas investigaciones que se llevan a cabo en esta empresa están focalizadas en las resinas, un componente importante dentro del proceso de fabricación de dichas palas.

El objetivo de esta investigación es analizar cómo repercute la variación de la proporción de la mezcla de las resinas y los endurecedores, denominado Mixing Ratio, respecto de la ideal, en las propiedades mecánicas tales como la rigidez y la tensión, y las propiedades térmicas, como la temperatura de transición vítrea (Tg) en dos tipos de compuestos laminados de fibra de vidio empleados en la fabricación de palas de aerogeneradores fabricados por la compañía Suzlon.

Para ello, se ha procedido a fabricar los distintos tipos de compuestos laminados, que van en función de la disposición de las fibras reforzadas, empleando en cada una de ellas, una proporcion distinta de mezcla Resina/Endurecedor y analizar sus propiedades mecánicas. Para dichos compuestos laminados se ha empleado fibra de vidrio tipo E, con disposiciones diferentes, 0° y 45°. La resina empleada en esta investigación fue una resina Epoxy y un agente de curado de tipo Amina.

La técnica empleada para fabricar dichos compuestos laminados ha sido la denominada 'Vacuum infusion', que es una variante de la técnica 'Resin Transfer Molding'.

Hecho esto, se ha procedido a fabricar las correspondientes muestras de cada lámina siguiento los correspondientes estándares, ISO 525-7 para laminas con fibras dispuestas a 0° e ISO 14129 para laminas con fibras a 45°. Para el estudio de las propiedades mecánicas, tales como la tensión, elongación y rigidez, se ha empleado la prueba de ensayo de tracción simple.

Además, este estudio se ha apoyado en el uso de la formulación de Halpin-Tsai para el cálculo del Módulo de Young para comprobar si los datos obtenidos experimentalmente concuerdan con los teóricos esperados.

En cuanto a las propiedad térmica de la temperatura de transición vítrea Tg, se ha obtenido una muestra de cada diferente compuesto laminado y se ha analizado mediante el proceso denominado Differential Scanning Calorimetry (DSC).

El estudio ha revelado, que a pesar de que disminuyen las propiedades mecánicas de los compuestos laminados al variar dicho Mixing Ratio, no es una gran pérdida significativa, lo cual permite seguir empleando dichas laminas con cierta seguridad en las palas de los aerogeneradores eólicos, aún sufriendo dichas mezclas de resinas, ligeras desviaciones respecto del ideal.

ABSTRACT

Suzlon Blade Technology is a company dedicated to researching, improving and manufacture wind turbine blades in the field of materials. One of the many research carried out in this company are focused on the resins, an important component of the manufacturing process of blades.

The objective of this research is to analyze, how it affects varying the proportion between Resin and the Hardener, called Mixing Ratio, respect to the ideal on the mechanical properties such as strength and stiffness, and the thermal properties, as the Glass transition temperature, in two types of composite laminates used in the blades manufactured by Suzlon.

For this purpose, it has manufactured two types of composite laminates, depending on the arrangement of reinforcing fibers, using in each one of them, a different mixing ratio and analyze its mechanical properties. The Epoxy resin and Amine hardener were used combining it with The E-glass fiber as reinforcement, in two different displacement, 0° Unidirectional composite laminate and 45° Biaxial composite laminate.

The technique used for performed these composite laminates was the 'Vacuum infusion', which is a variant of the 'Resin transfer molding' technique. The corresponding samples were tested following the respective ISO standards, ISO 525-7 for Unidirectional composite laminate and ISO 14129 Biaxial composite laminates.

For the study of mechanical properties such as strength, elongation and stiffness, the samples were tested by simple tensile traction test. Furthermore, this study has relied on the use of the Halpin-Tsai formulation to calculate the Young's modulus of the composite as a function of the variation of the resin mixing ratio, for checking whether data obtained experimentally are consistent with theoretical expectations.

Regarding to the thermal properties, as Glass transition temperature, a sample was obtained from each different composite laminate and it has been analyzed by a Differential Scanning Calorimetry.

The study revealed that even though decreasing the mechanical properties of laminates made by varying the mixing ratio, it was not a significant loss, allowing to use these composite laminates with some confidence on the blades of the wind turbines, even if these mixtures of these resins have suffered slight deviations from the ideal.

TABLE OF CONTENTS

1. INTRODUCTION. 8
   1.1. Suzlon company. 8
   1.2. Mixing ratio project. 9
2. STATE OF ART. 10
   2.1. A brief description of composite materials, wind energy and the concept of mixing ratio. 10
3. MOTIVATION AND OBJECTIVES. 16
4. MATERIAL AND CHARACTERIZATION TECHNIQUES. 17
   4.1. Materials. 17
      4.1.1. Glass fibres. 17
      4.1.2. Thermosetting polymers. Epoxy Resins. 19
      4.1.3. Curing Agents. (Hardeners). 22
      4.1.4. Curing Reactions. 24
      4.1.5. Laminates of composite materials. 25
   4.2. Characterization Techniques. 27
      4.2.1. Resin Transfer Molding (RTM). Vacuum infusion. 27
      4.2.2. Tensile Test. 29
      4.2.3. Glass transition Temperature (Tg). DSC Analyse. 30
   4.3. Theory prediction. 33
      4.3.1. Effects of the variation of mixing ratio on Young's modulus. Halpin-Tsai. 33
5. EXPERIMENTAL PART. 46
   5.1. Materials used. 46
   5.2. Sample preparation. 48
   5.3. Tensile tests 57
   5.4. Thermal analysis. 59
6. DISCUSSION OF RESULTS. 61
   6.1. Analyse of Tensile results 61
   6.2. Analyse of DSC. 69
   6.3. Comparation with the theorical prevision. 71
7. CONCLUSIONS. 74
8. RECOMMENDATION AND FURTHER STUDY. 75
9. BIBLIOGRAPHY. 77
10. LIST OF FIGURES. 80
11. LIST OF TABLES. 82
12. APPENDIX. 83
   12.1. Parameters of report for UD laminates: 83
   12.2. Parameters of report for Biax laminates: 90
   12.3. Parameters of report for DOW resin coupons: 101
   12.4. Analyse of DSC 104
13. ATTACHMENTS. 112

NOMENCLATURE

Acronyms

CMP	Composite Material Process.
RTM	Resin Transfer Molding.
UTS	Ultimate Tensile Strength.
DSC	Differential Scanning Calorimetry.
UD	Uni-directional Glass fibers.
Biax	Bi-axial Glass fibers.
Tg	Glass Transition Temperature.

Greek Symbols

Δl	Variation of length	mm
ε	Strain	%
σ	Stress	MPa

Latin Symbols

A_o	Initial section	mm^2
E	Young Modulus	GPa
F	Force	N
s	Standard Deviation	

1. INTRODUCTION.

1.1. Suzlon company.[1]

Suzlon Blade Technology is a division of Suzlon Energy, which it was conceived in 1995 with just 20 people and now is one of the leading wind turbine manufacturing groups in the world.

It is the largest wind turbine manufacturer in Asia and it is pioneer in the application of composites in the rotor blade industry. It works across America, Asia, Australia and Europe and offer a fully integrated supply chain with manufacturing facilities in three continents. It has sophisticated R&D capabilities in Denmark, Germany, India and The Netherlands.

Suzlon is a vertically integrated wind power company. Suzlon delivers end-to-end wind power solutions from assembly, installation to commissioning. The company manufactures blades, generators, panels, and towers in-house, as well as gearboxes through its partial ownership of Hansen Transmissions and state-of-the-art large or offshore turbines through its subsidiary REpower. The company is integrated downstream and delivers turnkey projects through its project management and installation consultancy, and operations & maintenance services. Suzlon is a multinational company with offices, R&D and technology centers, manufacturing facilities and service support centers spread across the globe.

Suzlon has design and R&D teams and facilities in Germany, India and The Netherlands to retrofit blades for clients. The international sales business of Suzlon is managed out of Aarhus, Denmark, while its global management office is in Pune, India.

Figure 1-1. Suzlon wind turbine.[1]

1.2. Mixing ratio project.

The Mixing Ratio project is an research and development coordinated by Composite Materials Process (CMP) Department of Suzlon. Within Suzlon Blade Technology there was a wish to know the consequence of variation in the resin mixing ratio's.

A mix ratio for a two component epoxy is the ratio used to determine the amount of resin and catalyst (may also be referred to as hardener or curing agent) required to obtain a full cure of the system.

During rotor blade production, large quantities of resin are used and need to be mixed just prior to blade infusion.

Temperature variation in the Rotor Blade production unit and extensive usage of the mixing machines now and then leads to mixtures that deviate from the ideal ratio between epoxy resin and amine based hardener. If the mixture is off ratio, curing of the blade will not result in complete netting of the resin as there will be an excess amount of one of the component.

A consequence of the incomplete curing is probably that the mechanical properties of the glass fibre reinforced composites are lower than theoretically possible. For this reason, an investigation to get a range of mixing ratio where there are no significant variations of the mechanical properties is needed.

2. STATE OF ART.

This chapter introduces the present knowledge on which this study is based on.

2.1. A brief description of composite materials, wind energy and the concept of mixing ratio.

Currently, researches in the field of materials are focused on composite materials. It offers an exciting and diverse alternative to traditional materials. The number of applications for composite materials is increasing everyday.

According to the "Composite Materials" by Nodal Consultants and published in 2002 in the journal Le 4 Pages Statistiques Industrielles des Ministry of Economy, Finance and Industry of France, the world market for composites materials (MC) has grown since 1994 until 2000 at 5.7% per year in quantity. In 2000 there were worldwide, seven million tons, of which over 95% of compounds widely [2].

The following Figure 2-1. shows the situation of the world market by geographical area composites. The U.S. market is by far the most important accounting for 47% of the global transformation of composites, however, market growth in Asia and Europe is higher than in the United States.

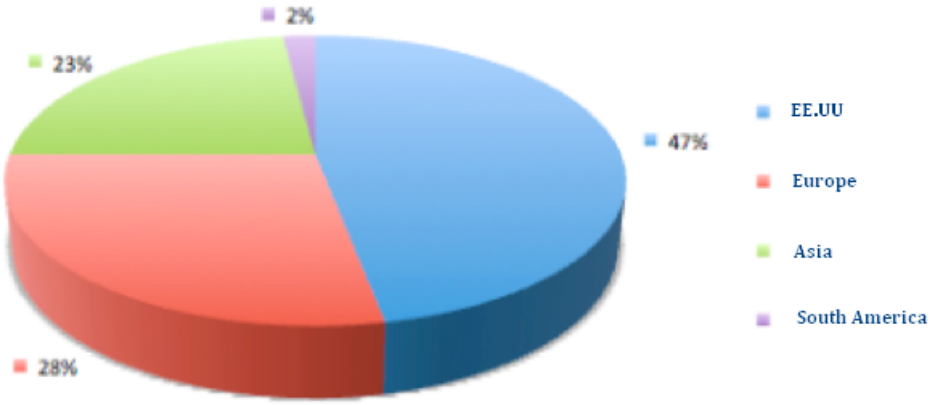

Figure 2-1. World Market Situation of composites by geography (2002).[1]

With 8% of European production (Figure 2-2), the Spanish production of composites lies behind Germany (28%), Italy (18%) and French (15%).

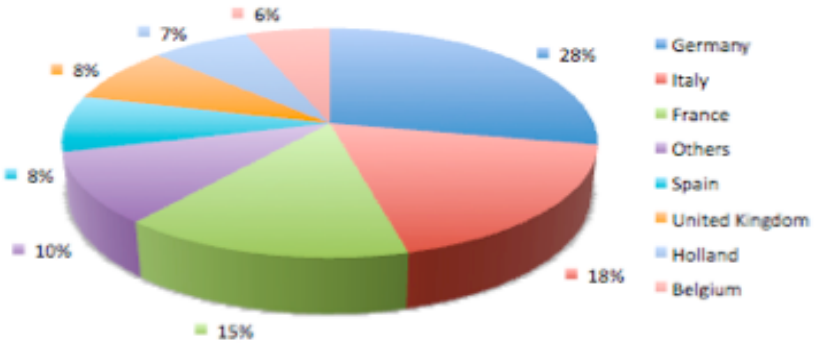

Figure 2-2. Track composites market in Europe, by geographical area (2002).[1]

According to the "Introduction to the analysis and design with composite materials" by F.P.Carballo, J.C.Delgado, J.C.Marin Vallejo, from School of Industrial Engineering of the University of Sevilla [3], the high-tech composite materials (epoxy resin with carbon fibers, boron or Kevlar) have been used in the aircraft industry, mainly in the wings, fuselage and landing gear, so clearly incremental.

Thus while the Airbus 300 (year 1974) the weight percentage of the composite structure to the weight of the total structure was 6% in the Airbus 310-200 (Year 1982) was 8% and the Airbus 320 (Year 1988) is about 20%. In the automobile industry has been used for the whole body only in prototypes. In large production models has been included in grills, bumpers, seat springs and racks. Only very isolation has been used in engine parts.

In naval engineering have been used especially in covered hulls and spars, especially in sports vessels where high performance is required of the materials used and lightweight. In the chemical industry are being increasingly used in pipes and pressure vessels, achieving inner layers of resins with specific properties adequate corrosion resistance against chemical agents. These applications often use fiberglass polyester resin. Inside the sports industry has been applied widely in tennis rackets, fishing rods, golf clubs, skis, canoes, poles, etc., With surprising results.

Advanced composite materials offer an exciting and diverse alternative to traditional materials. Their high strength and stiffness-to-weight ratios combined with a wide range of design options have allowed them to be a popular material in performance- driven areas such as aerospace and sporting goods industries. In addition, they can provide a competitive, low-cost solution in piping, storage tank, and marine applications [4][5].

Another application where advanced composites have a lot of popularity is the wind industry. E-glass reinforced polyester, vinyl-ester and epoxy composites are the materials of choice for producing wind turbine blades. Their high strength and stiffness-to-weight ratios combined with a wide range of design options have allowed them to be a popular material in performance. In addition, these composites allow designers to make lighter more efficient blades at an affordable price. These composites allow designers to make lighter more efficient blades at an affordable price.

Currently, wind power has a mature technology, in 2005 wind power was 59,091 MW (megawatts) worldwide and were projected to continue to increase, considering that the signatories of the Kyoto Protocol must honor their commitments and reduce emission elements which destroy the ozone layer.

Against this background, the wind farms are gaining ground in the world are generating energy and environmentally friendly, in the next Figure 2-3, we can notice the annual evolution of the installed wind power capacity by 2008 and their numbers [6].

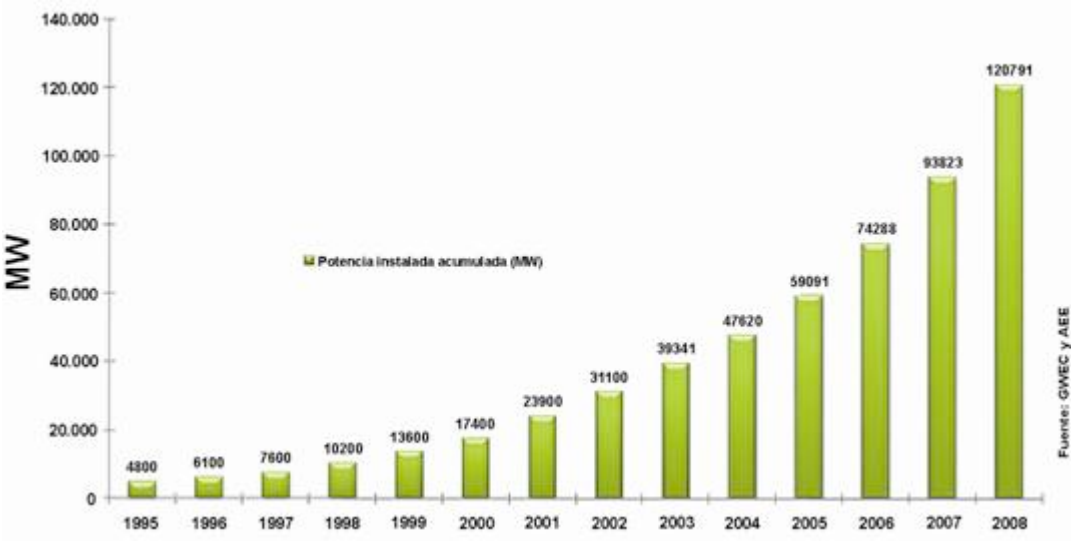

Figure 2-3. Annual evolution of the installed wind power capacity by 2008 and their numbers.[5]

The danish consultancy company "Make Consulting" has just released a preview of his report on the market shares of wind turbine manufacturers.

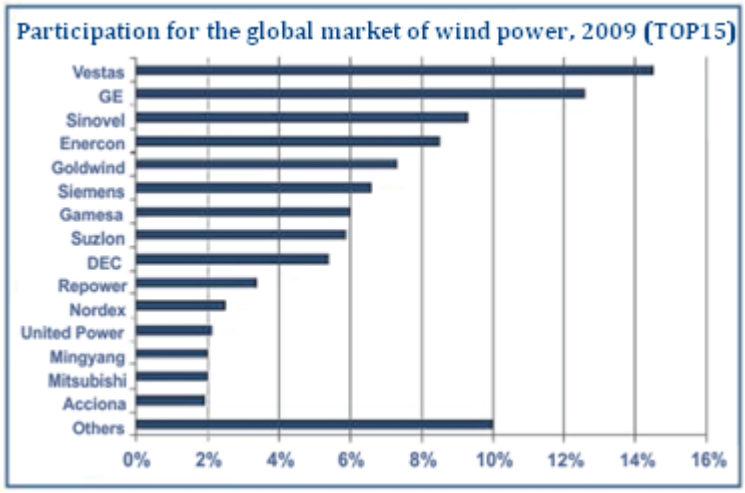

Figure 2-4. Wind Turbine Manufacturers in the global market.[5]

The Figure 2-4 indicates that the global market share of the Danish company Vestas ranked first, the most remarkable fact of balance 2009 is the meteoric rise of China, which manages to put two in the top five manufacturers: Sinovel (third in the ladder) and Goldwind (fifth). The first signed 3495 MW installed in 2009, while 2722 MW Goldwind reached. Chinese Momentum, joined the force (in the American market) of the U.S. multinational GE Energy (second place) and the presence (in the European market) of the German Enercon (third place) were relegated to the Spanish company Gamesa to seventh place, with 6% of the world market, and behind it is the Indian company Suzlon [6].

Wind energy is a clean, renewable source of energy. Despite the potential benefits of wind energy, its cost per kilowatt-hour remains high enough to limit its growth in the United States.

Based on the article "Wind Power Blades Energize Composites Manufacturing" of Joseph A. Large [7], a wind turbine is composed of several composite parts; but the blades, made of fiber-reinforced epoxy or unsaturated polyester, represent the largest use of this material.

The following Figure 2-5 shows a blade geometry and its structure:

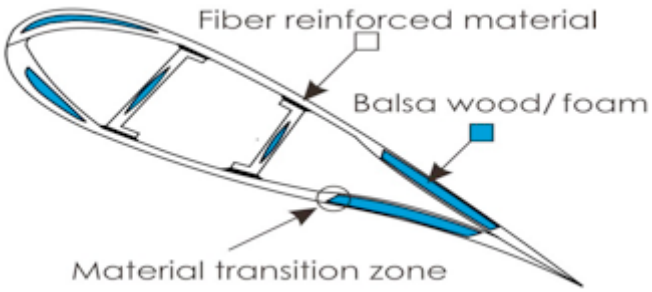

Figure 2-5. Generic Blade cross section.

E-glass is by far the most used reinforcement, while more costly carbon fiber is employed on a limited basis for greater stiffness and reduced weight in longer blades. – Carbon fiber bonded with same resins (less common, although provides high stiffness and less weight for longer turbine blades).

Typically composed of 70% to 75% glass by weight, these aerodynamically designed blades must meet very strict mechanical requirements such as high rigidity and resistance to torsion and fatigue. High static and dynamic loads over a wide temperature range are typical during a 20-years service life. A standard 35- to 40-meter blade for a 1.5-MW turbine weighs 6 to 7 tons.

Currently, blades of 50 meters have small fraction of the market, however, by 2012, blades over 50 meters will have a large market share. As blades get bigger, weight and cost needs to decrease.

One area where wind energy can see a cost reduction is in the manufacturing of wind turbine blades. Glass fibers/epoxy composites system is the most common used material in current wind turbine blade application, and vacuum infusion technique is the process used in wind turbine blade manufacturing. The low cost of raw materials and tooling makes it suitable for mass production of such huge product.

Many of the parts of the blade are composed of fiber reinforced material. Resin transfer molding (RTM) is the process used for manufacturing these materials reinforced with fibers. The mixing ratio of the resin is important for the healing process of the resin to obtain the desired mechanical properties.

The resin infusion process has developed as a low cost method for manufacturing large fiber reinforced plastic parts. This process still presents some challenges to industry

with regards to reliability and repeatability, resulting in trial and error development being expensive and inefficient. However, it still has its advantage of fabricate large-scale composite structures that can have substantial laminate thicknesses, especially in wind turbine blade manufacturing industry.

RTM offers the potential of making lighter, more efficient blades while at the same time lowering production costs of the blades [8][9]. The main advantage is that high fibre volume laminates can be obtained with very low void contents.

E-glass fibers in polyester, vinyl-ester or epoxy resin are currently the composite materials of choice for wind turbine blades because of their strength and stiffness to weight ratios, environmental resistance, and low cost [10][11].

Generally, resin systems are processed as liquids. Resin systems cure by either forming cross-linked polymer chains, thermosets, or by making very long, entangled polymer chains, thermoplastics [12].

The cure time of a resin system is very important to RTM. Although vacuum infusion is considered a recent development, the first production trials date back to the 1940s with a method called the Marco Process [13][14].

Regarding to a mix ratio for a two component epoxy is the ratio used to determine the amount of resin and curing agent required to obtain a full cure of the system. In a typical epoxy resin, there is a fixed ratio of the Resin and the Curing agent, determined by relative molecular weights and the amount of reactive groups they have per that weight.

This typical mixing ratio exist, due to the chemistry of the chemicals and how they react to one another, in which the amount of bonding sites of both chemicals determine the perfect ratio.

Adding more or less hardener will not yield a faster or slower reaction, rather, it will result in an incomplete cure which cannot be corrected. The exact ratio of resin and hardener depends on the kind of resin. These ratios are determined by the chemicals that make up both the resin and the catalyst, and must be followed or curing difficulties can occur. Cure has mainly to do with how much the product has reacted. So how far the reaction has completed. Some common cure problems are:

- Soft Cure
- High Exotherm during Reaction.

Mix ratios can be expressed by weight, by volume, or parts per hundred (PHR) in which, one of the components will be hundred. Due to differences in density between resins and catalysts the ratio by weight and the ratio by volume will be different in many cases. The most common expressions for materials that are to be mixed by hand are by weight or PHR.

One component is the epoxy and the other a chemical that will form bonds with the epoxy. What it forms is a polymer. Each particular epoxy product has a mixture ratio designed into it. Epoxy is the resin in most cases.

The end product is a newly formed thermosetting polymer. Leftover resin or leftover hardener has the effect of creating a weaker end product.

The concept of Mixing Ratio and its influence on other properties have been studied before as it proves some of the following scientific investigations.

J.R.M. d'Almeida & S.N. Monteiro conducted an investigation [15] focused on the variation of the mechanical properties of an epoxy system formulated with eight resin/hardener ratios. The ratios used covered a range of epoxy rich and hardener rich, as well as stoichiometric compositions. The tests were performed in compression and the results obtained were correlated with the macromolecular network developed.

Another research related to the concept of mixing ratio was done by A. Foyet, T.H. Wu, L. van der Ven, A. Kodentsov, G. de With, and R. van Benthem [16], where they studied the influence of substrates as well as the epoxy/amine mixing ratio on the water permeation coefficient.

H.L. Liu, A. Deng, and J. Chu carried out another investigation [17], where it was focused on the formation of a lightweight fill material by blending soil with polystyrene pre-puff (PSPP) beads and other binders such as cement is presented in this paper. The effects of different compositions and different ratios between PSPP beads and soil, cement and soil, water and soil on the density, unconfined compressive strength and deformation of the lightweight fill formed were studied.

3. MOTIVATION AND OBJECTIVES.

The Epoxy resin is widely used within Suzlon, so it is important to get a better understanding of the mechanical properties of this resin used in laminate's fabrication as function of the deviating mixing ratio. The ideal Mixing Ratio between Resin and Hardener from DOW Chemical company is the 100:31 ratio.

The main purpose of this project, was try to find out at what point or Mixing Ratio we see significant changes in the mechanical properties due to changes in the mixing ratio of the resin and try to establish a range of mixing ratio with a safe tolerance of these mechanical properties.

This can then lead to a broader allowable mixing range of this particular resin system.

It is intended that the investigations are focusing on the inter fibre properties of unidirectional (UD) and biaxial (Biax) reinforced epoxy laminates. Laminates will be produced in the Suzlon Blade Technology laboratory following its Standard laminate production method.

Test results will be analyzed on Strength, stiffness and critical strain as per test standard, failure mechanism, crack initiation and propagation by observation.

Extra aspect analyzed in this investigation was to achieve the glass transition temperature (Tg) after standard cure and potential Tg, and attempt to relate it to the mechanical properties.

4. MATERIAL AND CHARACTERIZATION TECHNIQUES.

This chapter describes the different materials involved in this experiment, the different methods used for testing the parameters required, followed by an explanation of the vacuum infusion in the form of descriptions.

The chapter closes with a brief background about mechanical properties of laminates and a prediction of how the mechanical properties changes if the mixing ratio varies.

4.1. Materials.

4.1.1. Glass fibres.[18]

Many different compositions of mineral glasses have been used to produce fibres. The most common are based on silica (SiO_2) with additions of oxides of calcium, boron, sodium, iron and aluminium.

These glasses are usually amorphous although some crystallisation may occur after prolonged heating at high temperatures. This usually leads to a reduction in strength properties. Typical compositions of the three well-know glasses used for glass fibre are given in the Table 4-1.

Table 4-1. Composition of glass used for fibre manufacture (all values in weight %). [18]

	E glass	C glass	S glass
SiO_2	52.4	64.4	64.4
Al_2O_3	14.4	4.1	25.0
CaO	17.2	13.4	-
MgO	4.6	3.3	10.3
Na_2O, K_2O	0.8	9.6	0.3
Ba_2O_3	10.6	4.7	-
BaO	-	0.9	-

E glass (E for electrical) is the most commonly used glass because it draws well and has good strength, stiffness, electrical and weathering properties.
C glass (C for corrosion) has a higher resistance to chemical corrosion than E glass but is more expensive and has lower strength properties.
S glass is more expensive than E glass but has a higher Young's modulus and is more temperature resistant. It is used in special applications such as the aircraft industry where the higher modulus may justify the extra cost.

The diameter of the glass fibers is between 8 and 15 microns. Unlike the carbon fibers, glass fibers are isotropic, direct consequence of the three-dimensional network structure of glass. The breaking strength of the glass is greatly influenced by surface damage they may suffer when touching each other during handling. Therefore they are often apply a protective layer which can additionally generate a chemical bond between the glass surface and the matrix, creating a high-resistance interface.

In this investigation the E glass fibre was used and their properties with other kind of fibres are shown in the Table 4-2.

Table 4-2. Properties of the fibres of carbon, glass, kevlar49 at 20ºC. [18]

Properties	Units	Carbon Base PAN Type I	Carbon Base PAN Type II	E Glass	Kevlar 49 Polyamide
Diameter	μ m	7,0-9,7	7,6-8,6	8-14	11.9
Density	10^3 kgm $^{-3}$	1.95	1.75	2.56	1.45
Young´s Modulus E_{11}	GPa	390	250	76	125
Young´s Modulus E_{22}	GPa	12	20	76	
Tensile Strength	GPa	2.2	2.7	1.4-2.5 (typical) 3.5 (recently stretched)	2.8-3.6
Elongation	%	0,5	1.0	1.8 - 3.2	2.2 - 2.8
Coefficient of thermal expansion (0 a 100 ° C)	10^{-6} C^{-1}	-0.5 a -1.2 (parallel) 7-12 (radial)	-0.1 a -0.5 (parallel) 7-12 (radial)	4.9	-2 (parallel) 59 (radial)
Thermal conductivity (Parallel to the fiber axis)	W m^{-1} C^{-1}	105	24	1.04	0.04

The stress-strain diagrams of the four fibers are shown in Figure 4-1. Kevlar fiber only has a certain rupture ductility with local narrowing in the fracture zone.

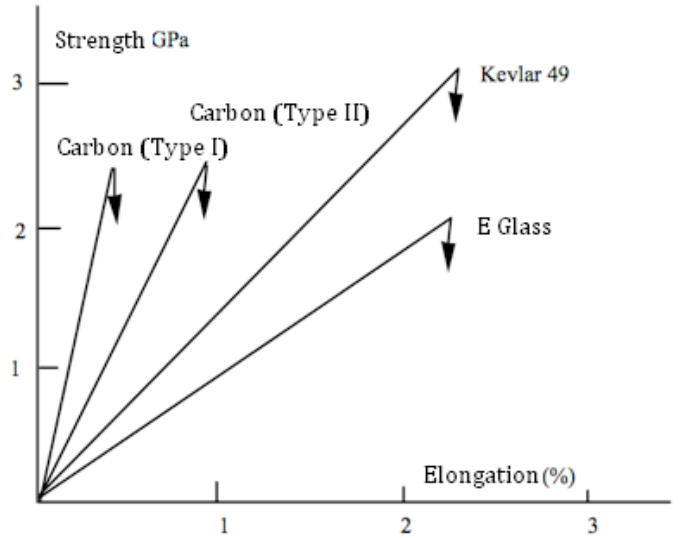

Figure 4-1. Stress-strain diagrams of carbon fibers, glass and Kevlar 49.[18]

From the viewpoint of properties it can be said that the absolute Kevlar fiber is stronger and the more rigid carbon, the glass being less resilient and less rigid, although cheaper.

The strength is strongly dependent on processing conditions and testing environment. The strength decreases when the fibres are tested in humid air owing to absorption of water on the glass surface and there is a more marked decrease when the surface has been in contact with mineral acids.

The most important factor determining the ultimate strength of glass is the damage which fibres sustain when they rub against each other during processing operations. The application of a size coating at a very early stage in manufacture helps to minimize the damage.

4.1.2. Thermosetting polymers. Epoxy Resins.

The raw materials most commonly used as matrices for composite materials include epoxy and polyester resins with a variety in their mechanical and chemical properties. Their most interesting property that gives them name (thermoset) is its response to heat and which do not melt when heated (unlike plastics) while lose stiffness properties from a certain temperature so that this value (to 300ºC to 110ºC for epoxy and polyester) represents a real limitation to its use.

The thermosetting polymers are defined as a polymer network formed by the chemical reaction of various monomers in which at least one of them has functionality equal to or greater than 3. The formation of the polymer network occurs through a chemical reaction called the curing reaction of the system to form a molecular structure of three-dimensional lattice form. The curing of thermoset polymers, either thermally or by UV radiation is an irreversible process and the polymer can not recover its previous structure [19].

The synthesis starts from thermoset polymers soluble phase formed by monomers (Figure 4-2a). As the reaction proceeds the monomers together and form polymeric chains with a degree of branching increasing (Figure 4-2b). At one point during the conversion of the functional groups takes place the phenomenon of gelation, in which appears a macromolecule that encompasses the entire system (Figure 4-2c). The transition point between the phase and the phase soluble gel is the gel point and is one of the main parameters of this class of polymers.

Another way to understand this phenomenon from the viewpoint of viscosity. Initially the fluid system has a behavior, with a viscosity that increases with the degree of cure and fully soluble until gelation occurs, after which the viscosity becomes infinite system and a first insoluble fraction appears. After the gel point, the soluble phase decreases until disappearing at the end of the crosslinking reaction in which the material is part of the three-dimensional network or gel. (Figure 4-2.d) [20].

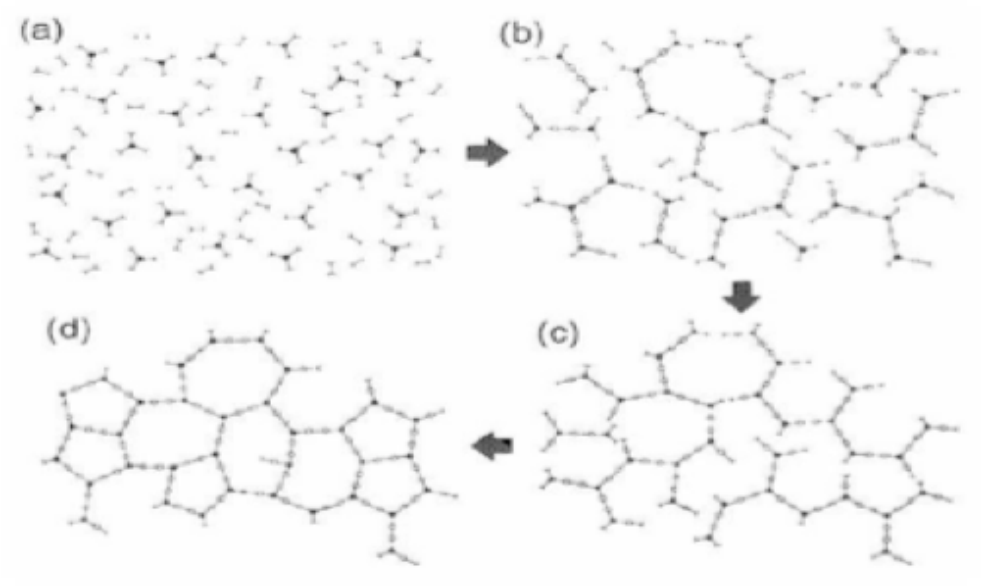

Figure 4-2. Representation of curing a thermosetting polymer.[20]

Epoxy resins are thermosetting polymers that, before curing, have one or more active epoxide or oxirane groups at the end(s) of the molecule and a few repeated units in the middle of the molecule [21]. Chemically, they can be any compounds that have one or more 1,2-epoxy groups and can convert to thermosetting materials. Their molecular weights can vary greatly. They exist either as liquids with lower viscosity or as solids. Through the ring opening reaction, the active epoxide groups in the uncured epoxy can react with many curing agents or hardeners that contain hydroxyl, carboxyl, amine, and amino groups [21][22].

Epoxy resins are one of the most important thermoset materials due to their good mechanical properties and thermal resistance both chemical. However, due to the high crosslinking is formed during the curing reaction, also exhibit a brittle behavior.
Epoxy resins are widely used in fiber reinforced composites, adhesives and surface coatings and other applications. Due to its high crosslinking, have a fragile behavior, with fracture energy values well below the thermoplastic therefore low impact resistance, which limits their use in certain applications.

The Table 4-3 presents some typical properties of Epoxy matrices.

Table 4-3. Properties of Epoxy matrix. [18]

Matrix	Density ρ (kg/m^3)	Young's Modulus E (GPa)	Tensile stress σ_{max}(MPa)		Tensile strain ε_{max} (%)		Coeff. of Thermal Expansion α ($\times 10^{-6}$/°C)
			Yield	Failure	Yield	Failure	
Epoxy	1150-1200	3.5		50 - 70		2 – 4	90
80 + 140[6]	1150-1200	3.5		60 - 80		3 – 5	60
120 + 160	1200-1300	3.5		80 - 90		4 – 5	65

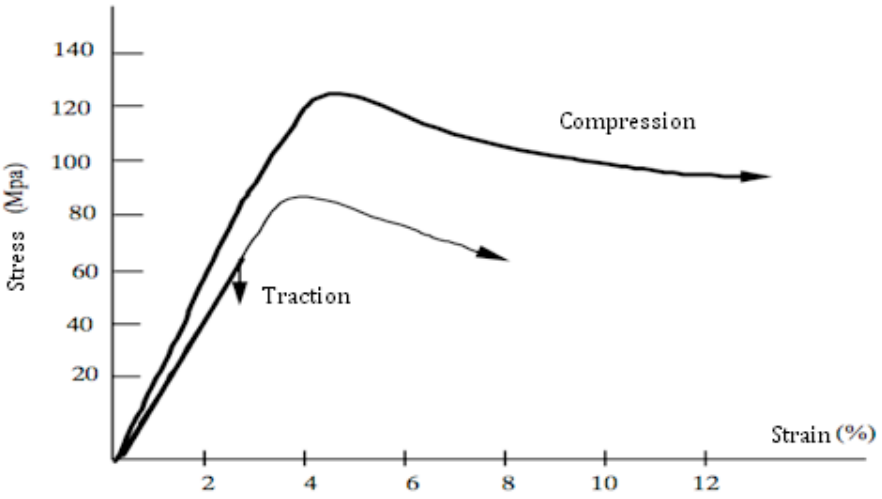

Figure 4-3. Stress-strain diagram of thermosetting resins.

The thermosetting resins are ductile materials as seen in stress strain curves included in Figure 4-3. The dashed line which appears in the tensile test represents the evolution that would not occur in case of premature breakage due to the concentration and intensification of tensions caused by surface defects and / or microcracks, which do not affect the compression behavior, where shows a large plastic deformation before the break appears.

This characteristic of the resins together ductility to justify isotropic behavior nonlinear behavior of composite materials, with stresses in the matrix plays an important role in the mechanism of resistance of the composite.

Epoxy resins can be divided into two groups: glicidílicas and cycloaliphatic. The first is obtained from the reaction of bis (4-hydroxy phenylene) -2.2 propane (bisphenol A) and 1 - chloropropane 2-oxide (epichlorohydrin) in the presence of sodium hydroxide to form the diglycidyl ether of bisphenol A (DGBEA), Figure 4-4:

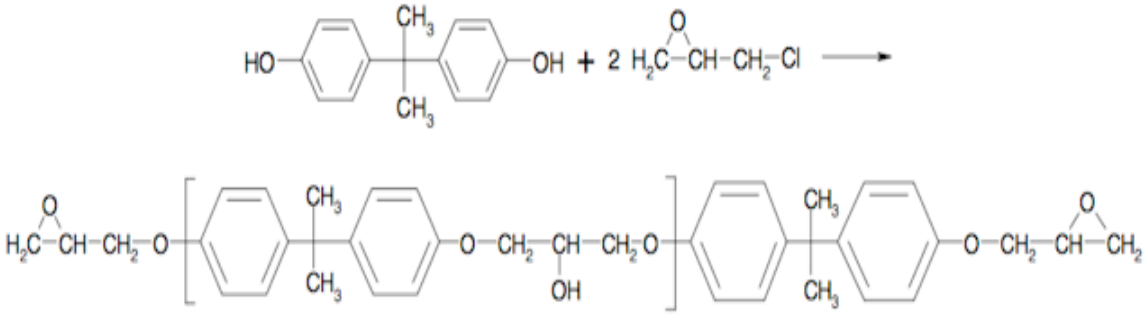

Figure 4-4. Scheme of the reaction of bisphenol A with epichlorohydrin to form DGBEA.

Cycloaliphatic resins are obtained by oxidation of aliphatic dienes. They exhibit greater thermal stability, greater rigideza and tensile strength and better electrical properties than the glicidílicas. These properties make these resins are widely used in the electronics industry [23].

The resins or epoxy-based formulations are very versatile because of the possibilities of reaction with the epoxy groups of a variety of hardeners such as amines, anhydrides, isocyanates or isocyanurates [24]. Epoxy resins generally exhibit high reactivity due to the tension of oxirane ring cycle.

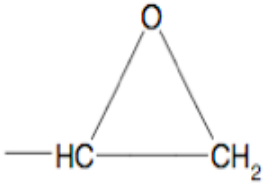

Figure 4-5. Schematic molecular structure of the epoxy group.

Epoxy resins are generally formed by the three membered epoxy group rings. Epoxy groups could be located in different locations other than the ends. At least two epoxy groups have to be on the polymer molecule for crosslinking. Epoxies usually have high viscosities at room temperature, therefore diluents that also contain epoxide groups are used to lower the viscosity.

The most common type of epoxy used is known as the diglycidyl ether of bisphenol A. (DGBEA), and it was used in this investigation.

4.1.3. Curing Agents. (Hardeners).

Curing agents play an important role in the curing process of epoxy resin because they relate to the curing kinetics, reaction rate, gel time, degree of cure, viscosity, curing cycle, and the final properties of the cured products.

Mika and Bauer [25] gave an overview of the epoxy curing agents and modifiers. They discussed three main types of curing agents:

1) The first type of curing agents includes active hydrogen compounds and their derivatives. Compounds with amine, amides, hydroxyl, acid or acid anhydride groups belong to this type. They usually react with epoxy resin by polyaddition to result in an amine, ether, or ester. Aliphatic and aromatic polyamines, polyamides, and their derivatives are the commonly used amine type curing agents. The aliphatic amines are very reactive and have a short lifetime.

   Their applications are limited because they are usually volatile, toxic or irritating to eyes and skin and thus cause health problems. Compared to aliphatic amine, aromatic amines are less reactive, less harmful to people, and need higher cure temperature and longer cure time. Hydroxyl and anhydride curing agents are usually less reactive than amines and require a higher cure temperature and more cure time. They have longer lifetimes.

Polyphenols are the more frequently used hydroxyl type curing agents. Polybasic acids and acid anhydrides are the acid and anhydride type curing agents that are widely used in the coating field. Table 4-4 gives a list of commonly-used type 1 curing agents and their chemical structures.

Table 4-4. Type 1 curing agents and their chemical structures. [25]

COMPOUNDS	CHEMICAL STRUCTURE
DDS	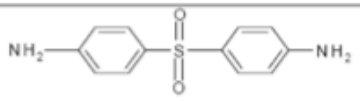
DDM	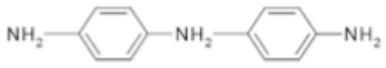
MCDEA	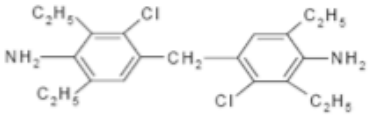
Methylaniline	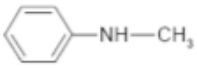
TETA	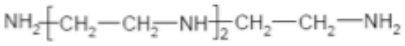
Phenol novolac	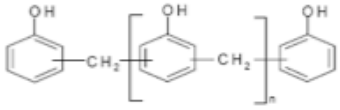
Phthalic anhydride	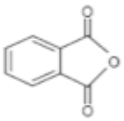

2) The second type of curing agents includes the anionic and cationic initiators. They are used to catalyze the homopolymerization of epoxy resins. Molecules, which can provide an anion such as tertiary amine, secondary amines and metal alkoxides are the effective anionic initiators for epoxy resins.

   Molecules that can provide a cation, such as the halides of tin, zinc, iron and the fluoroborates of these metals, are the effective cationic initiators. The most important types of cationic initiators are the complexes of BF3.

3) The third type of curing agents is called reactive cross linkers. They usually have higher equivalent weights and crosslink with the second hydroxyls of the epoxy resins or by self-condensation. Examples of this type of curing agents are melamine, phenol, and urea formaldehyde resins.

Hardeners are used to crosslink epoxies. Amine hardeners are the most common; hardener should be added in amounts such that the number of epoxide groups is equivalent to the number of crosslinking sites provided by the hardener.

If the hardener is added in the right amounts, a well cross-linked structure with the maximum properties will result. Some epoxies are formulated to crosslink at room temperature, but most epoxies used in composite applications require an increased temperature to initiate the crosslinking.

The nature of the epoxide resins and the reagents causes the molecular structure of the cross-linked epoxy resins to differ. Consequently, the mechanical properties and the useful temperature range of epoxies, as well as processing viscosity can vary over a wide range.

4.1.4. Curing Reactions.

The curing reaction of epoxide is the process by which one or more kinds of reactants, i.e., an epoxide and one or more curing agents with or without the catalysts are transformed from low-molecular-weight to a highly crosslinked structure.

As mentioned earlier, the epoxy resin contains one or more 1, 2-epoxide groups. Because an oxygen atom has a high electronegativity, the chemical bonds between oxygen and carbon atoms in the 1, 2-epoxide groups are the polar bonds, in which the oxygen atom becomes partially negative, whereas the carbon atoms become partially positive. Because the epoxide ring is strained (unstable), and polar groups (nucleophiles) can attack it, the epoxy group is easily broken. It can react with both nucleophilic curing reagents and electrophilic curing agents.

The curing reaction is the repeated process of the ringopening reaction of epoxides, adding molecules and producing a higher molecular weight and finally resulting in a three-dimensional structure. The chemical structures of the epoxides have an important effect on the curing reactions.

Tanaka and Bauer [26] provide more details about the relative reactivity of the various epoxides with different curing agents and the orientation of the ring opening of epoxides. It was concluded that the electron-withdrawing groups in the epoxides would increase the rate of reaction when cured with nucleophilic reagents, but would decrease the rate of reaction of epoxides when cured with electrophilic curing agents.

Curing conditions and therefore the cross-link density also have an important effect on the mechanical properties. For example, the complete reaction of the epoxide groups can only be achieved after long time at high temperature. This is mostly achieved by post-curing and is important for an increase in Young's modulus, chemical resistance and useful temperature range [27].

Physical and mechanical properties are also improved by increasing the molecular weight when curing. As for polyester resins, no condensation by-products are formed during epoxy curing reactions.

4.1.5. Laminates of composite materials.

A composite elemental form, is a combination of two or more different components, if we go deeper, must be a macroscopic combination of two or more different materials which can be seen in a clear interface there between [28][29]. However, depending on the level of study that are working there are many definitions.

One of the definitions of this type of material in which is reflected the purpose of the design is that cited by A. Miravete "Composite material consisting of two or more components, so that the properties of the final material are higher than those of the separate components" [30].

Other definitions that have been given to these materials are:

"A composite material is, or can be, a combination of two or more different substances and discrete, which when are interacting, allow minimize unwanted intrinsic properties of both substances and maximize the desired" *SW Bradstreet.*

"A composite is a material system composed of a mixture or combination of two or more macroconstituents different in shape and / or composition, and which are essentially insoluble each" *MM Schwartz.*

"A composite material is an artificial and intentional mixture of two or more phases, which remain separate macroscopically or association forming an assembly which combine the advantages and less favorable aspects are offset component" *A. Madroñero*.

So, composite materials, by definition, are made from combining two or more different materials. These materials can be as simple as straw and clay, or as complex as carbon fibre and epoxy resin. A typical composite material consists of strong, light fibres held in-place by a polymeric matrix material.

There are three main points to be included in a definition of an acceptable composite material for use in structural applications [18].

1. It consists of two or more physically distinct and mechanically separable materials.
2. It can be made by mixing the separate materials in such a way that the dispersion of one material in the other can be done in a controlled way to achieve optimum properties.
3. The properties are superior, and possibly unique in some specific respects, to the properties of the individual components.

The last point provides the main impetus for the development of composite materials.
In fibre reinforced plastics, fibres and plastics with some excellent physical and mechanical properties, are combined to give a material with new superior properties.

The characteristics obtained in the different composites are the result of the combination between the matrix and the reinforcement depends in turn on the proportions in which the reinforcement appears within the matrix of the form in which it is and the manufacturing process. They can be designed to meet specific engineering reinforcement varying the type and amount of matrix. The modern composite materials are usually optimized to achieve a balance of properties for a range of applications [31].

Regarding to the properties of the composites materials [32][33], they have advantages and disadvantages, which must be taken into account. Among the most important are the following:

Advantages:

- Mechanical resistance.
- Stiffness (its elastic limit corresponds to rupture).
- Wear resistance.
- Corrosion resistance.
- Thermal properties: is possible to design compounds with low or zero coefficient of thermal conductivity in the case required.
- Fatigue: is possible to design compounds where fatigue is negligible according to the application you want to work.
- Electrical properties: compounds can be obtained with high or low electrical characteristics. Glass reinforced plastics are excellent insulators.
- Electromagnetic characteristic may be estimable in a certain range for composite structures.
- Lightness.
- Acoustic insulation.

Disadvantages:

- Loss of ductility.
- Complexity in its preparation.
- Advanced technology sometimes.
- Costly manufacturing.

E-glass fibres are considerably stronger than the polyester matrix material. The fibres serve as the primary load bearing material in the composite.

The role of the matrix is to hold the composite together. It also protects the fibres from the environment and helps distribute loads between fibres. Generally, the composite with the higher volume fraction of glass fibres will be stronger if all other things are equal. Also, the strength of a composite is highly dependent on the orientation of the fibres to the direction of load. The composites are much stronger in the fibre direction.

There are different possibilities orientations of the layers to combine a composite laminate as it is showed in the followed picture, Figure 4-6.

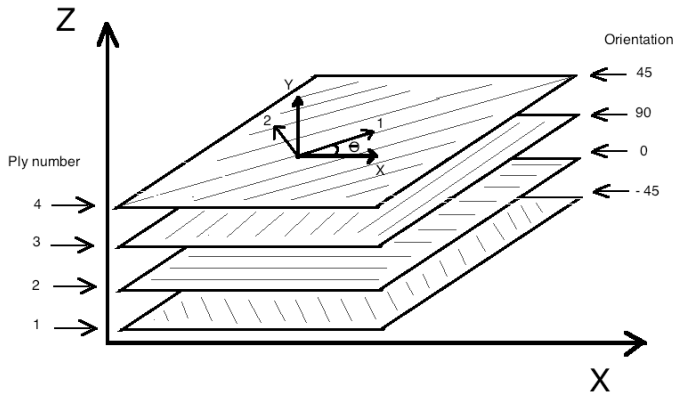

Figure 4-6. Sample of orientation of the different layers in a composite laminate.

The mainly challenging problems which influence the development of these materials are:

- The reversible or irreversible changes in property which occur owing to contact with humid environments and to temperature fluctuations.
- The design of products with optimum fibre content.
- The design of composites with energy absorbing capability.
- The development of materials with resistance to stress and strain corrosion.
- The improvement of the wear resistance of particulate composite material.

E-glass fibres in polyester, vinyl-ester or epoxy resin are currently the composite materials of choice for wind turbine blades due to their strength and stiffness to weight ratios, environmental resistance, and low cost.

4.2. Characterization Techniques.

4.2.1. Resin Transfer Molding (RTM). Vacuum infusion.

In any of the multiple processes for the manufacture of fiber reinforced composite materials can distinguish two phases: the laminated configuration and curing. The first includes a general set of actions that need to be made until the final configuration of the composite. Thus, it may for some materials, consist of the arrangement of fibers in a matrix to obtain a sheet and then the provision of a series of plates for a given laminate.

Curing is the drying or curing of the matrix to form permanent bonds between the matrix and fibers into a sheet and in turn between the sheets themselves. Curing may

occur naturally or may be required to accelerate the polymerization process, the independent or combined application of heat and pressure in autoclaves, ovens, etc.

Vacuum infusion is a resin injection technique and is derived from Resin Transfer Molding (RTM). A resin injection technique generally consists of the following production steps:

- Dry reinforcement is placed in a mold.
- A vacuum bag is placed on dry glass fiber laminates.
- Edges are sealed.
- Vacuum is made with the aid of a pump.
- Resin flows through the mold and impregnates the reinforcement.
- The resin cures.
- The vacuum bag is removed and the product is extracted.

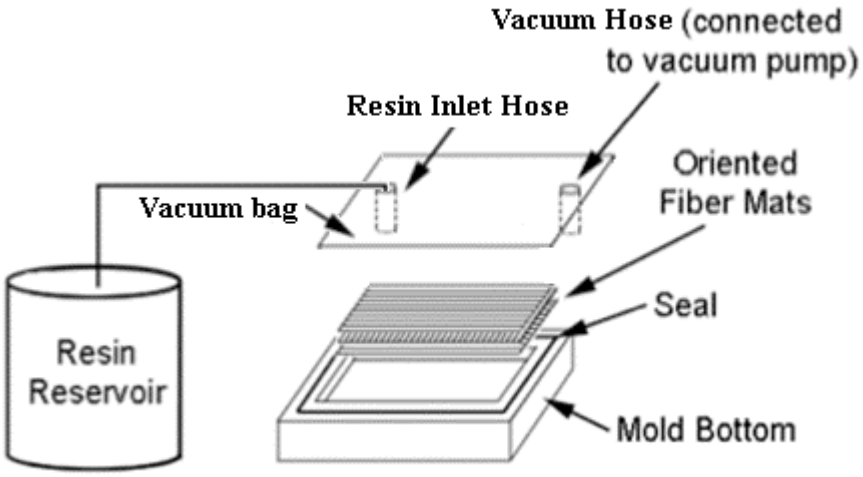

Figure 4-7. Diagram of a simple Vacuum infusion setup.

A general way of distinguishing between different resin injections techniques is how the pressure gradient is applied to force the resin to flow through the mold.

In the case of vacuum infusion the pressure gradient is created by vacuum on the outlet port. The resin injection tank and inlet port are at ambient pressure, as opposed to resin injection techniques (such as RTM) where the resin injection tank is pressurized.

The use of vacuum as the driver behind resin flow has a large impact on the application of the technique and the actual process in the workshop. The major advantage of using vacuum is the absence of large forces on the mold. Standard RTM techniques require strong and stiff tooling. The larger the product, the more difficult and expensive this becomes.

This is why the first success for vacuum infusion has been in large products that are made in small quantities. The major disadvantage of using vacuum is the sensitivity to leakage. A leak will result in air flowing into the mold. This often results in void-rich areas in the cured part. In RTM (with a pressurized resin tank and an outlet at ambient pressure), a leak in the mold would just result in resin spillage.

Besides, air will flow into the mold much easier than resin will flow out of the mold (i.e., the viscosity of air is much smaller than the viscosity of the resin).

Most of parts of a wind turbine blade are made by this process. The parts produced must pass a control (visual inspection, X-ray, ultrasound tests) to detect major defects that may arise:

- Discontinuities between sheets produced by the existence of trapped air.
- Incomplete curing of the resin.
- Excess resin between sheets.
- Porosity and holes in the laminates.
- Incorrect orientation of the sheets to form the laminate.
- Fiber damage.
- Inclusions.
- Variations in thickness.

4.2.2. Tensile Test.

Tensile test is probably the most fundamental type of mechanical test that can be performed on a material. Important design properties of materials can be determined by this test, such as ultimate tensile strength (UTS), elastic limit or Young's modulus.

The procedure is simple: the sample is clamped from its extremities to the tensile tester and an increasing traction load is applied uniaxially along its axis. Instant load and elongation are measured simultaneously with a load cell and an extensometer respectively.

The test ends when the sample is unable to withstand the applied load and consequently fractures. The instant load and the elongation data gathered is normalized so that it is not specific to the geometry of the test sample. Operating this way, two new parameters are defined: nominal stress and nominal deformation.

Nominal stress is defined by the relation.

$$\sigma = \frac{F}{A_0}$$

Where σ is the nominal stress in Megapascals (1MPa = 10^6 N/m^2), F is the instant force applied perpendicularly to the section of the sample in Newton (N), and A_o is the area of the original section before applying the load in square millimeters (mm^2).

Nominal deformation is defined as

$$\varepsilon = \frac{l_i - l_o}{l_o} = \frac{\Delta l}{l_o}$$

Where l_o is the original length before applying the load, and l_i is the instant longitude, so that Δl represents the change in longitude in a determined instant with respect to the initial longitude. Nominal deformation has no units, but it is commonly expressed in percentage.

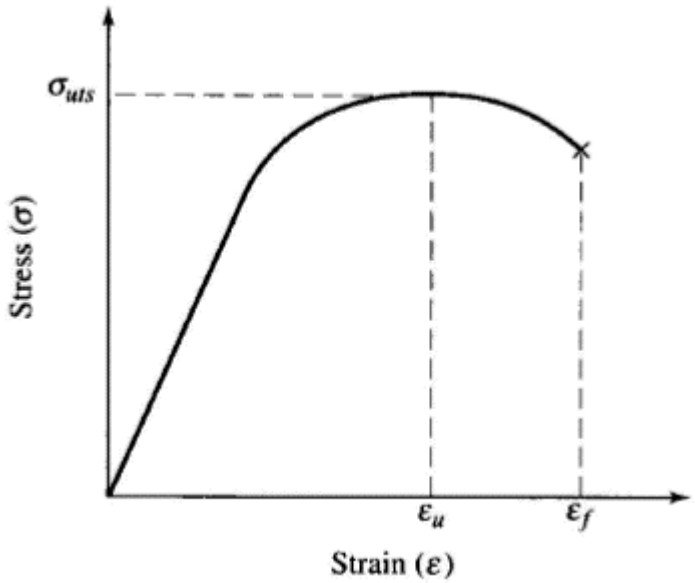

Figure 4-8. Stress - Strain curve.

From this curve (Figure 4-8) the parameters Ultimate Tensile Strength (UTS), maximum elongation and reduction in area can be directly observed. Other important properties can be calculated using of the curve, such as Young's Modulus (E), elastic limit, ductility or toughness [34].

4.2.3. Glass transition Temperature (Tg). DSC Analyse.

A major concern in the application of composite materials is with the elevated temperature properties and the maximum use temperature; these properties are dictated by the polymer matrix.

The glass transition temperature (Tg) is defined as the temperature at which mobility between molecules and segments in amorphous regions is possible. Above this temperature the polymer is rubbery; below it, the polymer is rigid. A partially crystalline polymer retains some rigidity up to the melt temperature (Tm), which is higher than Tg, even though the amorphous part of the material is soft and rubbery.

The glass transition temperature is the point where there is adequate thermal energy to overcome secondary bonds; thus, segments of chains are then free to move, restrained

at points of crosslinking (thermosets), chain entanglement (amorphous thermoplastics) or crystallites (semi crystalline thermoplastics). The polymer softens significantly as Tg is approached.

The maximum use temperature for an amorphous polymer used as a composite matrix is usually below Tg. The specific heat capacity of a polymer is higher when the molecules are free to move, so it decreases with decreased cross-linking, and increases with temperature increases, as Tg is approached.

A differential scanning calorimeter (DSC) apparatus represents one way to measure Tg trough heat capacity change. DSC is a technique that detects thermal phenomena such as phase changes, chemical reactions or properties such as heat capacity using the temperature difference between a reference sample and other one subjected to a temperature program, or the power which is required to be provided or removed from the sample so that its temperature is equal to the reference, subject to the same temperature program.

In the case of a chemical reaction, the heat absorbed or released is proportional to the degree of conversion of the system and the reaction speed is proportional to the heat liberated.

DSC defines the glass transition (Tg) as a change in the heat capacity as the polymer matrix goes from the glass state to the rubber state (Figure 4-19). This is a second order endothermic transition (requires heat to go through the transition) so in the DSC the transition appears as a step transition and not a peak such as might be seen with a melting transition.

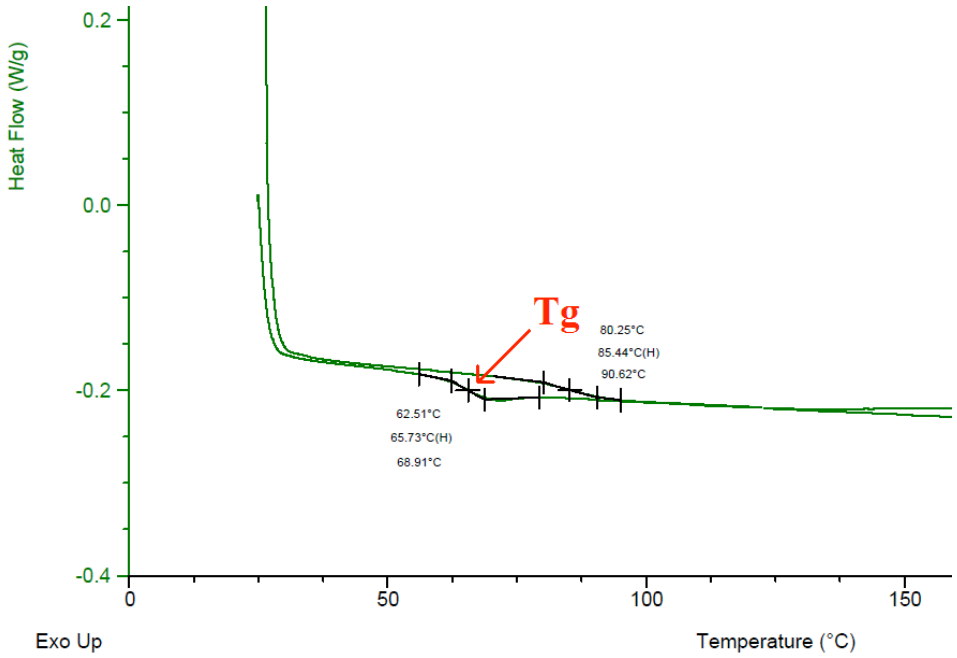

Figure 4-9. Measurement of Tg on DSC machine.

Thermosetting materials are those which undergo an irreversible, chemical reaction,

known as curing, which produces a crosslinked structure. Thermosets remain amorphous, although, above Tg, the liquid state goes from a freely flowing state for the uncured material to a rubbery state for the cured thermoset.

The degree of cure is a very important parameter in determining the end-use properties, such as stiffness or creep, for the material. The Tg of a thermoset material is related to the degree of cure. Tg increases significantly as the curing reaction proceeds to completion due to the establishment of a crosslinked molecular structure. Eventually, as the degree of cure of the thermoset approaches 100% or complete cure, the Tg of the material will reach a limiting value, $Tg(\infty)$ [35].

4.3. Theory prediction.

4.3.1. Effects of the variation of mixing ratio on Young's modulus. Halpin-Tsai.[36]

The micromechanical analysis recognizes the existence of two components: fiber and matrix but excluding the internal structure of each of them. The objective of this analysis is, for example, to define the properties of a homogeneous film and orthotropic to behave equivalently, from the mechanical standpoint, the actual composite sheet formed by a certain distribution of fibers embedded in a matrix.

To perform this equivalence must perform some additional hypotheses that represent possible to calculate properties of the sheet from the properties of the components and the percentage of those present in the compound.

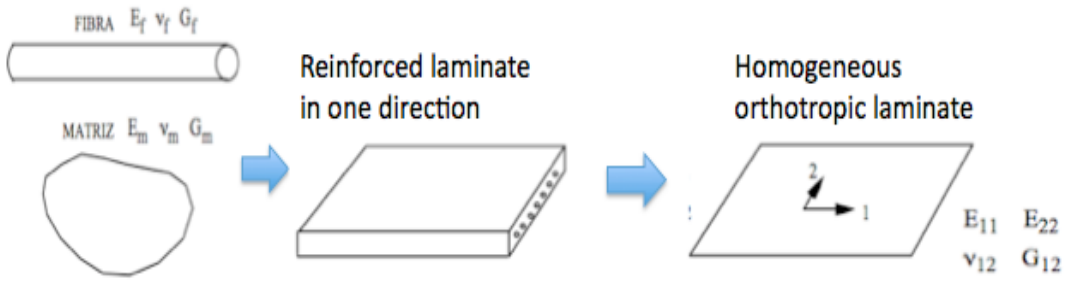

Figure 4-10. Diagram of assumptions for micromechanical analysis.

Tension and compression tests are used to determine the yield and ultimate strengths and ductility of a material. For a composite material, the stress-strain response is a function of the combination of the properties of the matrix and fiber.

The composite is considered as homogeneous. A block of composite containing fibre and matrix as show in the next figure is simplified to block containing two volumes.

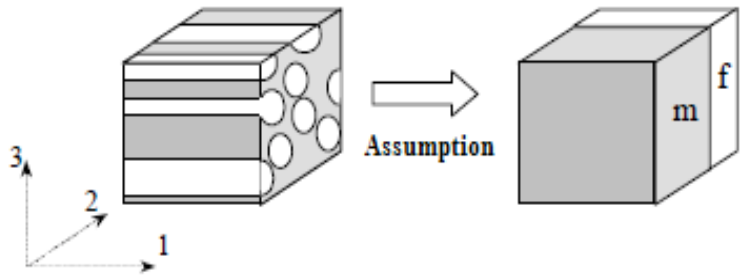

Figure 4-11. Representative matrix and fibre volume elements.[36]

These two volumes are connected together and represent the matrix (m) and the fibre (f) with their respective properties and volume fractions (V_f = fibre volume fraction, V_m = matrix volume fraction).

An elasticity E modulus is then obtained by performing a simple experiment, where the two representative volumes are subjected to an average stress. We are going to determinate E modulus in this situation.

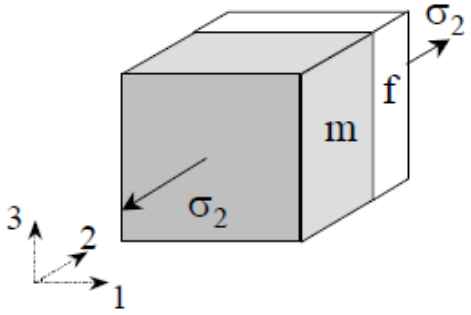

Figure 4-12. Experiment for the transverse modulus (Reus model).[36]

The transverse modulus is obtained by considering the matrix (m) and fibre (f) representative element in series. An average stress is applied along the 2-axis as shown in the Figure 4-12.

The total deformation is the sum of the deformations occurring on the two volumes. This can be expressed in terms of strain:

$$\varepsilon_2 L = \varepsilon_m L_m + \varepsilon_f L_f$$

Where L_m and L_f are the lengths of the matrix and fibre volumes. We can express this equation in terms of the volume fraction, cause the relative content of the constituents is mostly quoted as a volume content or fraction (of fibres for example). Whatever the amount of constituents, we have:

$$\sum_{i=1}^{n} v_i = 1 \quad \text{With} \quad v_i = \frac{V_i}{V_c}$$

Where:

v_i is the volume fraction of the i_{th} constituent,
V_i is the volume of the i_{th} constituent,
V_c is the total volume of the composite.

$$\varepsilon_2 = \varepsilon_m v_m + \varepsilon_f v_f$$

We assume that the 1D (uniaxial loading) Hooke's law (Figure 4-13) is applied relates the normal stress and normal strain as:

$$\sigma = E\varepsilon$$

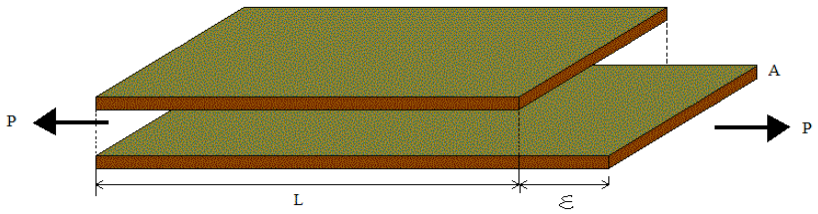

Figure 4-13. 1D Hooke's law.

$$\frac{P}{A} = E \cdot \frac{\varepsilon}{L} \qquad \sigma = E \cdot \varepsilon$$

$$\text{Therefore } \varepsilon = \frac{\sigma}{E}$$

It should be noted that the development carried out so far is based on a linear elastic behavior. Therefore it would be also desirable to check that such behavior occurs. It is therefore advisable to check:

Hence, the equation before can further be developed as:

$$\frac{\sigma_2}{E_2} = \frac{\sigma_m v_m}{E_m} + \frac{\sigma_f v_f}{E_f}$$

From the series volume arrangement, the stress in matrix, fibre and the composite are equal.

$$\sigma_m = \sigma_f = \sigma_2 = \sigma$$

An expression for the transverse elasticity modulus E_2 is obtained:

$$\frac{1}{E_2} = \frac{v_m}{E_m} + \frac{v_f}{E_f}$$

This relation is often called the inverse rule of mixture.

Note again that the fibre transverse modulus should be used. But this equation is generally known as being inadequate for predicting the transverse modulus. This is due to the fact the assumption made on the equality of the stress in the matrix and the fibre in the volume-in-series model is not valid in a real composite. This can be shown on basis of strain energy approach.

A second reason for the inaccuracy of models for the transverse modulus composite based on orthotropic fibre is that the fibre transverse modulus is difficult to measure (and has actually never directly been measured). Quoted values for the transverse modulus of fibres are actually derived from the comparison between micromechanical model results and experiments. The same actually applies for the shear modulus of these orthotropic fibres.

The Reuss model can be improved by simply adding a matrix volume in parallel to the series model as shown in the Figure 4-14.

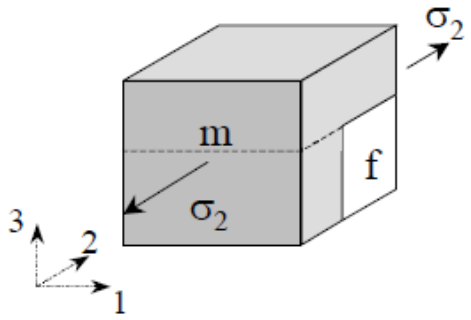

Figure 4-14. Parallel-series model for the transverse modulus.[36]

This geometrical model is an approximation of a square fibre packing.
This result in the following equation:

$$E_2 = (1-\sqrt{v_f})E_m + \frac{\sqrt{v_f}E_m E_{f2}}{v_f E_m + \sqrt{v_f}(1-\sqrt{v_f})E_{f2}}$$

E_2 has been determined in function of the E_{f2} and E_m, which it's depends of the different mixing ratio of the resin. But there is other model more accurate to determinate the E_2.
In the transverse direction, perpendicular to the fibre axis, the modulus E_2 is approximated by Halpin-Tsai equation [37], which developed an interpolation procedure that is an approximate representation of more complicated micromechanics results. The beauty of the procedure is twofold.

First, it is simple so it can readily be used in the design process. Second, it enables the generalization of usually limited, although more exact, micromechanics results.
Moreover, the procedure is apparently quite accurate if the fibre volume fraction (v_f) does not approach one.

The Halpin-Tsai equation, use similar assumptions as the inverse rule of mixture, but adds a "stress partitioning factor η" in order to take into account the mismatch in stress in the fibre and in the matrix.

The Halpin-Tsai relationship,

$$E_2 = E_m \cdot (1 + \zeta \cdot \eta \cdot v_f)/(1 - \eta \cdot v_f)$$

Where:

$$\eta = \left(E_{2f} - E_m\right)/\left(E_{f2} + \zeta \cdot E_m\right)$$

ζ = the curve fitting parameter.

ζ is a measure of fiber reinforcement of the composite that depends on the fiber geometry, packing geometry and loading conditions.

The only difficulty in using the Halpin-Tsai equations seems to be in the determination of a suitable value for ζ . Halpin and Tsai obtained a good approximation with ζ = 10 for calculation of E_2.

So it was shown that using ζ =10 gives similar results as more complex elasticity solutions.

In polymer matrix composites, the transverse modulus is dominated by the matrix modulus, while the longitudinal modulus is dominated by the fibre modulus.

The stress-strain curve for unidirectional materials is usually approximately linear to failure. The tensile strength in the longitudinal direction occurs approximately when the strain in the fibre reaches a value close to the fibre ultimate strain.

The transverse strength (and shear strength) is matrix dominated, with the mode of failure being a crack growing parallel to the fibers in the matrix and fibre/matrix interface. The limiting value for the transverse tensile strength is the matrix ultimate strength.

For brittle resins and/or poorly bonded fibers, the transverse strength will be lower than the matrix strength. So, firstable, the datas of fibre volume fraction (V_f), and the matrix volume fraction (V_m) is needed. To calculate it, the following assumptions are taken:

$$\sum_{i=1}^{n} V_i = 1$$

Therefore $V_f + V_m = 1$ and $V_m = 1 - V_f$

$$\rho_{composite} = V_f \cdot \rho_f + V_m \cdot \rho_m = V_f \cdot \rho_f + \left(1 - V_f\right) \cdot \rho_m$$

The densities of the E-glass fibre ρ_f and the Resin ρ_m are:

$$\rho_f = 2620 kg/m^3$$
$$\rho_m = 1102 kg/m^3$$

These datas were extracted from the data specifications sheet of the suppliers (it can be seen in attachments). Regarding the ρ_m in addition, was made under the following assuming. Considering the 100:31 mixing ratio as reference following the suppliers recommendations:

Hence, there is a 76% of resin and a 24% of hardener

$$\rho_{mix} = 76\% \cdot \rho_{\text{Resin}} + 24\% \cdot \rho_{Hardener}$$
$$\rho_{mix} = 0.76 \cdot 1.15 {}^{g}\!/_{cc} + 0.24 \cdot 0.95 {}^{g}\!/_{cc} = 1.102 {}^{g}\!/_{cc} = 1102 {}^{kg}\!/_{m^3}$$

This $\rho_m = 1102 kg/m^3$ was made for the formulation, but this data could not be exactly, and it will change as function of the variation of the mixing ratio due to the difference of density of resin and the hardener, and the amount of each one in the total mixture as well.

A UD coupon with the following size was taken for this calculation (Figure 4-15):

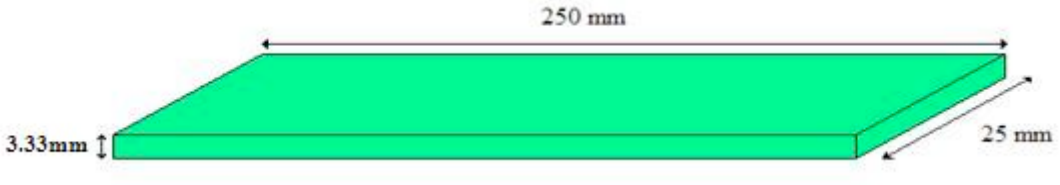

Figure 4-15. Dimensions of UD coupon.

So, $V_{composite}$ are:

$$V_{composite} = 0.250 \times 0.025 \times 0.00333 = 2.081 \cdot 10^{-5} m^3$$

The mass of this coupon was measure using a balance:

$$m_{composite} = 0.040 kg$$

Hence $$\rho_{composite} = \frac{m_{composite}}{V_{composite}} = \frac{0.040 kg}{2.081 \cdot 10^{-5} m^3} = 1922.15 kg/m^3$$

The fibre volume fraction (V_f), and the matrix volume fraction (V_m) is possible to calculate:

$$\rho_{composite} = 1922.15 kg/m^3 = V_f \cdot \rho_f + (1 - V_f) \rho_m = V_f \cdot 2620 kg/m^3 + (1 - V_f) 1102 kg/m^3$$

$$V_f = \frac{\rho_{composite} - \rho_m}{(\rho_f - \rho_m)} = \frac{1922.15kg/m^3 - 1102kg/m^3}{(2620kg/m^3 - 1102kg/m^3)} \approx 0.54$$

Finally,

$$V_f = 54\,\%$$
$$V_m = 46\,\%$$

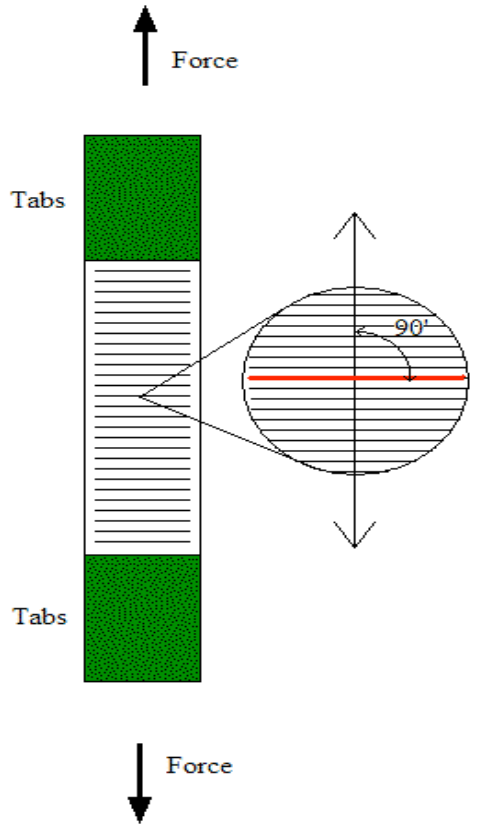

Figure 4-16. Scheme of UD coupon under tensile test.

To apply the formula of Halpin-Tsai formula:

$$E_2 = E_m \cdot (1 + \zeta \cdot \eta \cdot v_f)/(1 - \eta \cdot v_f)$$

Where:

$$\eta = (E_{2f} - E_m)/(E_{f2} + \zeta \cdot E_m)$$

ζ = the curve fitting parameter.

The datas of the Young's modulus on transverse direction of E-Glass fibres are needed.

$$E_{fL} = 72 \text{ Gpa}$$
$$E_{fT} = E_{2f} = 72 \text{ Gpa}$$

As it said before, ζ =10 is taken for the calculation due to it gives similar results as more complex elasticity solutions.

For the E_m, data of the matrix (Epoxy resin), it changes in function of the different resin mixing ratio. To obtain these datas, five resin coupons of each different mixing ratio from 100:28 to 100:34 were fabricated and tested following the standard ISO 527-2 on the tensile machine. The Figure 4-17 shows one coupon of 100:32 mixing ratio as an example of all of them.

All datas of these resin coupons are in the appendix chapter. The average of the results from each mixing ratio are shown in the Table 4-5.

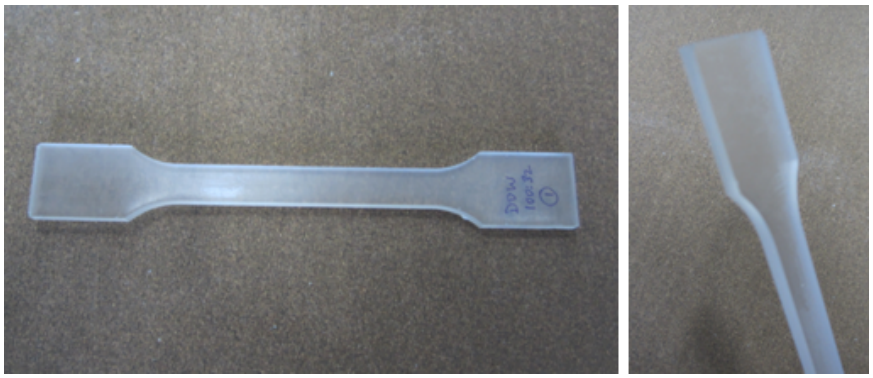

Figure 4-17. Resin coupon of different mixing ratio.

Table 4-5. Values of E_m of different resin mixing ratios.

Resin	Different mixing ratios						
	100:28	100:29	100:30	100:31	100:32	100:33	100:34
E_m (GPa)	1.96	2.22	2.48	2.77	2.58	2.39	2.37

Therefore, the Table 4-6 shows the influence of the resin mixing ratio on the Young's modulus of the composite laminate could be predicted by Halpin-Tsai formulation:

Table 4-6. Values of the E modulus as function of different resin mixing ratios.

UD	Mixing ratio						
	100:28	100:29	100:30	100:31	100:32	100:33	100:34
E_2 (Gpa)	17.12	18.50	19.76	21.05	20.22	19.34	19.24
η	0.765	0.741	0.719	0.694	0.710	0.726	0.728

$$\zeta = 10$$
$$E_{2f} = 72 \text{ GPa}$$
$$V_f = 54\,\%$$

The predicted results of E modulus of UD laminates are shown below in Figure 4-18:

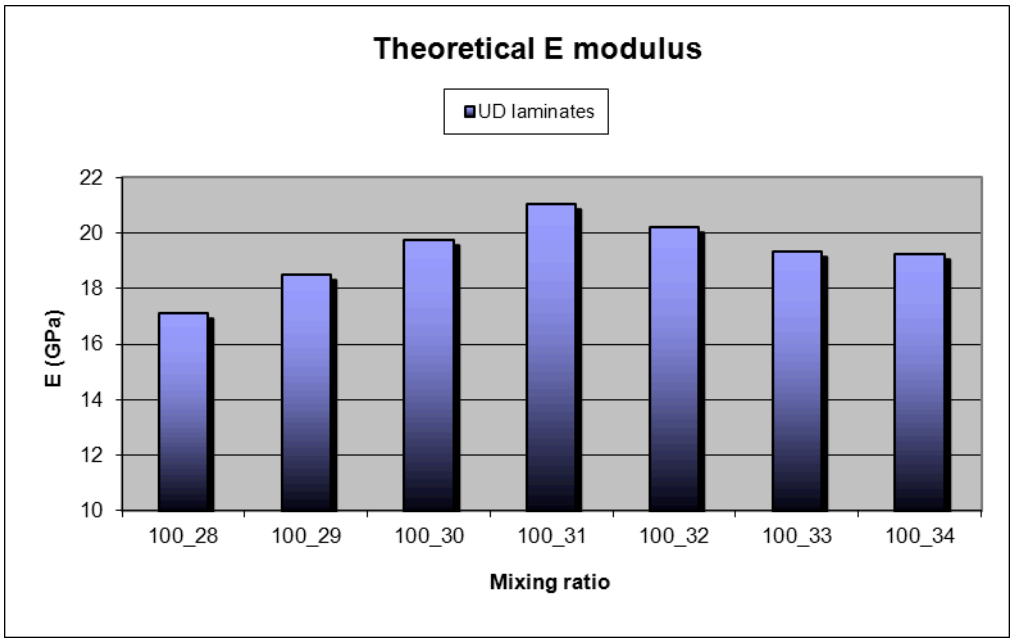

Figure 4-18. Variation of the E modulus vs resin mixing ratio in UD laminates.

After these results of the predicted formulation, the mixing ratio 100:31 is expected as the ratio that it has the highest E modulus, which, it will provide the highest stiffness to the final composite UD laminate.

The decreasing of the value of the predict E modulus on mixing ratios lower than 100:31 were more accused than mixing ratios over 100:31.

One conclusion might be taken after this results, as far as the E modulus is concern, to increase the amount of the curing agent in the mixing ratio, it is not as bad as decreasing it.

It is expected than UD laminates infused with resins mixed with lower mixing ratio than 100:31 are more flexible than higher mixing ratio as consequences of its loss of stiffness.

For the Biax laminates, a coupon (Figure 4-19) with the following size was taken for this calculation:

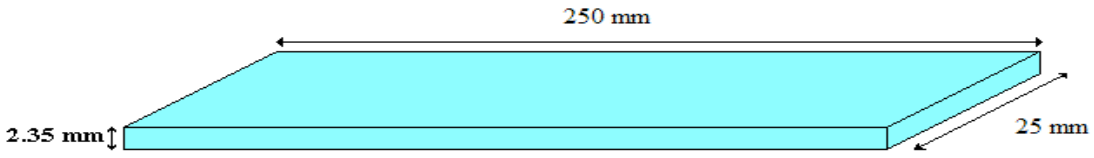

Figure 4-19. Dimensions of Biax coupon.

So, its $V_{composite}$ was:

$$V_{composite} = 0.250 \times 0.025 \times 0.00235 = 1.469 \cdot 10^{-5} m^3$$

The mass of this coupon was measured using a balance:

$$m_{composite} = 0.028kg$$

Hence $$\rho_{composite} = \frac{m_{composite}}{V_{composite}} = \frac{0.028kg}{1.469 \cdot 10^{-5} m^3} = 1906.1kg/m^3$$

The fibre volume fraction (V_f), and the matrix volume fraction (V_m) is possible to calculate:

$$\rho_{composite} = 1906.1kg/m^3 = V_f \cdot \rho_f + (1 - V_f)\rho_m = V_f \cdot 2620kg/m^3 + (1 - V_f)1102kg/m^3$$

$$V_f = \frac{\rho_{composite} - \rho_m}{(\rho_f - \rho_m)} = \frac{1906.1kg/m^3 - 1102kg/m^3}{(2620kg/m^3 - 1102kg/m^3)} \approx 0.53$$

Finally,

$$V_f = 53\,\%$$
$$V_m = 47\,\%$$

In case of Biax laminates, the principle of linearity was assumed, so it was possible to apply Superposition principle (Figure 4-20).

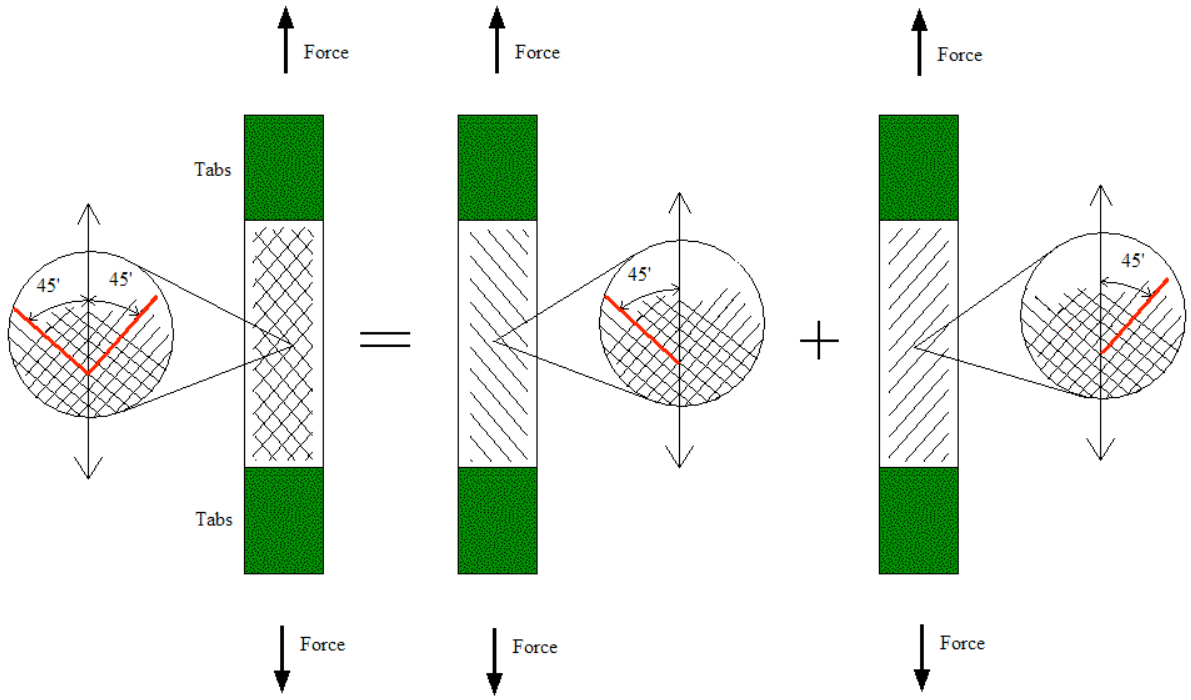

Figure 4-20. Scheme of Superposition principle of Biax coupon under tensile test.

To apply the formula of Halpin-Tsai formula:

$$E_2 = E_m \cdot (1 + \zeta \cdot \eta \cdot v_f)/(1 - \eta \cdot v_f)$$

Where:

$\eta = (E_{2f} - E_m)/(E_{f2} + \zeta \cdot E_m)$

ζ = the curve fitting parameter.

The datas of the Young's modulus on transverse direction of E-Glass fibres are needed.

$$E_{fT} = E_{2f} = 72 \text{ Gpa}$$

In this case, the force is not applying in the direction of E_{fT}. The simple trigonometry is applied to bound it.

$$E_{ft} = E_{ft} \cdot \cos(45) + E_{ft} \cdot \cos(-45) = E_{ft} \cdot 2 \cdot \cos(45) = 72GPa \cdot 2 \cdot \cos(45) = 75.65 \text{ GPa}$$

$$E_{fT} = E_{2f} = 75{,}65 \text{ Gpa}$$

As it said before, ζ =10 is taken for the calculation due to it gives similar results as more complex elasticity solutions.

For the E_m, data of the matrix (Epoxy resin), it changes with the different resin mixing ratio.

The datas obtained before for the UD laminates were taken in count here due to it was the same mixture of resin and hardener for both kinds of composite laminates. The results are shown again in Table 4-7.

Table 4-7. Values of E_m of different resin mixing ratio.

Resin	Different mixing ratios						
	100:28	100:29	100:30	100:31	100:32	100:33	100:34
E_m (GPa)	1.96	2.22	2.48	2.77	2.58	2.39	2.37

So, the influence of the resin mixing ratio on the Young's modulus could be predicted as well by Halpin-Tsai formulation and shown on Table 4-8:

Table 4-8. Values of the E modulus as function of different resin mixing ratio.

Biax	Mixing ratio						
	100:28	100:29	100:30	100:31	100:32	100:33	100:34
E_2 (Gpa)	16.94	18.35	19.63	20.95	20.10	19.20	19.10
η	0.774	0.750	0.728	0.705	0.720	0.736	0.738

$$\zeta = 10$$
$$E_{2f} = 75.65 \text{ GPa}$$
$$V_f = 53\,\%$$

The predicted results of E modulus of Biax laminates are shown below in Figure 4-21:

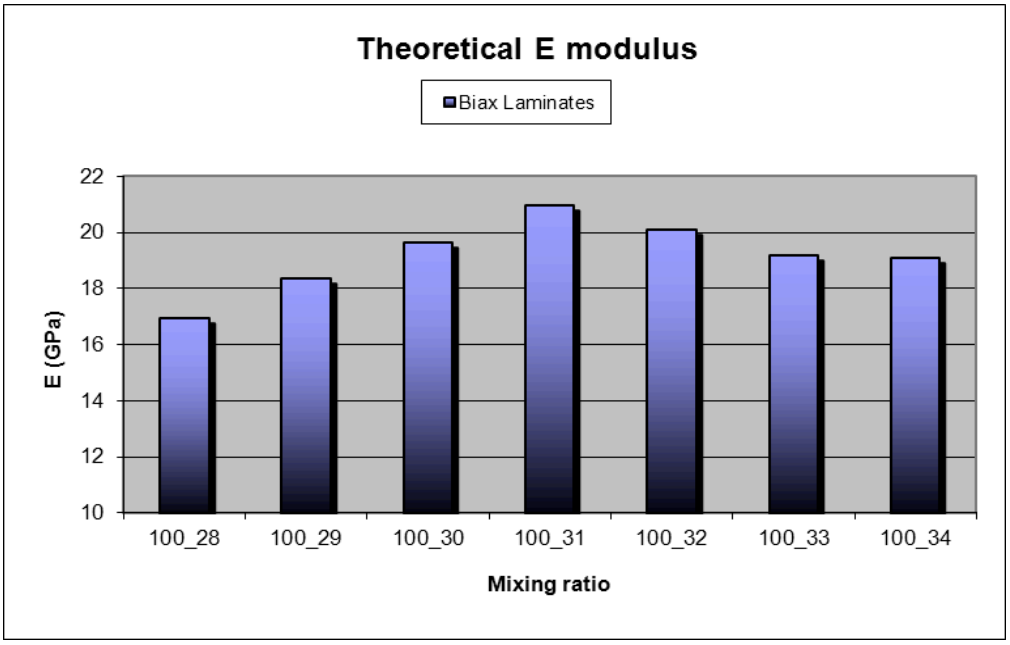

Figure 4-21. Variation of the E modulus vs resin mixing ratio in Biax laminates.

Based on the theory prediction, the highest E modulus of Biax laminate is provide by the mixing ratio 100:31 as well as the same case of UD laminates.

Deviating the mixing ratio around the 100:31, the value of the E modulus decreases. That decreasing of stiffness is in major proportion for the poor mixing ratio than excess mixing ratio. The variation of the E modulus is not symmetric in both sides of the 100:31 mixing ratio.

The prediction results of E modulus of UD and Biax laminates were compared on Table 4-9:

Table 4-9. Values of the E modulus of UD and Biax laminates as function of mixing ratio.

		Mixing ratio						
		100:28	100:29	100:30	100:31	100:32	100:33	100:34
UD	E_2 (Gpa)	17.12	18.50	19.76	21.05	20.21	19.34	19.24
Biax	E_2 (Gpa)	16.94	18.35	19.63	20.95	20.10	19.20	19.10

The comparison could be seen in the Figure 4-22.

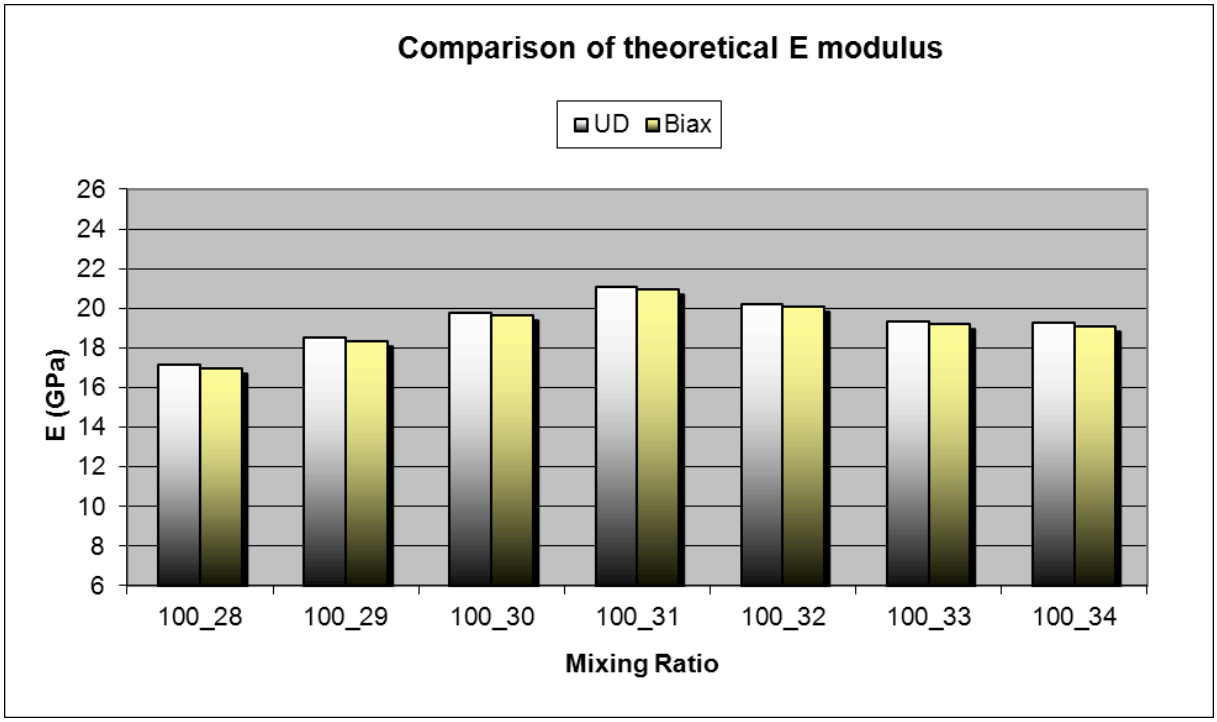

Figure 4-22. Comparison of the theorist E modulus of UD and Biax laminates.

The E modulus of both kinds of laminates follows a similar behaviour as function of the mixing ratio. Is expected, the mixing ratio 100:31 has the highest E modulus in both cases. For Biax laminates, if a 5% is assuming as an acceptable decreasing of the value of E modulus, the safe range of mixing ratio could be from 100:31 to 100:32 (the E modulus are between 20.95 and 19.90 GPa).

For UD, assuming a 5 % as well, the range of mixing ratios would be only from 100:31 to 100:32 as well, where the E modulus are more than 19.99 Gpa.
In general, decreasing of E modulus is bigger in lower mixing ratios than 100:31 in comparison with the mixing ratios over the 100:31.

5. EXPERIMENTAL PART.

This chapter gives details of the experiments conducted for the purposes of the present study and the results obtained.

In a first part, a description of the materials utilized and their preparation steps is presented.

5.1. Materials used.

For the present work, for the vacuum infusion, the unidirectional (UD) fiber fabrics are provided by the company KUSH. The UD glass fibers are held together by ±90º E-glass fibers and PES stitching.

The materials that were used were E-Glass Fabrics from Kush company (Figure 5-1). In this investigation two different E-Glass fabrics were used according to the orientation of the fibres, Unidirectional (UD) fibres and Bi-axial (Biax) ±45 fibres.

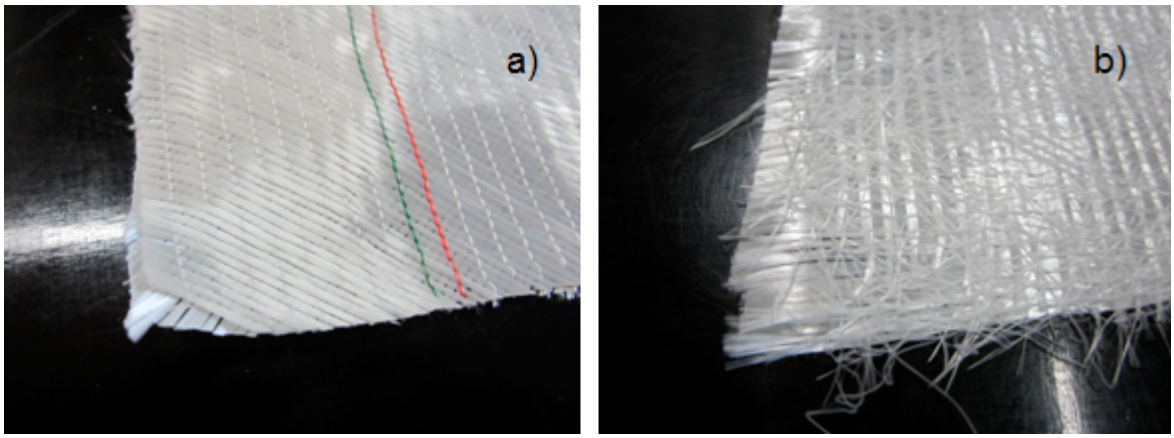

Figure 5-1. a) Biax fabric. b) UD fabric.

Their properties are shown in the Table 5-1:

Table 5-1. Properties of the E-Glass from KUSH company.

Property	UD	Biax
Orientation of the E-Glass fibres	0°	+45°/-45°
Orientation of the Stitches	90°	90°
Areal weight	1265 g/m^2	800 g/m^2
E modulus (long/transv)	72GPa	72GPa

In this experiment, the resin system used was DOW Airstone 780E/785H from DOW chemical company (Figure 5-2).

Figure 5-2. Resin and Hardener from DOW cheminal company.

Their properties are shown in Table 5-2:

Table 5-2. Properties of Dow Resin and Hardener.

Property[1]	AIRSTONE 780E Epoxy Resin	AIRSTONE 785H Hardener
Viscosity @ 25°C (mPa·s) ASTM D-445	1400	16
Density @ 25°C (g/cc) ASTM D-4052	1.15	0.95

The density of the mixture resin + hardener was assumed, taking the 100:31 mixing ratio as reference cause following DOW chemical specifications.

Hence, there is a 76% of resin and a 24% of hardener in the mixture resin/hardener.

$$\rho_{mix} = 76\% \cdot \rho_{\text{Resin}} + 24\% \cdot \rho_{Hardener}$$

$$\rho_{mix} = 0.76 \cdot 1.15 \, {}^{g}/_{cc} + 0.24 \cdot 0.95 \, {}^{g}/_{cc} = 1.102 \, {}^{g}/_{cc} = 1102 \, {}^{kg}/_{m^3}$$

5.2. Sample preparation.

The steps followed for the preparation of the coupon samples of the different composite laminates used on Suzlon's blades were the followings.

Composite laminates with different types of E-Glass (UD or Biax) have to be fabricated and cut in the size needed. For this experiment 4 fabrics of UD and 4 fabrics of Biax were used in each laminate. A schematic of the layup sequence is shown below (Figure 5-3). These processes of infusion are the same for the UD laminates and Biax laminates.

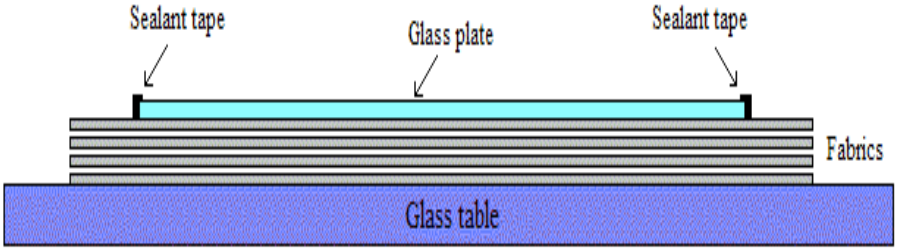

Figure 5-3. Layup of fabrics.

The Vacuum infusion process was used (Figure 5-4).

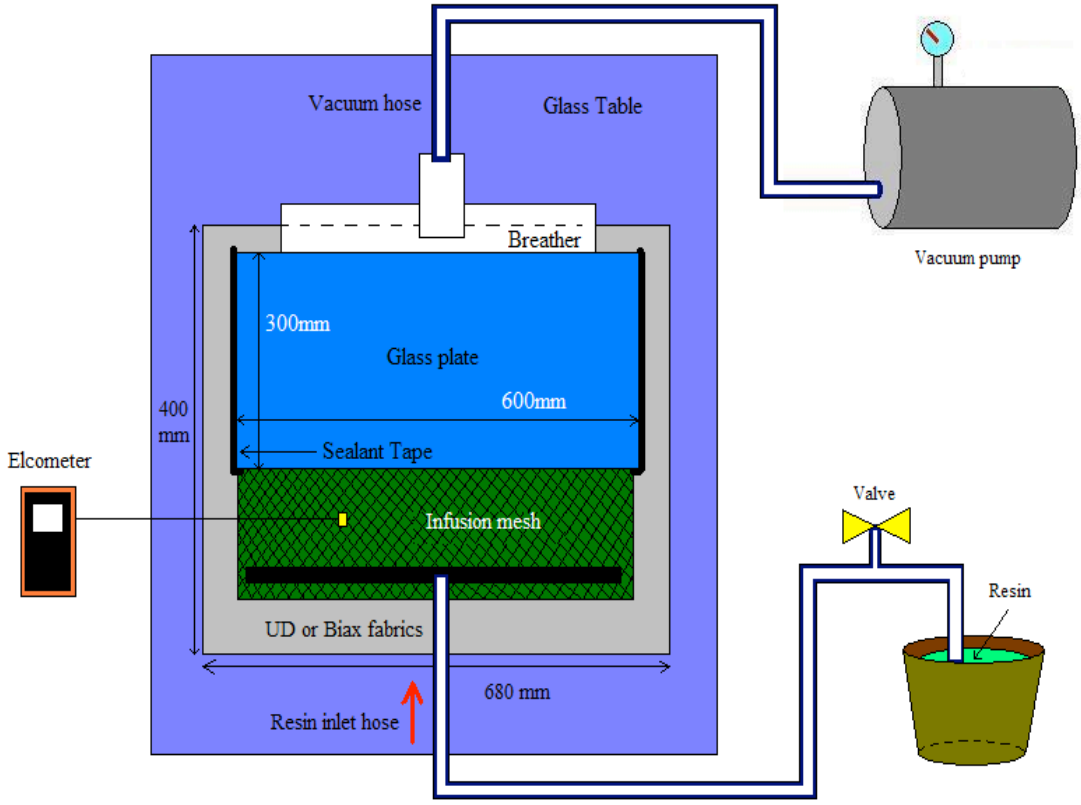

Figure 5-4. Process of laminate fabrication.

The laminate's build up is shown by cross-sectional view (Figure 5-5):

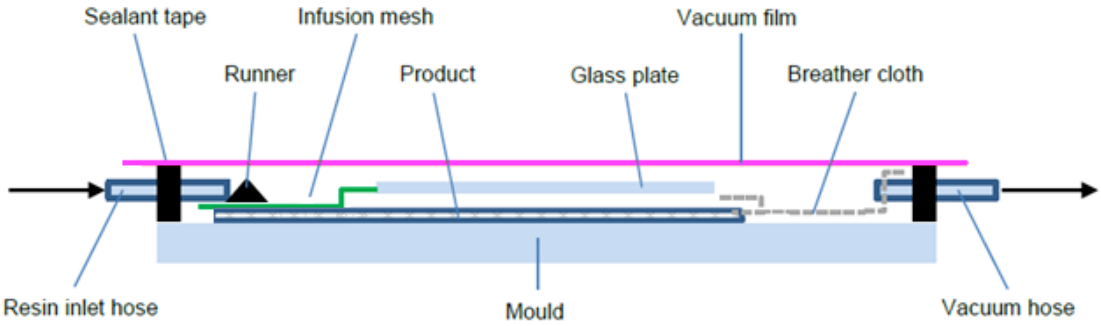

Figure 5-5. Cross section view of laminate build-up.

Firstable, the glass table was cleaned applying a release agent, such as Loctite Frekote for a good release of laminates after infusion process. After placed the fabrics with the properly dimension required and the glass plate above them, vacuum sealing tape was applied around.

Next, the runner was placed to get a distribution of the resin across the width of the fabric. The resin exit must be arranged, therefore, the breather cloth was placed at the opposite side to absorb the resin. Two pieces of breather cloth are needed. One is insert a small distance into the fabric package to establish contact between the fabric and the breather cloth, and the second one, can be placed at the top, covering a small piece of the top fabric layer and the other breather cloth.

After this, the infusion mesh, and the different hose (resin inlet and vacuum) were placed and fixed to the mould by sealing tape. The mouth of the vacuum hose was wrapped in breather cloth, this way; the vacuum can be transferred from the hose to the breather cloth touching the laminate.

Then, all was covered by the vacuum film and made sure it was completely sealed (Figure 5-6).

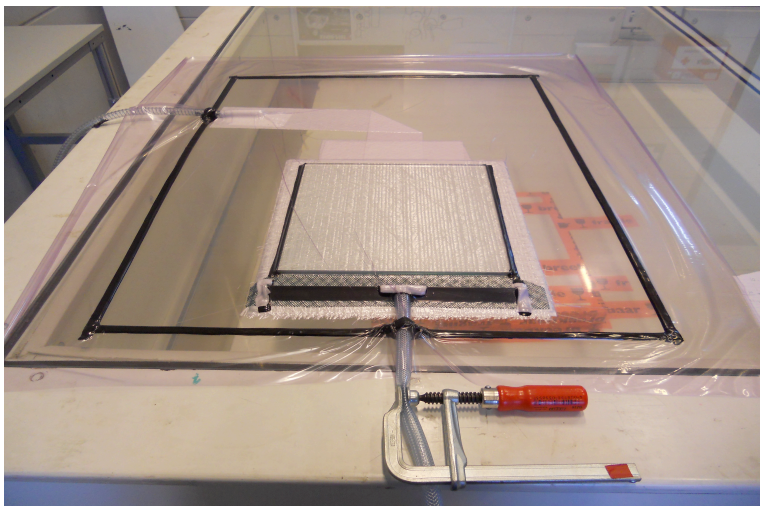

Figure 5-6. Build up before infusion starts.

A thermocouple was attached to the top of the package for measure the temperature during infusion, and a clamp was put on the resin inlet hose as a valve.

Vacuum was applied and make sure there was no leaks in the vacuum bag. Any leakage may spoil the whole fabrication process. The mould was preheated to 35°C before start infusion.

By the other hand, the resin for the infusion must be in the workshop at least 24 hours before the infusion to allow the resin to reach the same temperature as the workshop. Only after the leak rate is considered acceptable can the resin components be mixed. Mixing needs to be done carefully to prevent dragging in excessive air (which can cause bubbles in the laminate).

The mixing ratio of the resin were prepared with the correctly amount of the resin and the hardener. Seven different mixing ratios by weight (from 100:28 to 100:34) were made. To determine the amount needed of each one, some calculations were done.
Firstable, a reference of resin amount is needed to be estimated.

Datas of dimensions of UD fabrics:
1 UD Layer: 0,36m X 0,40m = 0,144m^2
4 UD Layers: 4 X 0,144m^2 = 0,576m^2
0,576m^2 X 1200 g/m^2 = 691,2 g

Datas of dimensions of Biax fabrics:
1 Biax Layer: 0,68m X 0,40m = 0,272m^2
4 Biax Layers: 4 X 0,272m^2 = 1,088m^2
1,088m^2 X 800 g/m^2 = 870,4 g

At least 691,2 gr of mixed resin (resin with hardener) are needed for UD laminates and 870, 4 gr at least for Biax laminates. Therefore, the following references of amount of resin were taken for mix it with the appropriate amount of curing agent in base of the variation of the mixing ratio. The Table 5-3 shows all different amounts of Resin and Hardener used in this investigation.

Table 5-3. Amount of resin and curing agent of each different mixing ratio.

	UD		Biax	
Mixing ratio	Resin (gr)	Hardener (gr)	Resin (gr)	Hardener (gr)
100:28	700	196	1000	280
100:29	700	203	1000	290
100:30	700	210	1000	300
100:31	700	217	1000	310
100:32	700	224	1000	320
100:33	700	231	1000	330
100:34	700	238	1000	340

The correctly amount of resin and hardener were mixed slowly in a bucket with an agitator avoiding bring air into the resin mixture by whirlpools.
The air bubbles inside of the laminate are a big problem, because it makes decrease the mechanical properties of the laminate, especially the strength. For this reason, it is important to this part of the process avoid air bubbles as much as possible.

The resin can be degassed before and after mixing, depending on the purpose. Before mixing, the resin can be degassed thoroughly to remove dissolved air [38][39]. After mixing, degassing can be used to remove small bubbles that are dragged into the resin during mixing to prevent voids that might weaken the material.

Degassing can, however, affect resin cure. Checking the resin temperature, viscosity, and gel time is good practice to prevent mistakes, especially for large parts. In this investigation, the degassing processes were used only after mixing with each mixing ratio for extract all the air bubbles inside of the resin before start the infusion.

A desiccator was used to extract the gasses from the resin (Figure 5-7).

Figure 5-7. Desiccator and degassing process.

The principle of the desiccator is very simple; put some resin in a vacuum and all gasses captured in the resin will tend to expand into the vacuum, therefore leaving the resin. The easiest way of doing this is placing a bucket containing resin into a small space under vacuum. The only drawback of this method is the slow speed.

Gasses are pulled out of the surface at a decent rate, but due to the motionless resin the gasses inside the resin will have to travel a larger distance when located at the bottom. A way to increase the speed is moving or vibrating the resin and hereby creating a certain flow. If an electromagnetic agitator is used, this method is also suitable for combining mixing and degassing in one action, but this was not able to do in this investigation.

A scheme of this degassing process is shown in the Figure 5-8.

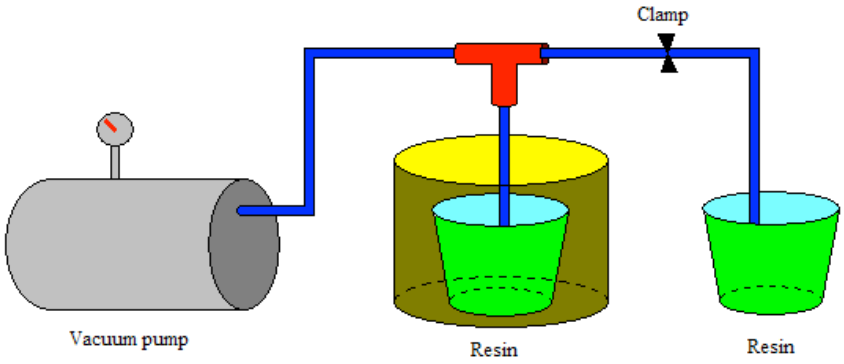

Figure 5-8. Degassing of resin process.

When the leak rate is acceptable, the injection pressure is set and checked, the resin is mixed and degassed, and the temperature of the resin is checked, then the infusion can start. In this simple method, a hose is fixed in a bucket with resin. The hose is opened (valve, or removal of a clamp) and the resin flows into the vacuum bag wetting the layers of fibers.

The infusion process of UD laminates are shown below (Figure 5-9, Figure 5-10):

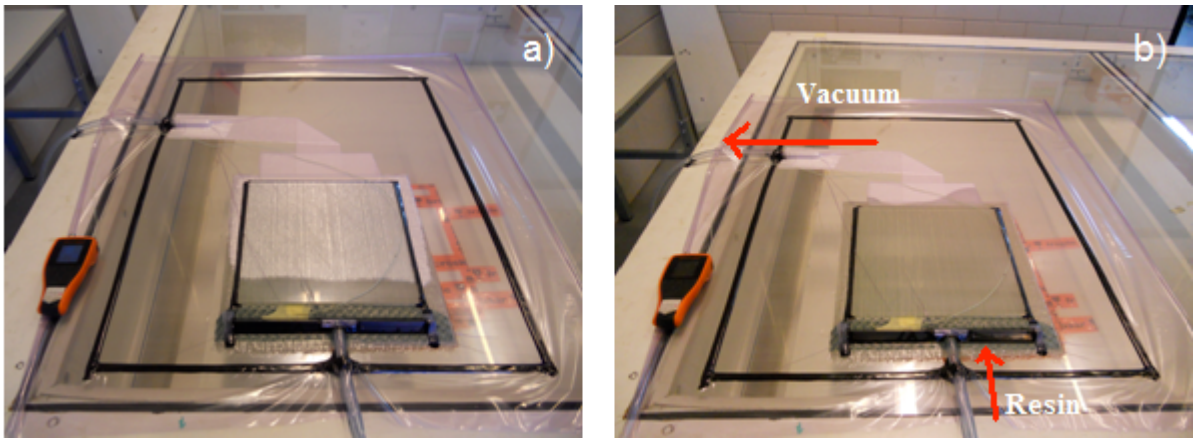

Figure 5-9. a) Start infusion UD laminate b) End infusion UD laminate.

And it was the same for the Biax laminates:

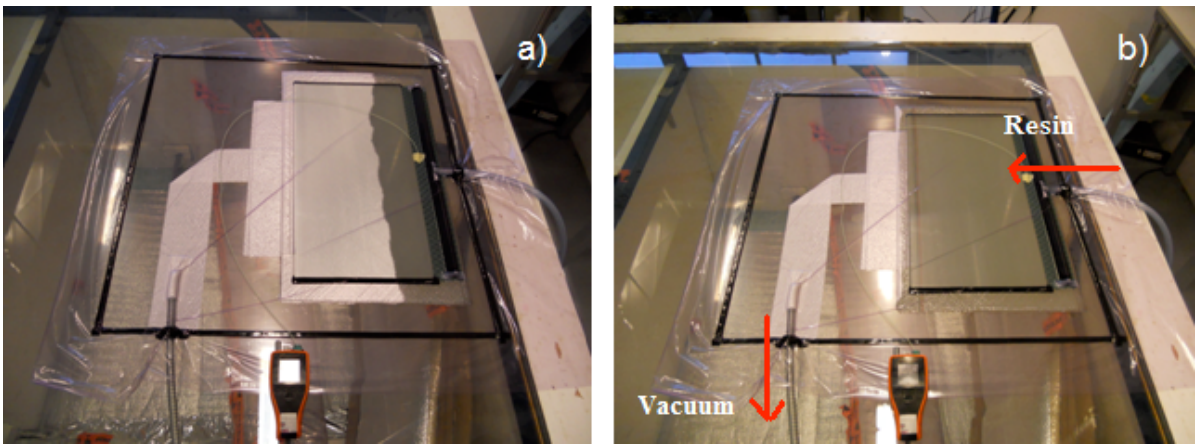

Figure 5-10. a) Start infusion of Biax laminate b) End infusion of Biax laminate.

When the infusion is done, the Pre-cure process of the laminate starts (Figure 5-11). The laminate was covered with insulation blankets to improve an even distribution of the heat and heated up to the curing temperature 65°C during three and half hours.

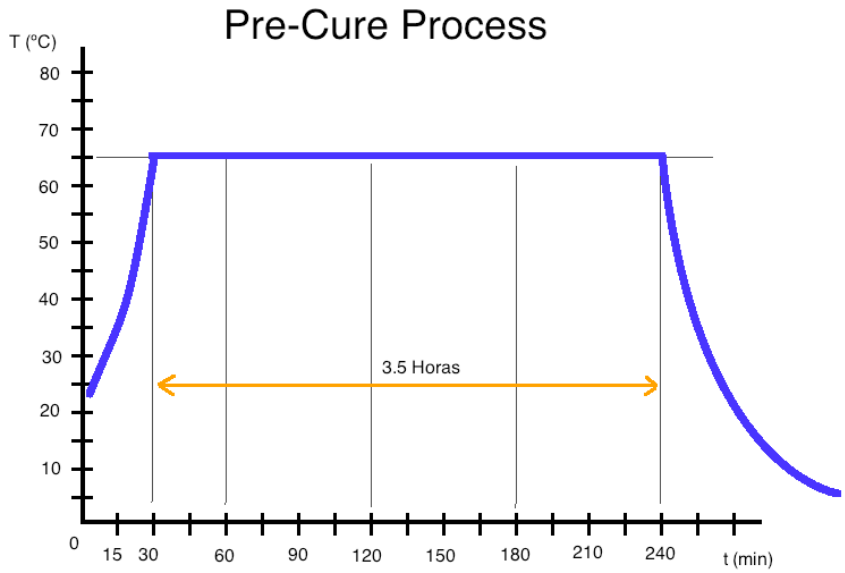

Figure 5-11. Graph of Pre-Cure of laminates.

Next, all aiding materials were removed, and the laminate was cut in the required dimension. The laminates were placed into the oven during 8 hours at 75°C for the Post-cure process (Figure 5-12).

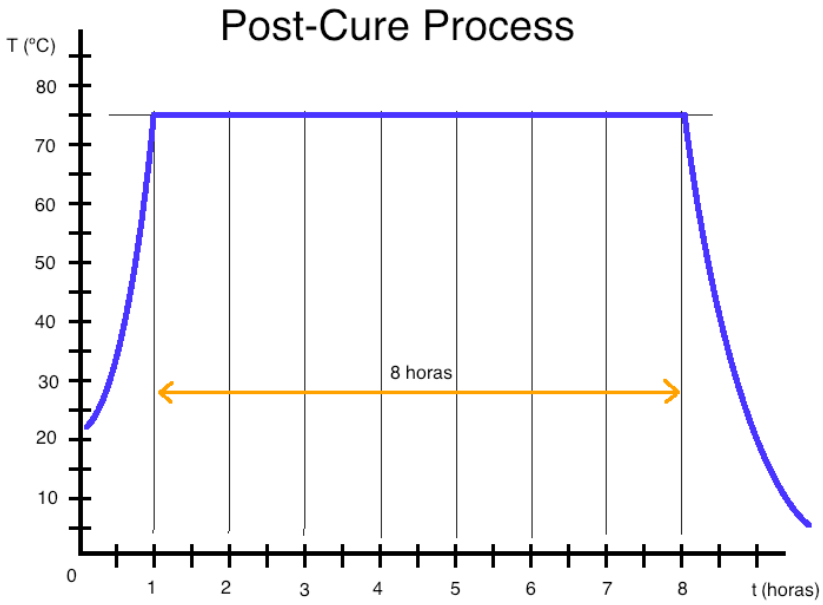

Figure 5-12. Graph of Post-Cure process of laminates.

The appreciation of the nature of the defects is increased by the direct observation in the manufacture of laminated fiber reinforced composite materials.

Some common defects to be controlled are the damage that may have on the surfaces of the composite laminate caused by the presence of dirt on the surface of the mold during the infusion process the laminate.

When all laminates were manufactured without damage that may make the material weaker and post-curing also ended, then it was possible to cut them into the required size for tensile coupons.

Some of the finished laminates are shown below (Figure 5-13 and Figure 5-14).

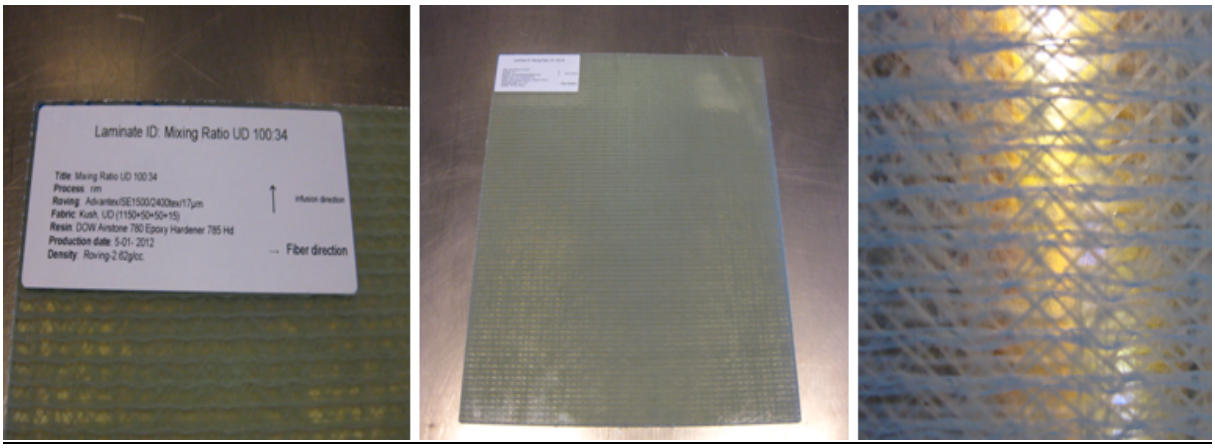

Figure 5-13. Sample of UD laminate.

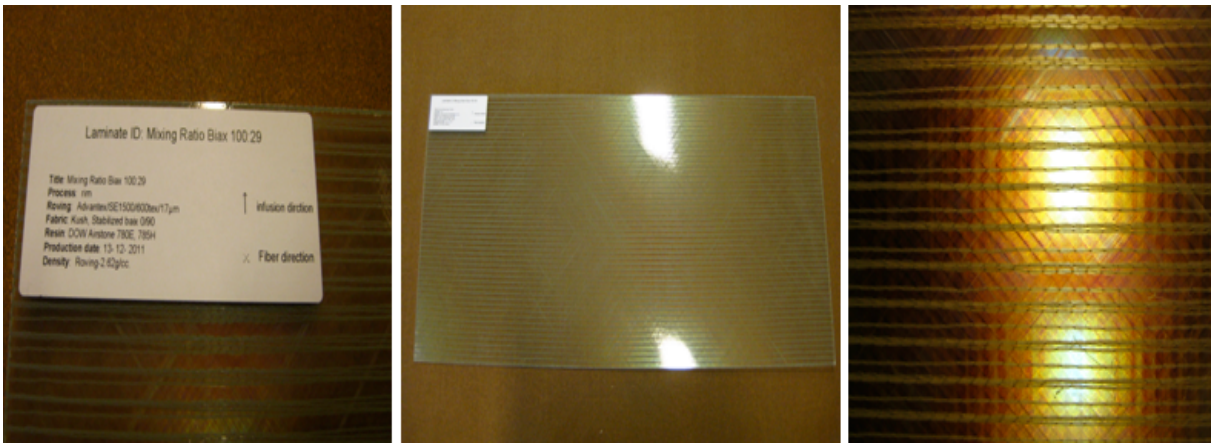

Figure 5-14. Sample of Biax laminate.

This fabrication process was done for each laminate (UD type and Biax type) with different resin mixing ratio, from 100:28 to 100:34. One laminate of each different mixing ratio was fabricated to extract from it, several coupons and tested under a tensile machine.

The steps followed for the preparation of the coupon samples of the different composite laminates for testing their mechanical properties were followed the different ISO standards, ISO 527 for UD and ISO 14129 for Biax laminates.

The following Figure 5-15 shown the required sizes for UD coupons:

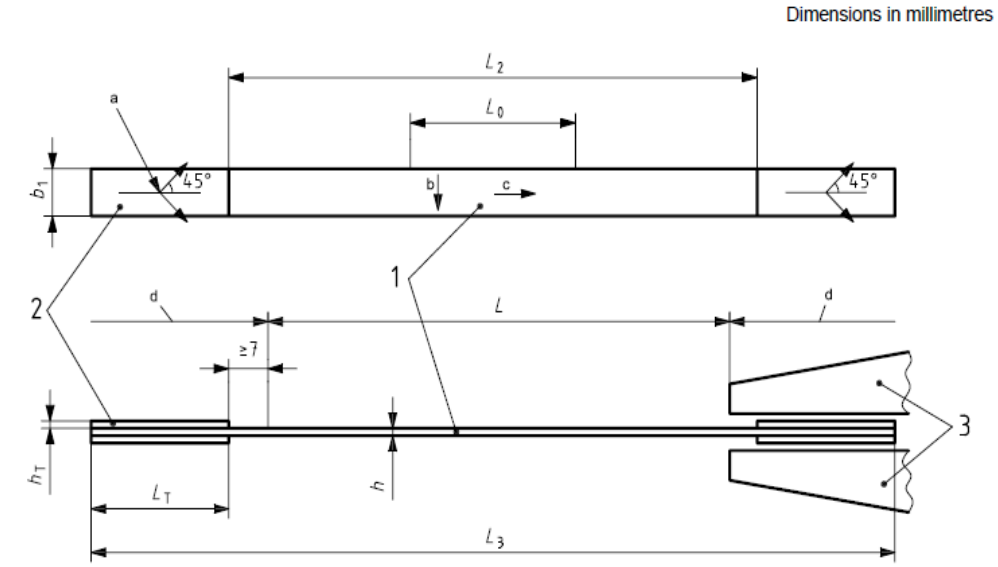

Key

1 specimen
2 tab
3 jaws

a Tab-fibre orientation.
b Fibre direction in type B specimen.
c Fibre direction in type A specimen.
d Zone covered by jaws.

Figure 5-15. Dimensions of UD coupon.

After added the tabs of peel ply material, seven coupons of the different mixing ratio were fabricated with the required sizes and specifications of the ISO standard 527-5 as its shown the Figure 5-16:

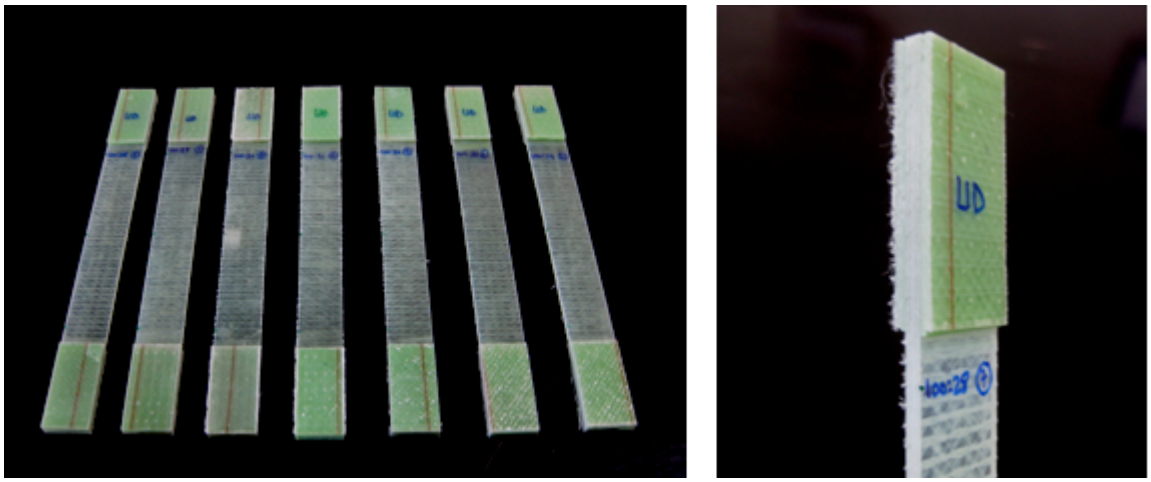

Figure 5-16. UD coupons before tensile tests.

For Biax coupons, the following sizes are required (Figure 5-17):

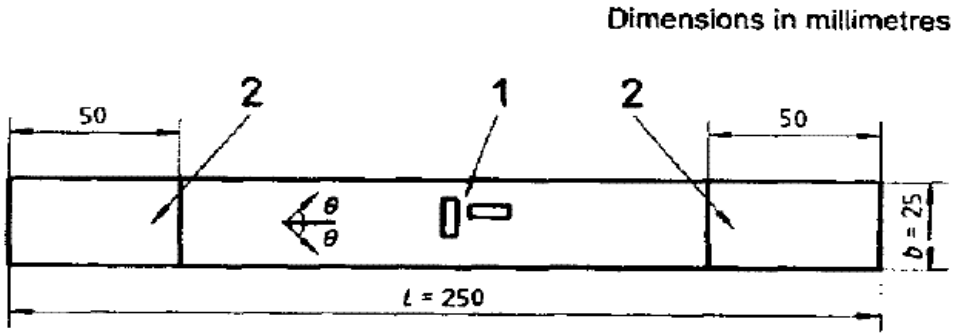

Key

1 Strain gauges
2 Tab
θ Fibre angle (= 45°)
Specimen thickness h = 2 mm

Figure 5-17. Dimensions of Biax coupons.

The same process as UD coupons were done for Biax, and seven coupons of the different mixing ratio were fabricated with the required sizes and specifications of the ISO standard 14129. The Figure 5-18 shows 7 coupons extracted from a Biax laminate infused by 100:32 mixing ratio:

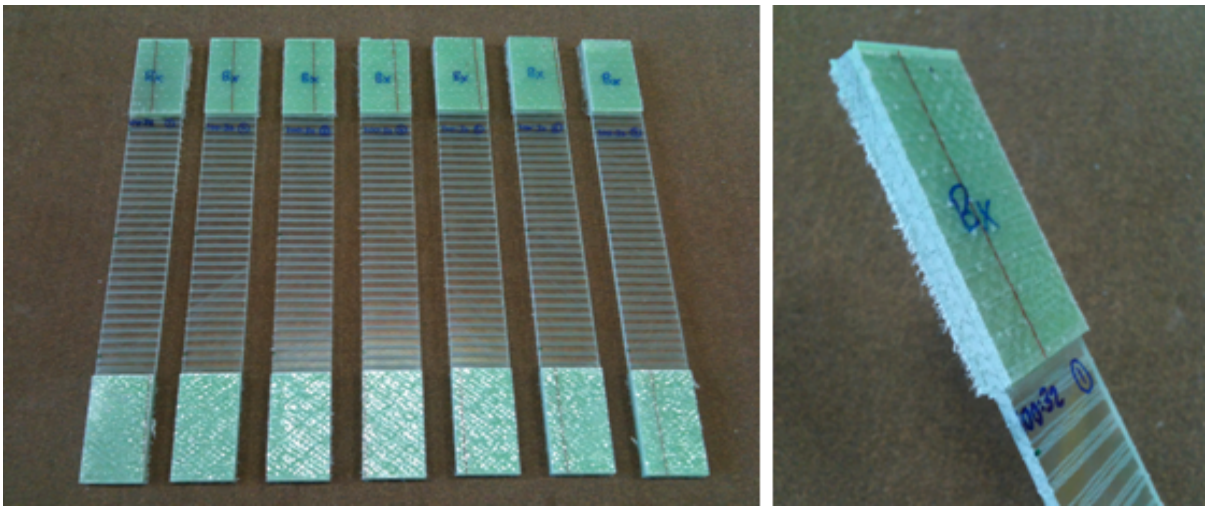

Figure 5-18. Biax coupons before tensile test.

7 coupons of each mixing ratio (from 100:28 to 100:34) were done of each type (UD and Biax) laminate. 49 samples of UD, and 49 samples of Biax.

5.3. Tensile tests

Tensile tests were performed on five samples of each different mixing ratio for UD and Biax laminates with the help of a Zwick/Roell tensile machine, equipped with an extensometer (Figure 5-19).

Figure 5-19. Tensile machine.

Test standard ISO 527-5 and ISO 14129 were used to perfome the tensile testing. An extensometer was used to measure the elongation of the tensile samples.

Firstable the peel ply of the tabs on coupons were removed to get more grip on the jaws The different coupons of different mixing ratios were clamped carefully following the ISO 527-5 conditions.

Only five coupons of each same mixing ratio from 100:28 to 100:34 of each type of laminate, UD and Biax were tested to obtain its average value. These tests were performed with a 20N pre-load and with a speed testing of 2 mm/min to obtain its tensile strength, E-Modulus and elongation at break and compared to find significant variation of these properties mentioned before as function of the differents resin mixing ratio.

After tensile test UD coupons were as follows (Figure 5-20):

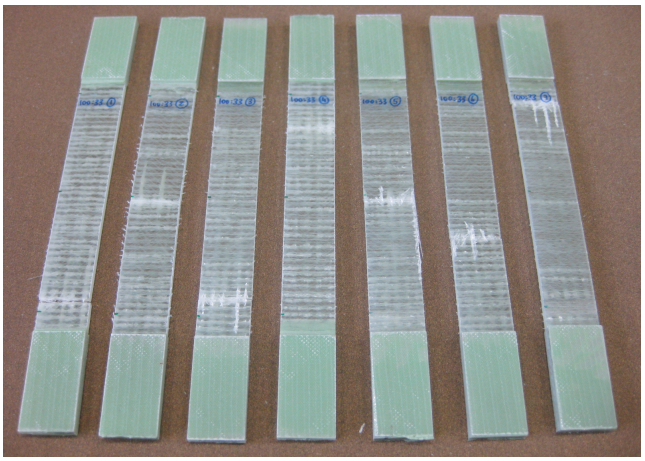

Figure 5-20. UD coupons after tensile test.

It is remarkable, that the number of stabilizer fibres on each UD coupons could not be exactly for each one. It is easy to see it after the coupon was failure. This situation might influence on the final results of the tensile test, in further way on tensile strength. In addition, the part where the coupons broke it wasn't the same for the each one.

Biax coupons were as follows after tensile test (Figure 5-21):

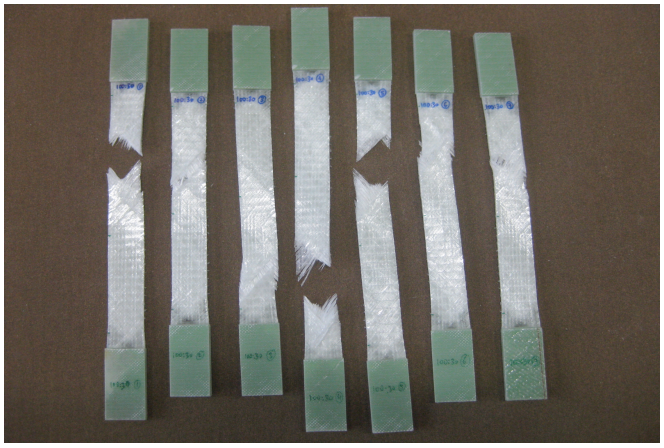

Figure 5-21. Biax coupons after tensile test.

The Biax coupons were experimented a considerable elongation after tensile tests. Some of them were totally broken up and got separated in two parts as it is possible to see at the picture. It is also remarkable that most of them experimented a slight twisting.

5.4. Thermal analysis.

The tests were carried out with an equipment calorimetry differential scanning (DSC), model Q-200 TA Instruments USA, (Figure 5-22) using nitrogen as a purge gas (50 ml / min). It sealed aluminium capsules prepared with a press for sealing, placing inside thereof an amount of sample of 5-20 mg. One sample was cut from the final laminates after Pre-cure and other after Post-cure, of each type of laminate (UD and Biax) of each mixing ratio (from 100:28 to 100:34) and analysed in DSC.

Figure 5-22. DSC model Q-200.

The Standard procedure was followed to determine the Tg:

-Equilibrate at 25 °C.
-Ramp 10 °C/ min to 200 °C.
-Isothermal for 1 min.
-Ramp 10 °C/ min to 25 °C.
-Ramp 10 °C/ min to 200 °C.
-Ramp 10 °C/ min to 25 °C.

Samples for DSC were about 10 mg, and filled into capsules of aluminum of about 40 µL of capacity (Figure 5-23).

Figure 5-23. Details of sample preparation for DSC analysis.

The amount of sample introduced into each capsule was measured on a balance (Figure 5-24).

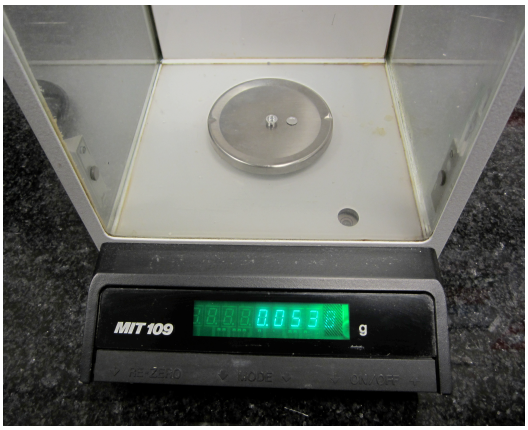

Figure 5-24. Measurement of the sample in the balance.

Best results, when testing a sample for its Tg, are obtained by using the following suggested guidelines:

- Keep the sample as thin and as flat as possible to minimize the occurrence of thermal gradients
- Start the experiment so that three minutes of 'run time' are obtained before the onset of the Tg is encountered, as this provides a better baseline response.

6. DISCUSSION OF RESULTS.

In this chapter show all the results and all the discussion.

6.1. Analyse of Tensile results

Curve graph of all datas of different mixing ratio of UD coupons obtained from tensile machine (Figure 6-1):

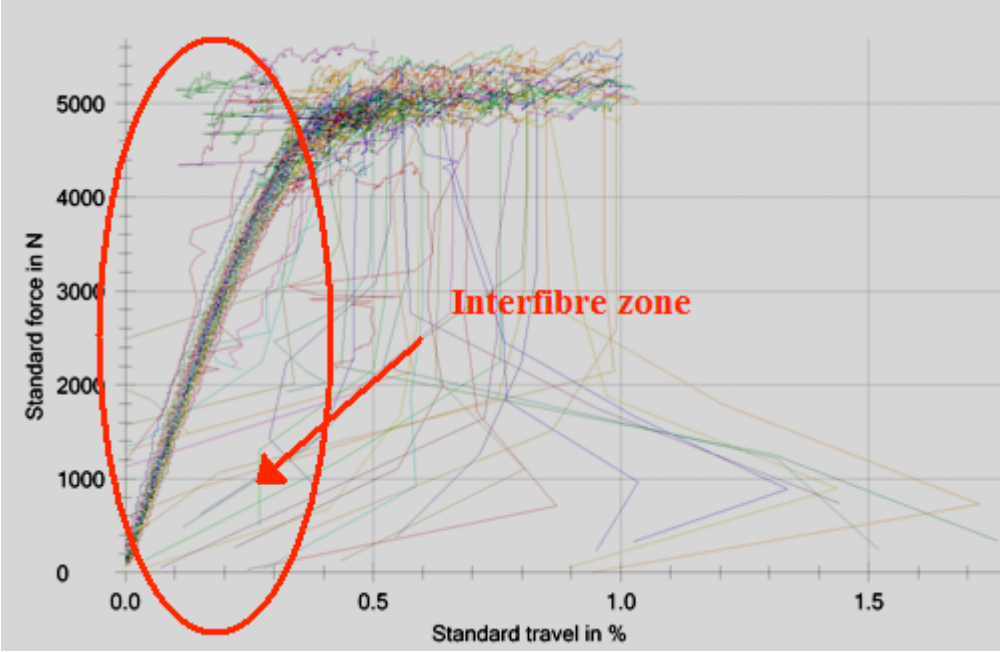

Figure 6-1. Curve graph of UD laminates.

The graph shows that there are clearly two different regions. At the beginning the curve Strength-Elongation is lineal behavior, and after a certain point, it doesn't follow any lineal formulation.

As this experiment was focused in the inter fibre (resin) properties as a function of the variation of it mixing ratio, only the first region is taken in count.

At the first region, the resin matrix, the UD fibres and the stabilizer were held together and supporting all the forces, after certain point, resin matrix crashed and got separated of UD fibres, consequence of that, the force is supported only by the stabilizer until it definitely was broken. That point is the maximum strength the resin was able to support.

Extracting each value of maximum strength when the curve changes its slope of each coupon of the same mixing ratio, and taking and average of them, and doing the same procedure for the all different mixing ratio, the following results were obtained, and are shown below in Table 6-1:

Table 6-1. A value of Strength of UD laminates.

UD	Mixing ratio						
	100:28	100:29	100:30	100:31	100:32	100:33	100:34
$\sigma_{máx}$ (MPa)	52.5	61.1	61.5	61.7	60.6	56	56.5
s (MPa)	3.27	2.51	2.41	3.71	1.46	4.07	1.71

All these datas shown in table 6-1 are contained in the Appendix chapter, and represented in the next graph, Figure 6-2.

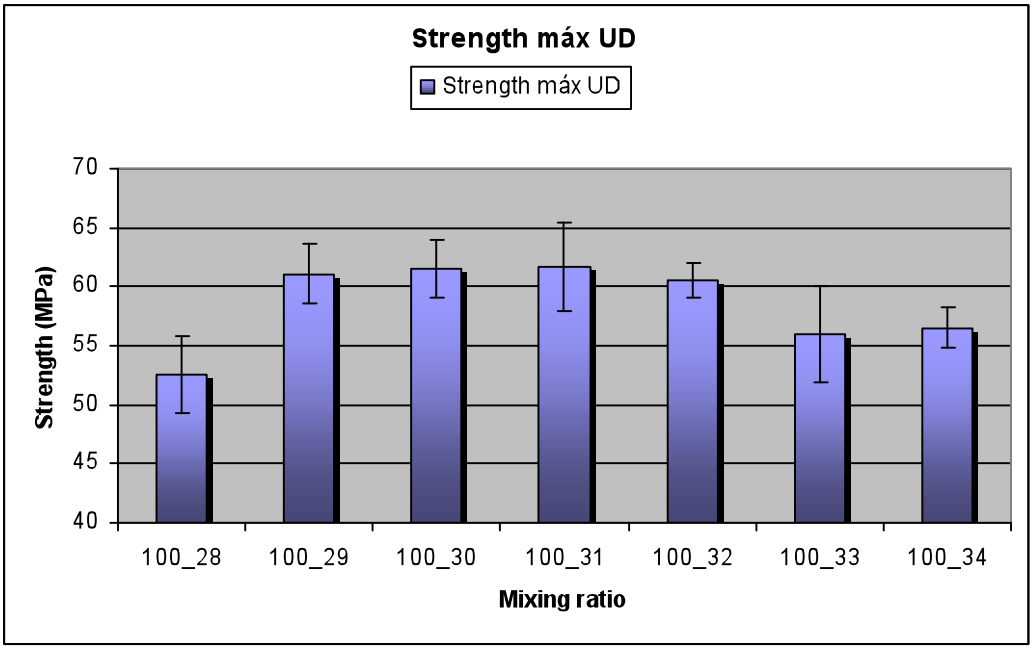

Figure 6-2. Strength of UD laminates as function of mixing ratio.

According to the results, the laminate infused with the mixing ratio 100:31, support the maximum strength of all of them. If a 2% loss in value of the maximum stress is assumed as acceptable, a range of mixing ratio could be defined from 100:29 to 100:32, where all maximum strength average were over 60 Mpa.

Out of this range, there was a considerable drop of the value of strength. The minimum value was at 100:28 mixing ratio. This situation maybe is due to a poor mixing ratio of the resin, and the resin was not fully cured.

At the other hand, excess of curing agent on mixing ratio, seems not so significant drop as a lack of it.

About the stiffness, the E modulus of this first lineal region of the experiment was obtained using the following formulation as ISO Standard 527-5 says:

$$E_{\text{mod}} = \frac{\Delta\sigma}{\Delta\varepsilon} = \frac{\sigma_{0.25\%} - \sigma_{0.05\%}}{\varepsilon_{0.25\%} - \varepsilon_{0.05\%}}$$

The final E modulus of each different mixing ratio was obtained making an average of each E modulus of the samples of the same mixing ratio. The results are shown below in Table 6-2 and represented in the following graph (Figure 6-3), these datas are contained in the Appendix chapter as well:

Table 6-2. Values of Stiffness of UD laminates.

UD	Mixing ratio						
	100:28	100:29	100:30	100:31	100:32	100:33	100:34
E_t (GPa)	16.2	16.3	16.9	17.6	16.4	16.3	15.9
s (GPa)	0.49	0.57	0.54	0.59	0.35	0.43	0.36

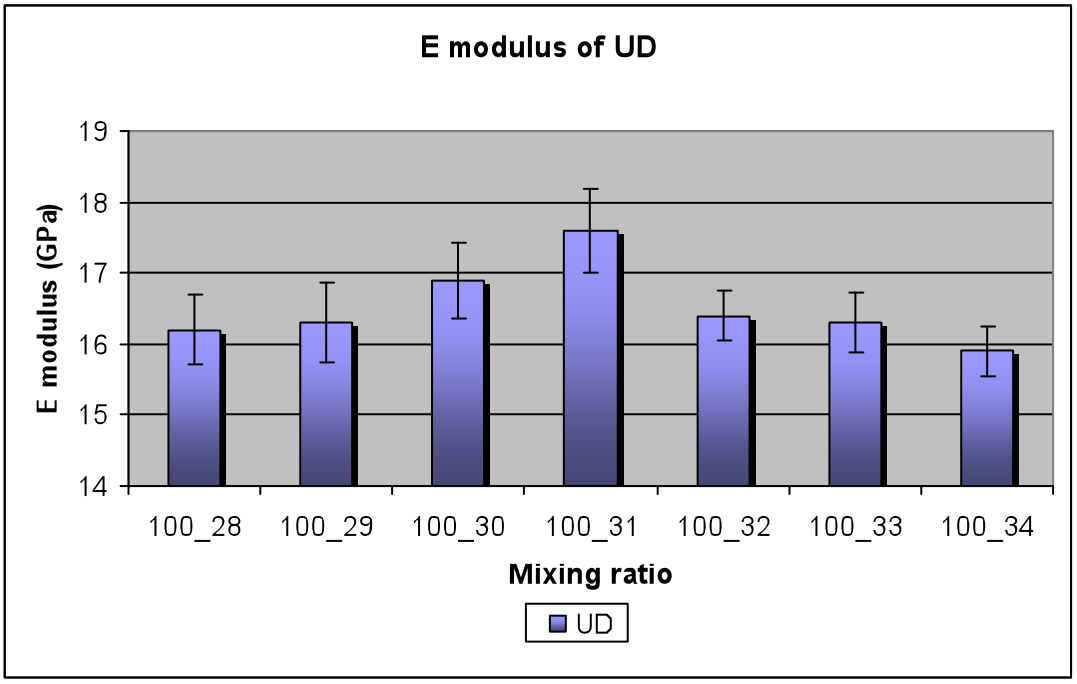

Figure 6-3. Stiffness of UD laminates as function of mixing ratio.

As it was predicted in the theory, the highest stiffness was at the 100:31 mixing ratio. The tends saw in the theory were also corroborate here, increasing or decreasing the mixing ratio around the 100:31 mixing makes lower the value of the stiffness of the laminate and make them more flexible.

The only mixing ratio that it has stiffness over 17 Mpa is the 100:31. Assuming a 5% loss as acceptable from the highest value, the range acceptable could be only from 100:30 to 100:31.

The 100:34 mixing ratio obtained the lowest value. With almost 10% of difference of lost from the highest.

As regards the elongation, extracting each value of maximum elongation when the curve changes its slope of each coupon of the same mixing ratio, and taking and average of them, and doing the same procedure for the all different mixing ratio, the following results were obtained, and are shown in Table 6-3:

Table 6-3. Values of elongation of UD laminates.

UD	Mixing ratio						
	100:28	100:29	100:30	100:31	100:32	100:33	100:34
$\varepsilon_{máx}$ (%)	0.3	0.6	0.5	0.6	0.6	0.4	0.4
S (%)	0	0.1	0.1	0.1	0.1	0.2	0

These datas are contained in the Appendix chapter and represented in the following graph, Figure 6-4.

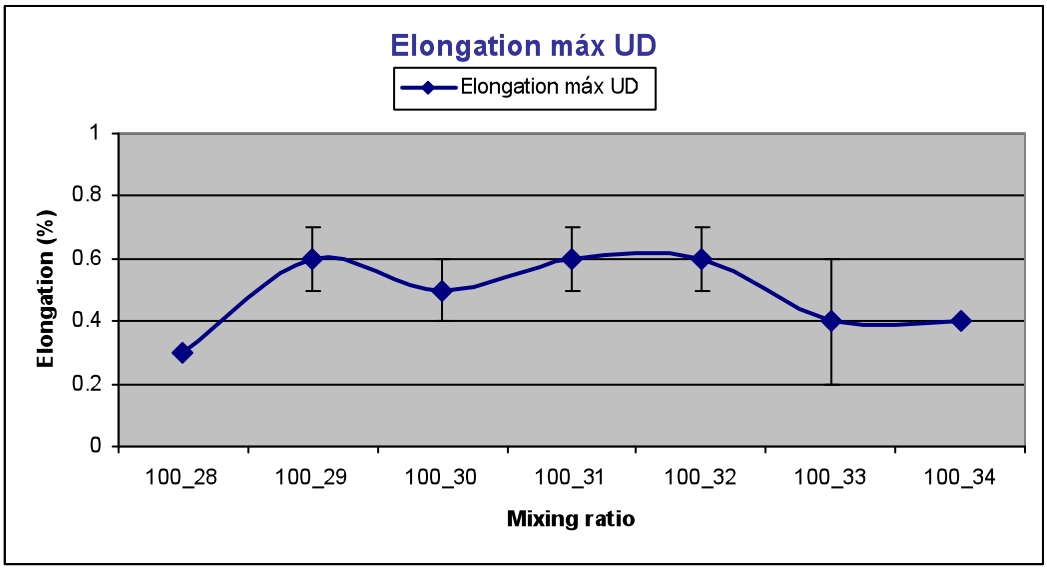

Figure 6-4. Elongation of UD laminates as function of mixing ratio.

There was not too much difference between the results regarding to the elongation. All average values obtained varied between 0.3% and 0.6%, and there were not a clearly trend.

The same procedure was applied for the Biax laminates. The Figure 6-5 shows all the datas obtained from the tensile tests:

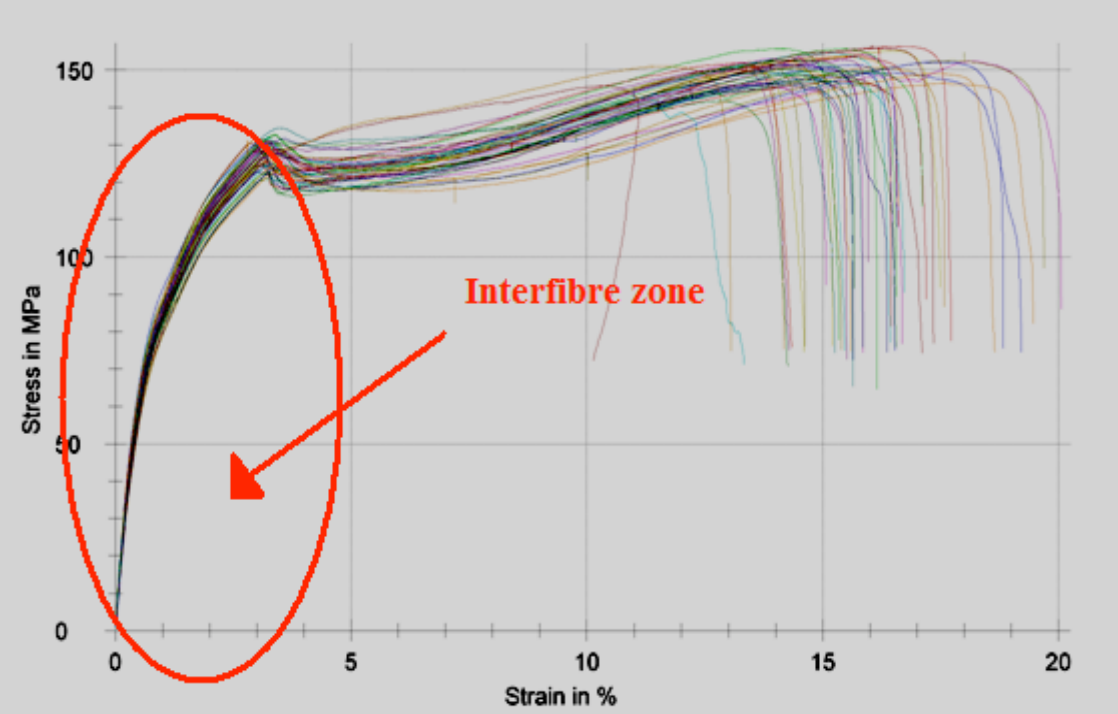

Figure 6-5. Curve graph of Biax laminates.

As it was mentioned before, this experiment was focused on inter fibre properties. Therefore, only the first region of the curve it was in taken in count. In this case it was easier to separate the two different regions, as it shows; there were a Yield Strength that it marks the final edge of the lineal and elastic part.

These averages of Yield Strength of each different coupons of each different mixing ratio were taken as Strength máx (UTS) of each different mixing ratio. The results are shown below in the Table 6-4:

Table 6-4. Values of Strength of Biax laminates.

Biax	Mixing ratio						
	100:28	100:29	100:30	100:31	100:32	100:33	100:34
$\sigma_{máx}$ (MPa)	127	128	128	138	131	127	122
s (Mpa)	1.95	0.614	1.75	6.78	0.357	2.13	1.76

It can also be shown graphically, Figure 6-6:

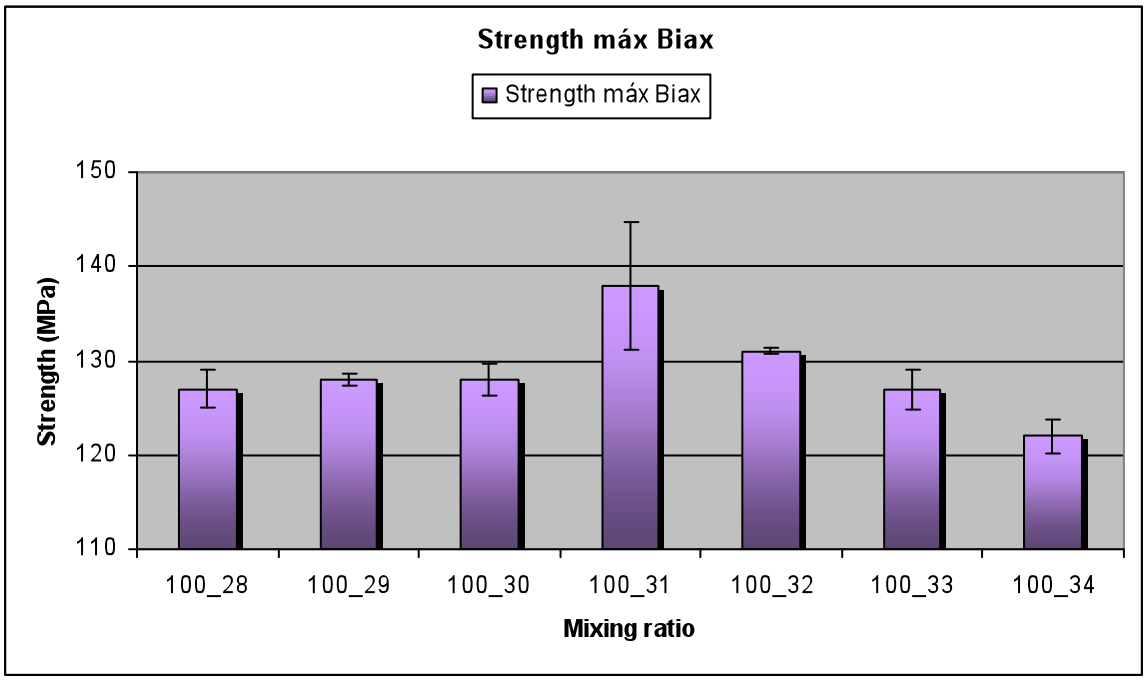

Figure 6-6. Strength of Biax laminates as function of mixing ratio.

According to the results, the laminate infused with the mixing ratio 100:31, supported the maximum strength of all of them with a value of 138 MPa.
The next highest value was 131 MPa, around a 5% less. The lowest value obtained was 122 MPa on 100:34 mixing ratio. That was almost a 12% of loss. It could be possible to see a trend, that increasing the amount curing agent in the mixing ratio over the 100:31 mixing ratio, it makes decreasing its maximum strength.

By the other hand, less amount of curing agent than 100:31 decreases the maximum strength as well, but not in staggered way as with excess of amount of curing agent. It seems that, excess or lack of curing agent, did not improve these mechanical properties.
This situation maybe is due to the amount of resin and curing agent was not in the best proportion, and it makes the laminate weaker.

If a 2% loss in value of the maximum stress is assumed as acceptable as the case of UD laminates, a range of mixing ratio could not be defined, because all the values experimented a drop higher than this percentage. Thus, the best mixing ratio regarding the strength was the 100:31.

In reference to the Stiffness of these laminates, the following results were obtained (Table 6-5).

Table 6-5. Values of Stiffness of Biax laminates.

Biax	Mixing ratio						
	100:28	100:29	100:30	100:31	100:32	100:33	100:34
E_t (MPa)	14.5	14.8	15	15.2	14.3	13.4	13.3
s (MPa)	0.72	0.50	0.58	1.05	0.20	0.17	0.38

These datas are represented in the next graph, Figure 6-7.

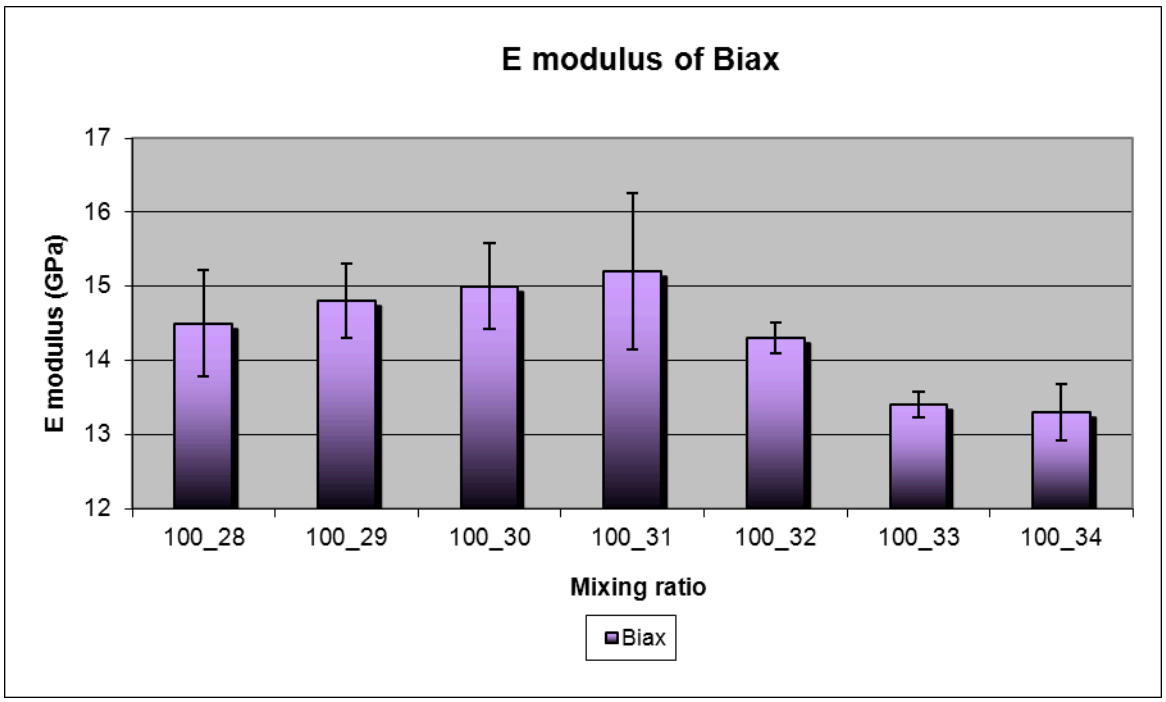

Figure 6-7. Stiffness of Biax laminates as function of mixing ratio.

As it possible to see, the highest stiffness was at 100:31 mixing ratio once again. It was the only mixing ratio that its laminate had a value of stiffness over 15 Mpa.

The stiffness of the Biax laminates in function of the different mixing ratio follows the trend seen in the theory prediction.

Increasing or decreasing the mixing ratio around the 100:31 mixing makes lower the value of the stiffness of the laminate, hence, gives them a more flexible behaviour.

Assuming a 2% loss from the highest value as acceptable, the range acceptable could be only from 100:30 to 100:31.

The 100:34 mixing ratio obtained the lowest value. With a 12.5% of difference of lost from the highest. It seems that, mixing ratio with less amount of curing agent than 100:31, keeps better the value of the stiffness than excess amount of curing agent.
Mixing ratios over the 100:31 loses its stiffness in a considerable way.

Regarding the elongation, the maximum elongation was obtained taking and average of each value of maximum elongation of each coupon of the same mixing ratio, at the point of the graphic curve, where it gives the maximum strength.

Doing the same procedure for the all different mixing ratio, the following results were obtained and shown in Table 6-6:

Table 6-6. Values of elongation of Biax laminates.

Biax	Mixing ratio						
	100:28	100:29	100:30	100:31	100:32	100:33	100:34
$\varepsilon_{máx}$ (%)	3.3	3.2	3.3	3.3	3.2	3.3	3.4
s (%)	0.1	0	0.1	0.3	0.1	0.3	0.2

These datas are contained in the Appendix and represented in the following graph, Figure 6-8.

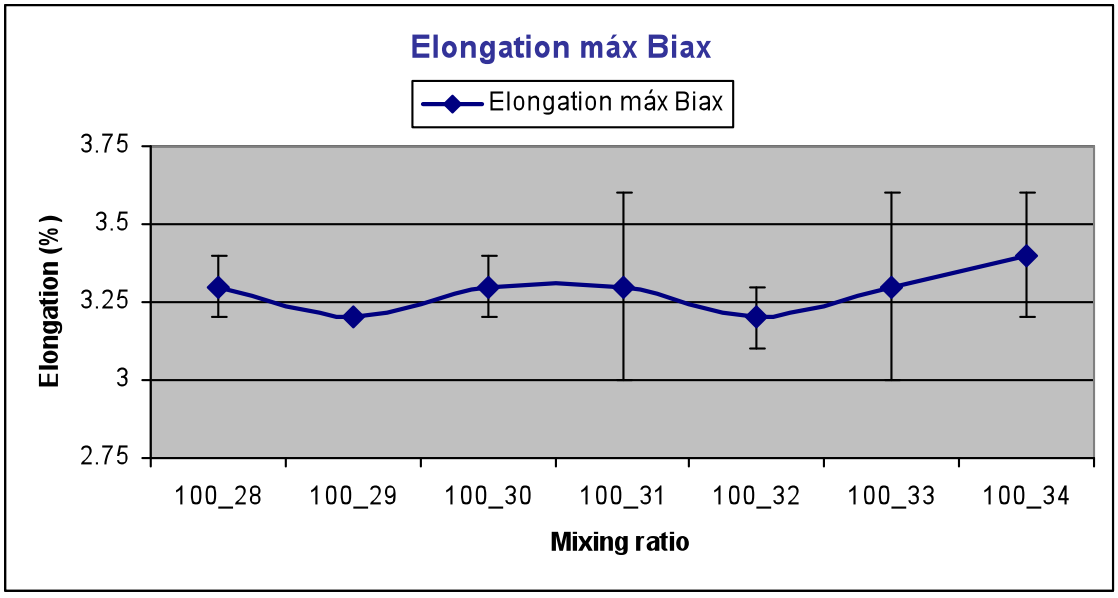

Figure 6-8. Elongation of Biax laminates as function of mixing ratio.

It seems, that variating the mixing ratio of the resin, does not give so much different among the elongation. All different ratios, has a similar elastic behavior.

The 100:34 mixing ratio was the least stiffness, so, more flexible, and also, with the most large elongation.

6.2. Analyse of DSC.

The following results of Tg temperature were obtained from the DSC machine
Concerning to the UD laminates, the results are shown below in Table 6-7:

Table 6-7. Statistics about Tg of different mixing ratio of UD laminates.

		UD			
		Tg (°C)			
		Pre Cure		Post Cure	
		I run	II run	I run	II run
RATIO	100/28	65.73	85.44	78.32	87.34
	100/29	70.42	89.76	81.84	87.33
	100/30	69.92	91.02	86.32	95.06
	100/31	68.48	91.44	82.12	93.72
	100/32	70.97	91.03	82.92	90.16
	100/33	67.49	86.23	83.91	87.99
	100/34	69.65	83.11	79.99	84.22

These data can be represented in the graph below, Figure 6-9.

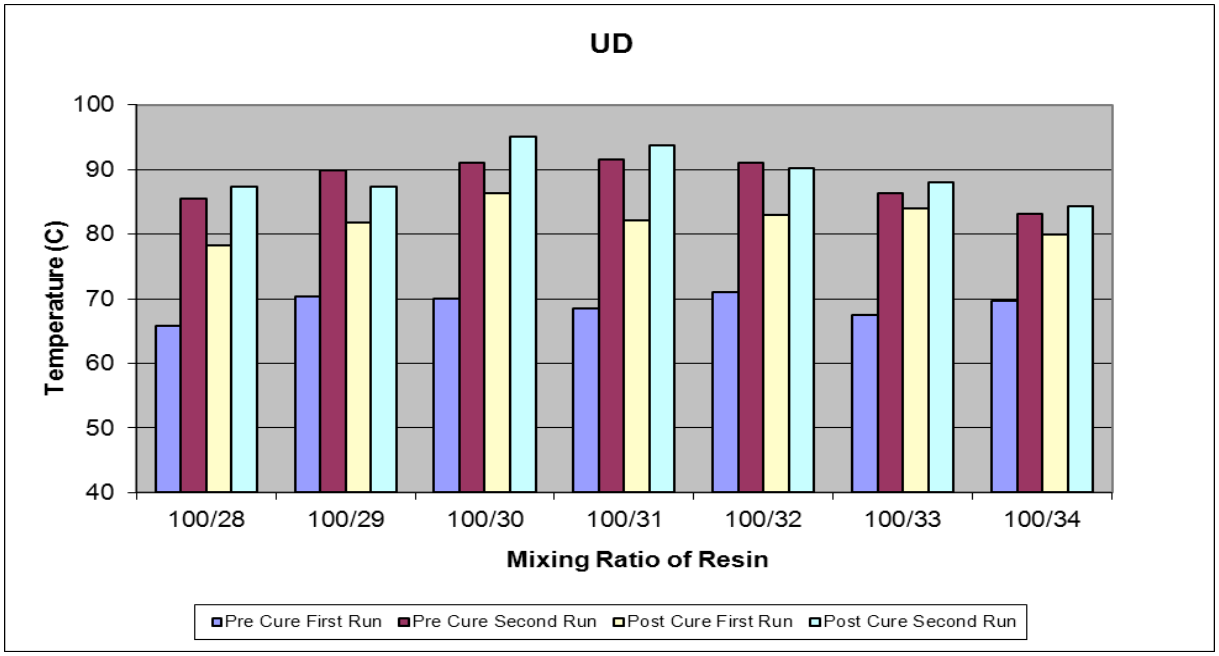

Figure 6-9. Tg temperature of UD laminates.

It was appreciate that the processing of Post cure increased the Tg temperature of the laminate and second run gets always a higher Tg than first run as well, no matter which mixing ratio of resin was. For the final analysis, only the Tg temperature of Post-cure is important and taken into account.

The highest Tg obtained was 95,06°C in Post-cure of 100:30 mixing ratio. Until now, the 100:31 mixing ratio was obtained the best values in terms of strength and stiffness.
In relation to this property, there was only a 4,2°C of difference respect to the highest.
This is only a 1,4% of variation of Tg between 100:30 and 100:31 mixing ratio.

If a safe tolerance is assuming as the mixing ratios that have Tg's over 90°C, a range of mixing ratio could be from 100:30 to 100:32. Out of this, the rest of Tg temperatures of the other mixing ratio are lower.

Regarding to the Tg temperature of Biax laminates (Table 6-8):

Table 6-8. Statistics of Tg of different mixing ratio of Biax laminates.

		BIAX			
		Tg (°C)			
		Pre Cure		Post Cure	
		I run	II run	I run	II run
RATIO	100/28	66.83	85.57	79.93	85.06
	100/29	71.71	92.04	82.38	89.47
	100/30	76.19	96.43	85.85	95.18
	100/31	79.55	94.41	84.34	93.72
	100/32	74.06	92.72	82.63	92.84
	100/33	72.54	89.52	81.33	90.39
	100/34	67.02	84.6	78.44	85.21

These data can be represented in the graph below, Figure 6-10.

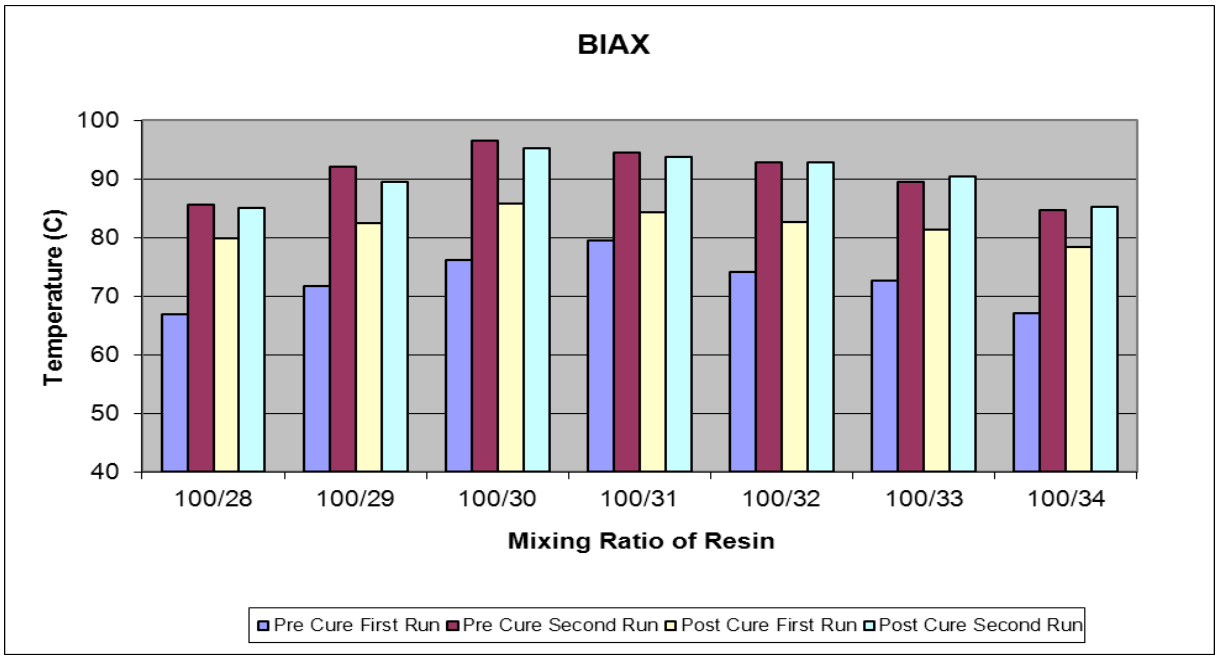

Figure 6-10. Tg temperature of Biax laminates.

As it was shown in the UD laminates case, after Post-cure processing, Tg temperature of Biax laminates, were increased from Pre-cure, and also second run gets higher Tg than first run as well, no matter which mixing ratio of resin was.

Based only on Tg temperature of Post-cure and second run for try to determine a safe tolerance, and assuming as acceptable Tg temperature over 90°C, only mixing ratios from 100:30 to 100:33 could be taken in account. The highest Tg obtained was 95,18°C in 100:30 mixing ratio. Comparing its Tg temperature against the 100:31 mixing ratio, which it was obtained the best values in terms of strength and stiffness until now, there was 1,46°C of difference, a 1,53% between them.

In relation to this property, the maximum difference of grades of Tg temperature between highest and lowest was 7,4°C, which is an 8,6% of variation.

6.3. Comparation with the theorical prevision.

According to the datas of theorical prediction of E modulus and the experimental E modulus in function of the mixing ratio obtained, it was possible to compare the results. In case of UD laminates (Table 6-9):

Table 6-9.Comparation of theorist and experimental E modulus. UD laminates.

E (GPa)	Mixing ratio						
	100_28	100_29	100_30	100_31	100_32	100_33	100_34
UD Theorist	17.12	18.50	19.76	21.05	20.22	19.34	19.24
UD Experimental	16.2	16.3	16.9	17.6	16.4	16.3	15.9

The graph below (Figure 6-11) shows this comparison.

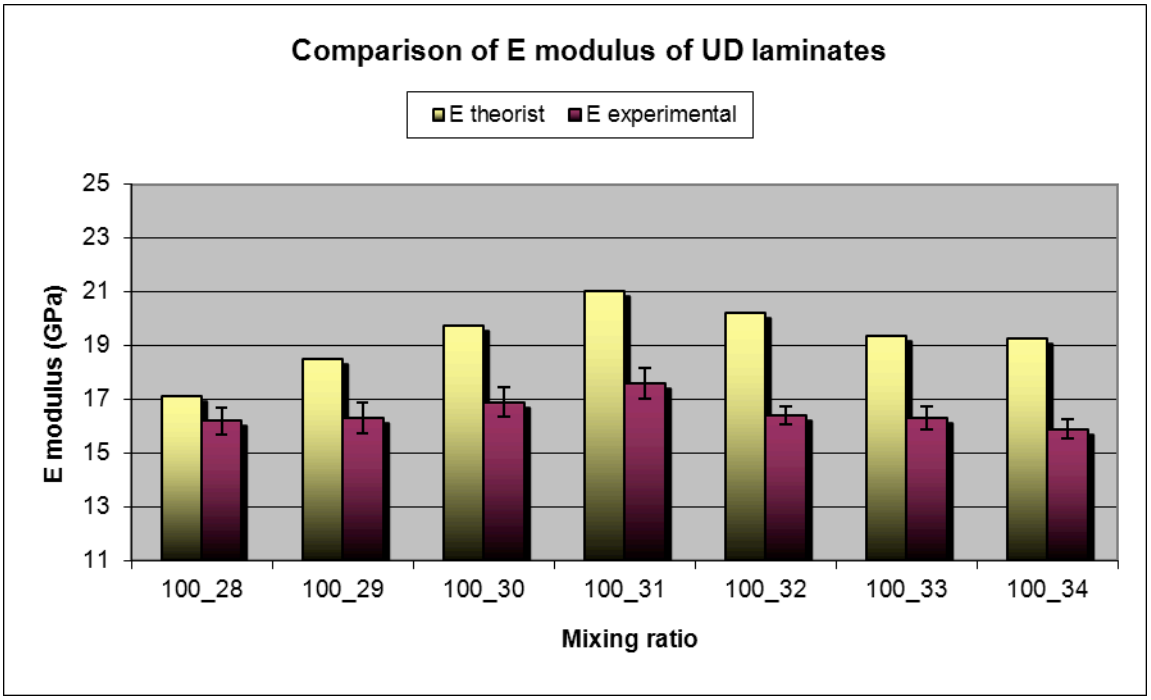

Figure 6-11. Graph of E theorist and experimental modulus of UD laminates.

As it can see, the data obtained experimentally are lower than theoretically expected. The theory predicted that varying the mixing ratio, the stiffness would be affected quite steeply, pretty much more with the mixing ratios under 100:31 ratio, but the experimental part shows no significant variations. In theoretically expected there was almost an 18.7% of difference between the highest E modulus and the lowest, but only a 9.7% was obtained by the experimental way.

Despite of the difference of the results obtained from the two ways, both can be concluded that the best mixing ratio regarding the stiffness is the 100:31 mixing ratio.
Even with the mixing ratio with the highest E modulus, which occurs in the 100:31 ratio, the difference with the theoretical value obtained is aprox an 18%.
In this case, it is possible to conclude that the theory prediction does not predict an approximate way all entire range of mixing ratios, such as it happens on 100:31 or 100:32 mixing ratios, which there are a significant difference of values between them, although in some exceptional case, very close value is obtained between the theoretical and experimental, as the case of 100:28 mixing ratio.
Regarding to Biax laminates (Table 6-10):

Table 6-10. Comparation of theorist and experimental E modulus. Biax laminates.

E (GPa)	Mixing ratio						
	100_28	100_29	100_30	100_31	100_32	100_33	100_34
Biax Theorist	16.94	18.35	19.63	20.95	20.10	19.20	19.10
Biax Experiment	14.5	14.8	15	15.2	14.3	13.4	13.3

The graph below (Figure 6-12) shows this comparison.

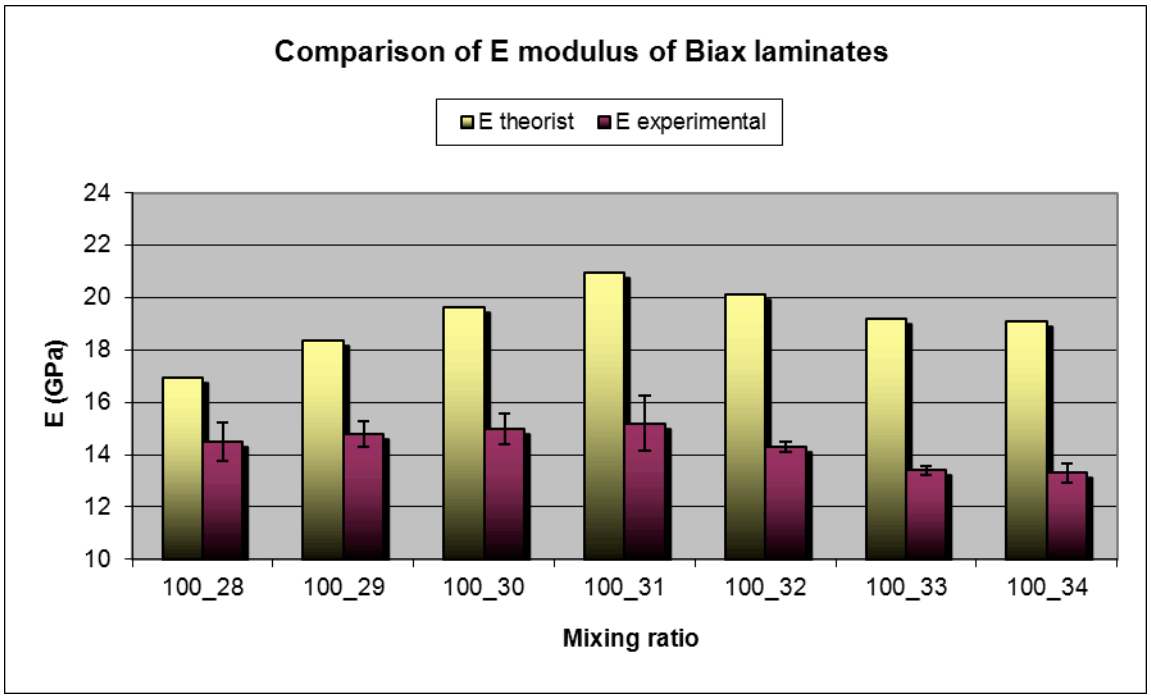

Figure 6-12. Graph of E theorist and experimental modulus of Biax laminates.

In this case also, the theoretically obtained values were significantly higher than those predicted experimentally. However, both ways of estimation of E modulus concluded that 100:31 mixing ratio is the best with reference to the stiffness.

Theory estimation may not predict accurately the values that should take the form E modulus, but however, shows that both methods, theoretical and experimental, agree in showing that the trend is the same. The value of E modulus decreases around the 100:31 mixing ratio. However, in this case the experimental way shown that the descent of E modulus is a more pronounced in ratios above 100:31 than below it, and that is opposite to the theoretically expected.

After tensile experiments, the results obtained are shown below (Table 6-11):

Table 6-11. Comparation of UD and Biax experimental E modulus.

E (GPa)	Mixing ratio						
	100:28	100:29	100:30	100:31	100:32	100:33	100:34
UD	16.2	16.3	16.9	17.6	16.4	16.3	15.9
Biax	14.5	14.8	15	15.2	14.3	13.4	13.3

The graph below (Figure 6-13) shows this comparison.

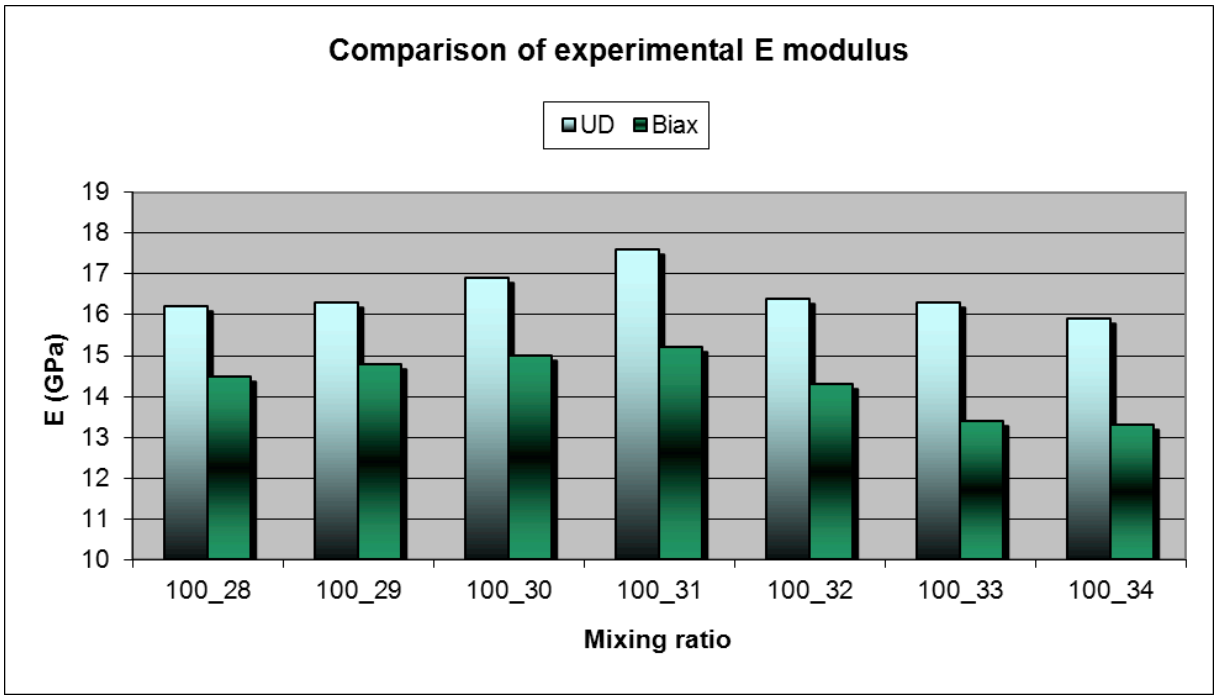

Figure 6-13. Graph of UD and Biax experimental E modulus.

The behavior in both composite laminates in terms of mechanical properties as E modulus in function of the variation of the mixture of resin and curing agent followed a similar trend. The only difference is that the values obtained in the case of the UD laminates were larger than Biax laminates.

The highest E modulus in both kinds of laminates was obtained with the 100:31 mixing ratio, so that provides them a more stiffness than the other ones.

7. CONCLUSIONS.

From the results discussed in the present study, the conclusions that can be drawn are presented in this chapter.

Two different kind of laminates (UD and Biax), were infused by the Vacuum process with seven different resin mixing ratio each one, and compared their mechanical properties in the project.

Analyzing each property in more detail, it is possible to extract the following conclusions:

- Strength:
    1. UD Laminates.

    There were no huge differences between all different results of the strength of UD laminates obtained from the tensile tests. There was no significant change in mechanical properties by varying the mixing ratio around the 100:31 mixing ratio. In fact, if the amount of curing agent is increased or decreased over a unit of the 100:31 mixing ratio, the loss of strength is only a 2%.

    2. Biax Laminates.

    The variation in the ratio of the resin mixture, the loss of strength was more significant than in the case of the UD laminates. If the proportion of the mixture is modified one unit around 100:31, loss of strength is about 5%.

- Stiffness:

    Both kind of composite laminates obtained similar datas in relation to the stiffness. Best values were obtained after testing was with the 100:31 mixing ratio. Although varying the proportion around this mixture mentioned, the loss of stiffness is around a 6% or 7%.

In both types of laminates, the loss of stiffness was less significant for mixing ratios lower than 100:31 than for ratios above this. So, in case the 100:31 mixing ratio is not possible to achieved, it is better a lack of curing agent in the mixture than an excess of it.

- Theory prediction of the E modulus:

    The theory prediction of the E modulus used in this investigation was not quite successful as it was expected. The results of that were not accurate, but it was helpful to get a better knowledge about this mechanical property behaviour in function of the mixing ratio of the resin before start the experiment. This theory and the experimental have confirmed that the 100:31 mixing ratio provides the best stiffness and strength.

That theory predicting of E modulus is not recommended for next further investigations, due to it does not provides reliable datas closes to the experimental datas, is only valid for get an idea or trend behavior of this mechanical property.

- Strain:

All samples were an average of around 0.6% elongation in the case of UD laminates and around 3.25% in the case of Biax laminates. As to the elongation undergone by the different films with different mixing ratios of resin, it is not possible to determine an accurate conclusion. The only conclusion that can be confirmed is that Biax laminates have a more elastic behavior, but this is perhaps due to the arrangement of glass fibers.

- Glass temperature transition (Tg):

The best choice for this property is the 100:30 mixing ratio in both types of composite laminates, as its highest value obtained in this ratio showed. In these case, the Tg temperature of 100:31 mixing ratio was lower than the 100:30 ratio. The difference between them was only 1.4% in the case of UD laminates and a 1.53% in the Biax. It is not a significant variation. Although the 100:30 mixing ratio provides the best Tg temperature, the Tg temperature of 100:31 mixing ratio is considered acceptable.

The main purpose of this project, was try to find out at what point we see significant changes in the mechanical properties due to changes in the mixing ratio of the resin and try to establish a range of mixing ratio with a safe tolerance of these mechanical properties.

The range of mixing ratio could be from 100:30 to 100:31 for both kind of laminates, due to the 100:31 provides to highest strength and the 100:30 the highest Tg. The difference between both mixing ratio on Strength and Stiffness are at most a 6% and about the Tg are only around 1.5%.

Due to the small variation in the values obtained, it can be concluded that a deviation from an ideal mixing ratio is not so significant in the end result of these properties studied. Actually, these mechanical properties are mainly determined by distributed fibers in the composite material instead of the resin/hardener mixture.

8. RECOMMENDATION AND FURTHER STUDY.

Some recommendations could be taken under consideration for develop this investigation and get a more reliable datas.

It would be more appropriate for future research to expand the range of mixing ratios to better see the variation of these properties.

As for the theoretical calculation of the modulus E, it has assumed the density of the mixture based on the ratio 100:31. It could better adjust the calculations for each mixing ratio to get more precision to compare to the experimental results.

Regarding to the measurement of the Tg, it was used a single sample of each laminate and analysed on DSC. It could be better take more samples of each sheet in different parts of it, and establish an average due to the temperature of the laminate in the oven,

might not been the same at the entire surface, and consequently, the value of Tg may vary.

Since the goal is to investigate the variating of the mechanical properties as function of different the mixing ratios of the resin, there is still quite some work that can be carried out in further study.

The basic material properties and related knowledge of the mixing ratio of resin used in composites laminates have been achieved in this project, but it could be possible to complement with extra aspects as analysis of released heat (Enthalpy) by DSC, damage threshold, change in viscous behaviour and as a result the infusion properties.

Another deeper study could be to get a better knowledge about what might happen chemically or what will happen to different mixing ratio's with respect to the time because, this project was only focused on static mechanical properties.

9. BIBLIOGRAPHY.

[1]. www.suzlon.com

[2]. Chalaye, H “Los materiales compuestos dinamismo e innovación” 2002 .Le 4 Pages des Statistiques Industrielles Nº 158.

[3]. F. P. Carballo, J. C. Delgado, J. C. Marin Vallejo, "Introducción al análisis y diseño con materiales compuestos" Escuela superior de ingenieros industriales. Universidad de Sevilla, Grupo de Elasticidad y Resistencia de materiales. Sevilla, 2006.

[4]. Swanson, R.W., Introduction to Design and Analysis with Advance Composite Materials, Prentice Hall, NJ, 1997.

[5]. Mallick, P.K., Fiber-Reinforced Composites, Marcel Dekker, Inc., New York, 1988.

[6]. www.energias-renovables.com

[7]. Joseph A.Grande, Wind power blades energize composites manufacturing. Plastics technology. October 2008.

[8]. Skramstad, J.D. “Evaluation of Hand Lay-Up and Resin Transfer Molding in Composite Wind Turbine Blade Manufacturing,” Master’s Thesis in Mechanical Engineering, Montana State University-Bozeman, August 1999.

[9]. Mandell, J.F., Sutherland, H.J. and Samborsky, D.D., “Effects of Materials Parameters and Design Details on the Fatigue of Composite Materials for Wind Turbine Blades,” Proceedings of 1999 European Wind Energy Conference and Exhibition, Nice, France, 1-5 March, 1999, WIP-Munich, Germany, 1999.

[10]. Orozco, R., “Effects of Toughened Matrix Resins on Composite Materials for Wind Turbine Blades,” Master’s Thesis in Chemical Engineering, Montana State University-Bozeman, July 1999.

[11]. Li, M., “Temperature and Moisture Effects on Composite Materials for Wind Turbine Blades,” Master’s Thesis in Chemical Engineering, Montana State University-Bozeman, March 2000.

[12]. Rosen, S. L., Fundamental Principles of Polymeric Materials, John Wiley & Sons, New York, 1993.

[13]. R.H. Sonneborn, A.G.H. Dietz, and A.S. Heyser, Fiberglass Reinforced Plastics, Reinhold Publishing Corporation, New York, 1954.

[14]. I.E. Muskat, Method of Molding, U.S. Patent 2,495,640, 1945.

[15]. J.R.M. d'Almeida & S.N. Monteiro. "The Effect of the Resin / Hardener Ratio on the Compressive Behavior of an Epoxy System", Polymer Testing, Volume 15, Issue 4, 1996, Pages 329-339.

[16]. A. Foyet, T.H. Wu, L. van der Ven, A. Kodentsov, G. de With, and R. van Benthem. "Influence of mixing ratio on the permeability of water and the corrosion performance of epoxy/amine coated un-pretreated Al-2024 evaluated by impedance spectroscopy", Progress in Organic Coatings, Volume 64, Issues 2-3, February 2009, Pages 138-141.

[17]. H.L. Liu, A. Deng, and J. Chu. "Effect of different mixing ratios of polystyrene pre-puff beads and cement on the mechanical behaviour of lightweight fill", Geotextiles and Geomenbranes, Volume 24, Issue 6, December 2006, Pages 331-338.

[18]. Derek Hull: An introduction to composite materials, Cambridge Solid Stage Science Series, 1981.

[19]. Pascault, J.P., et al., Thermosetting polymers. 2002, New York [etc.] :: Marcel Dekker.

[20]. Turi, E.A., ed. Thermal characterization of polymeric materials. 2nd ed ed. 1997, Academic Press: San Diego.

[21]. Lee, H., and Neville, K., "Handbook of Epoxy Resins", McGraw-Hill, Inc., New York, 1975.

[22]. Saunders, K. J., "Organic Polymer Chemistry", Chapman &Hall, New York, p. 412-435, 2 nd ed., 1988.

[23]. Fernández-Francos, X., et al., A new strategy for controlling shrinkage of DGEBA resins cured by cationic copolymerization with hydroxyl-terminated hyperbranched polymers and ytterbium triflate as an initiator. Journal of Applied Polymer Science, 2009. 111(6): p. 2822-2929.

[24]. Pascault, J.P., et al., Thermosetting polymers. 2002, New York [etc.] :: Marcel Dekker.

[25]. Mika, T. F. and Bauer, R. S. "Curing Agents and Modifiers" in Epoxy Resins Chemistry and Technology, May, C. A., 2 nd ed., Marcel Dekker, Inc., New York, p. 465-480, 1988.

[26]. Tanaka, Y., and Bauer, R. S., "Curing Reactions", in Epoxy Resins Chemistry and Technology, May, C. A., 2 nd ed., Marcel Dekker, Inc., New York, p. 285-295, 1988.

[27]. Katz, D.; Tobolsky, A.V., Polymer, v. 4, p. 417-421, 1963.

[28]. Mel Schwartz. "Composite materials Handbook" 2nd ed.1992 Ed. Mc Graw-hill.

[29]. "Engineered materials handbook, composites" vol.1 ASM international 1987.

[30]. A. Miravete. “Materiales compuestos I” 2000 Ed.Reverté.

[31]. D. Gay, S. V.Hoa, S. W. Tsai. “Composite materials desing and applications” 2003 Crc Press.

[32]. D. Hull, T. W. Clyne, “An Introduction to Composite Materials”, Cambridge Solid State Science Series, 1996.

[33]. University of Cambridge department of Engineering <www-materials.eng.cam.ac.uk>.

[34]. A. S. for Metals, Metals Handbook vol 8 - Mechanical testing and evalution. American Society for Metals, 2000.

[35]. Fernandez-Francos, X., Curat tèrmic i fotocurat de resines epoxi per al control químic de la contracció i millora de la degradabilitat, in Laboratori de Termodinàmica, ETSEIB. 2009, Universitat Politècnica de Catalunya: Barcelona.

[36]. Composites Course University of Twente 2008-2009, Eng.& Tech. Constituents and manufacturing techniques. Laurent Warnet & Remko Akkerman.

[37]. Halpin, J.C., and S.W. Tsai: Effects of Environmental Factors on Composite Materials, AFML-TR 67-423, June, 1969.

[38]. M. Labordus, M. Pieters, A. Hoebergen, and J. Soderlund, The Causes of Voids in Laminates Made with Vacuum Injection, Proc. 20th International SAMPE Europe Conference of the Society for the Advancement of Material and Process Engineering, April 1999, p 433–441.

[39]. M. Labordus, A. Hoebergen, J. Soderlund, and T. Astrom, Avoiding Voids by Creating Bubbles, Degassing of Resin for the Vacuum Injection Process, Proc. 21st International SAMPE Europe Conference of the Society for the Advancement of Material and Process Engineering, April 2000, p 47– 58.

10. LIST OF FIGURES.

Figure 1-1. Suzlon wind turbine.... 8
Figure 2-1. World Market Situation of composites by geography (2002).... 10
Figure 2-2. Track composites market in Europe, by geographical area (2002).... 11
Figure 2-3. Annual evolution of the installed wind power capacity by 2008 and their numbers.... 12
Figure 2-4. Wind Turbine Manufacturers in the global market.... 12
Figure 2-5. Generic Blade cross section.... 13
Figure 4-1. Stress-strain diagrams of carbon fibers, glass and Kevlar 49.... 18
Figure 4-2. Representation of curing a thermosetting polymer.... 20
Figure 4-3. Stress-strain diagram of thermosetting resins.... 21
Figure 4-4. Scheme of the reaction of bisphenol A with epichlorohydrin to form DGBEA.... 21
Figure 4-5. Schematic molecular structure of the epoxy group.... 22
Figure 4-6. Sample of orientation of the different layers in a composite laminate.... 27
Figure 4-7. Diagram of a simple Vacuum infusion setup.... 28
Figure 4-8. Stress - Strain curve.... 30
Figure 4-9. Measurement of Tg on DSC machine.... 31
Figure 4-10. Diagram of assumptions for micromechanical analysis.... 33
Figure 4-11. Representative matrix and fibre volume elements.... 33
Figure 4-12. Experiment for the transverse modulus (Reus model).... 34
Figure 4-13. 1D Hooke's law.... 35
Figure 4-14. Parallel-series model for the transverse modulus.... 36
Figure 4-15. Dimensions of UD coupon.... 38
Figure 4-16. Scheme of UD coupon under tensile test.... 39
Figure 4-17. Resin coupon of different mixing ratio.... 40
Figure 4-18. Variation of the E modulus vs resin mixing ratio in UD laminates.... 41
Figure 4-19. Dimensions of Biax coupon.... 42
Figure 4-20. Scheme of Superposition principle of Biax coupon under tensile test.... 43
Figure 4-21. Variation of the E modulus vs resin mixing ratio in Biax laminates.... 44
Figure 4-22. Comparison of the theorist E modulus of UD and Biax laminates.... 45
Figure 5-1. a) Biax fabric. b) UD fabric.... 46
Figure 5-2. Resin and Hardener from DOW cheminal company.... 47
Figure 5-3. Layup of fabrics.... 48
Figure 5-4. Process of laminate fabrication.... 48
Figure 5-5. Cross section view of laminate build-up.... 49
Figure 5-6. Build up before infusion starts.... 49
Figure 5-7. Desiccator and degassing process.... 51
Figure 5-8. Degassing of resin process.... 52
Figure 5-9. a) Start infusion UD laminate b) End infusion UD laminate.... 52
Figure 5-10. a) Start infusion of Biax laminate b) End infusion of Biax laminate.... 52
Figure 5-11. Graph of Pre-Cure of laminates.... 53
Figure 5-12. Graph of Post-Cure process of laminates.... 53
Figure 5-13. Sample of UD laminate.... 54
Figure 5-14. Sample of Biax laminate.... 54
Figure 5-15. Dimensions of UD coupon.... 55

Figure 5-16. UD coupons before tensile tests. 55
Figure 5-17. Dimensions of Biax coupons..... 56
Figure 5-18. Biax coupons before tensile test. 56
Figure 5-19. Tensile machine. 57
Figure 5-20. UD coupons after tensile test. 58
Figure 5-21. Biax coupons after tensile test..... 58
Figure 5-22. DSC model Q-200..... 59
Figure 5-23. Details of sample preparation for DSC analysis. 59
Figure 5-24. Measurement of the sample in the balance. 60
Figure 6-1. Curve graph of UD laminates. 61
Figure 6-2. Strength of UD laminates as function of mixing ratio. 62
Figure 6-3. Stiffness of UD laminates as function of mixing ratio..... 63
Figure 6-4. Elongation of UD laminates as function of mixing ratio..... 64
Figure 6-5. Curve graph of Biax laminates. 65
Figure 6-6. Strength of Biax laminates as function of mixing ratio..... 66
Figure 6-7. Stiffness of Biax laminates as function of mixing ratio. 67
Figure 6-8. Elongation of Biax laminates as function of mixing ratio. 68
Figure 6-9. Tg temperature of UD laminates. 69
Figure 6-10. Tg temperature of Biax laminates..... 70
Figure 6-11. Graph of E theorist and experimental modulus of UD laminates. 71
Figure 6-12. Graph of E theorist and experimental modulus of Biax laminates. 72
Figure 6-13. Graph of UD and Biax experimental E modulus. 73
Figure 12-1. Curve graph of UD laminates. 83
Figure 12-2. a) Failure mixing ratio 100:28UD. b) Failure mixing ratio 100:29UD. 89
Figure 12-3. d) Failure mixing ratio 100:31UD e) Failure mixing ratio 100:32UD 89
Figure 12-4 Curve graph of Biax laminates. 90
Figure 12-5. a) Failure mixing ratio 100:28Biax b) Failure mixing ratio 100:29Biax..... 100
Figure 12-6. d) Failure mixing ratio 100:31Biax e) Failure mixing ratio 100:32Biax..... 100
Figure 12-7. Curve graph of DOW resin coupons. 103
Figure 12-8. Tg of mixing ratio 100:28. UD Laminate. Post cure. 104
Figure 12-9. Tg of mixing ratio 100:29. UD Laminate. Post cure. 104
Figure 12-10. Tg of mixing ratio 100:30. UD Laminate. Post cure. 105
Figure 12-11. Tg of mixing ratio 100:31. UD Laminate. Post cure. 105
Figure 12-12. Tg of mixing ratio 100:32. UD Laminate. Post cure. 106
Figure 12-13. Tg of mixing ratio 100:33. UD Laminate. Post cure. 106
Figure 12-14. Tg of mixing ratio 100:34. UD Laminate. Post cure. 107
Figure 12-15. Tg of mixing ratio 100:28. Biax Laminate. Post cure. 108
Figure 12-16. Tg of mixing ratio 100:29. Biax Laminate. Post cure. 108
Figure 12-17. Tg of mixing ratio 100:30. Biax Laminate. Post cure. 109
Figure 12-18. Tg of mixing ratio 100:31. Biax Laminate. Post cure. 109
Figure 12-19. Tg of mixing ratio 100:32. Biax Laminate. Post cure. 110
Figure 12-20. Tg of mixing ratio 100:33. Biax Laminate. Post cure. 110
Figure 12-21. Tg of mixing ratio 100:34. Biax Laminate. Post cure. 111

11. LIST OF TABLES.

Table 4-1. Composition of glass used for fibre manufacture (all values in weight %). 17
Table 4-2. Properties of the fibres of carbon, glass, kevlar49 at 20ºC. 18
Table 4-3. Properties of Epoxy matrix. 20
Table 4-4. Type 1 curing agents and their chemical structures. 23
Table 4-5. Values of E_m of different resin mixing ratios. 40
Table 4-6. Values of the E modulus as function of different resin mixing ratios. 40
Table 4-7. Values of E_m of different resin mixing ratio..... 44
Table 4-8. Values of the E modulus as function of different resin mixing ratio. 44
Table 4-9. Values of the E modulus of UD and Biax laminates as function of mixing ratio. 45
Table 5-1. Properties of the E-Glass from KUSH company. 46
Table 5-2. Properties of Dow Resin and Hardener. 47
Table 5-3. Amount of resin and curing agent of each different mixing ratio. 50
Table 6-1. A value of Strength of UD laminates. 62
Table 6-2. Values of Stiffness of UD laminates. 63
Table 6-3. Values of elongation of UD laminates. 64
Table 6-4. Values of Strength of Biax laminates. 65
Table 6-5. Values of Stiffness of Biax laminates. 67
Table 6-6. Values of elongation of Biax laminates. 68
Table 6-7. Statistics about Tg of different mixing ratio of UD laminates. 69
Table 6-8. Statistics of Tg of different mixing ratio of Biax laminates. 70
Table 6-9.Comparation of theorist and experimental E modulus. UD laminates. 71
Table 6-10. Comparation of theorist and experimental E modulus. Biax laminates. 72
Table 6-11. Comparation of UD and Biax experimental E modulus. 73
Table 12-1. Statistics of mixing ratio 100:28 of UD laminate. 85
Table 12-2. Statistics of mixing ratio 100:29 of UD laminate. 85
Table 12-3. Statistics of mixing ratio 100:30 of UD laminate. 86
Table 12-4. Statistics of mixing ratio 100:31 of UD laminate. 86
Table 12-5. Statistics of mixing ratio 100:32 of UD laminate. 87
Table 12-6. Statistics of mixing ratio 100:33 of UD laminate. 87
Table 12-7. Statistics of mixing ratio 100:34 of UD laminate. 88
Table 12-8 Statistics of mixing ratio 100:28 of Biax laminate. 93
Table 12-9. Statistics of mixing ratio 100:29 of Biax laminate. 94
Table 12-10. Statistics of mixing ratio 100:30 of Biax laminate. 95
Table 12-11. Statistics of mixing ratio 100:31 of Biax laminate. 96
Table 12-12. Statistics of mixing ratio 100:32 of Biax laminate. 97
Table 12-13. Statistics of mixing ratio 100:33 of Biax laminate. 98
Table 12-14. Statistics of mixing ratio 100:34 of Biax laminate. 99
Table 12-15. Statistics of mixing ratio 100:28 of Dow resin. 102
Table 12-16. Statistics of mixing ratio 100:29 of Dow resin. 102
Table 12-17. Statistics of mixing ratio 100:30 of Dow resin. 102
Table 12-18. Statistics of mixing ratio 100:31 of Dow resin. 102
Table 12-19. Statistics of mixing ratio 100:32 of Dow resin. 102
Table 12-20. Statistics of mixing ratio 100:33 of Dow resin. 103
Table 12-21. Statistics of mixing ratio 100:34 of Dow resin. 103

12. APPENDIX.

The results of the tensile tests of the seven infused laminates of UD with different resin mixing ratio are shown below:

12.1. Parameters of report for UD laminates:

Test standard : ISO 527-5
Material : DOW Airstone & Kush UD
Specimen type : B
Machine data : AGW & OCV

Curve graph of all datas (Figure 12-1):

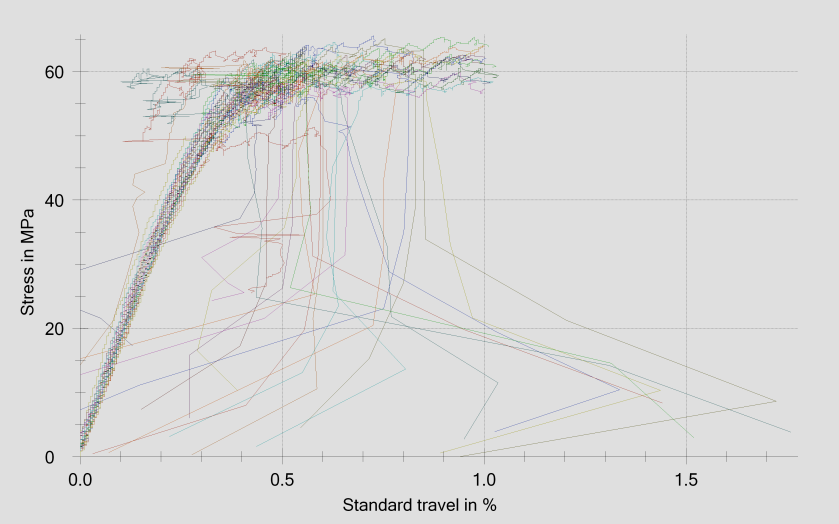

Figure 12-1. Curve graph of UD laminates.

Mixing Ratio	Specimen no.	Fmax	Et	σ_M	ε_M	σ_B	ε_B	h	b	A_0
		N	MPa	MPa	%	Mpa	%	mm	mm	mm^2
100:28	1	4217,07	15500	49,5	0,4	48,0	0,3	3,38	25,18	85,11
	2	4514,95	16400	53,2	0,4	51,7	0,4	3,37	25,17	84,82
	3	4272,97	16100	50,1	0,3	50,1	0,3	3,38	25,21	85,21
	4	4409,40	16700	52,0	0,3	52,0	0,3	3,37	25,16	84,79
	5	4894,48	16500	57,8	0,4	57,8	0,4	3,37	25,14	84,72

Mixing Ratio	Specimen no.	Fmax	Et	σ_M	ε_M	σ_B	ε_B	h	b	A_0
		N	MPa	MPa	%	Mpa	%	mm	mm	mm^2
100:29	1	5344,14	16700	63,1	0,7	61,4	0,7	3,41	24,83	84,67
	2	5341,57	17100	61,8	0,6	61,4	0,6	3,43	25,19	86,40
	3	5286,43	16200	62,5	0,7	61,6	0,7	3,41	24,79	84,53
	4	5180,57	15900	61,0	0,8	60,1	0,8	3,42	24,83	84,92
	5	4856,74	15800	56,8	0,5	56,5	0,5	3,4	25,15	85,51

Appendix

Mixing Ratio	Specimen no.	Fmax	Et	σ_M	ε_M	σ_B	ε_B	h	b	A_0
		N	MPa	MPa	%	Mpa	%	mm	mm	mm^2
100:30	1	5122,13	17100	61,7	0,4	61,3	0,4	3,28	25,29	82,95
	2	4775,14	17700	57,9	0,5	54,4	0,5	3,29	25,08	82,51
	3	5187,19	16700	61,9	0,4	53,9	0,6	3,35	25	83,75
	4	5464,70	16200	64,6	0,7	64,6	0,7	3,34	25,31	84,54
	5	5207,77	17000	61,4	0,6	60,2	0,6	3,37	25,17	84,82

Mixing Ratio	Specimen no.	Fmax	Et	σ_M	ε_M	σ_B	ε_B	h	b	A_0
		N	MPa	MPa	%	Mpa	%	mm	mm	mm^2
100:31	1	5100,81	17900	63,3	0,7	63,3	0,7	3,22	25,03	80,60
	2	5186,45	18400	64,2	0,6	63,2	0,6	3,23	25,02	80,81
	3	4910,40	17400	61,0	0,6	60,6	0,8	3,22	25,01	80,53
	4	4403,15	17100	55,6	0,4	55,3	0,5	3,24	24,45	79,22
	5	5219,90	17100	64,6	0,6	64,2	0,6	3,23	25,01	80,78

Mixing Ratio	Specimen no.	Fmax	Et	σ_M	ε_M	σ_B	ε_B	h	b	A_0
		N	MPa	MPa	%	Mpa	%	mm	mm	mm^2
100:32	1	5177,14	16700	62,6	0,6	62,6	0,7	3,35	24,69	82,71
	2	4963,51	16200	58,8	0,4	57,0	0,5	3,38	24,97	84,40
	3	5180,45	16300	61,2	0,6	60,4	0,7	3,4	24,88	84,59
	4	5258,77	15900	60,5	0,6	60,2	0,6	3,49	24,91	86,94
	5	5174,94	16800	59,6	0,6	58,6	0,6	3,46	25,08	86,78

Mixing Ratio	Specimen no.	Fmax	Et	σ_M	ε_M	σ_B	ε_B	h	b	A_0
		N	MPa	MPa	%	Mpa	%	mm	mm	mm^2
100:33	1	5178,25	16600	61,7	0,7	61,7	0,7	3,32	25,26	83,86
	2	4905,05	15500	55,6	0,3	55,5	0,4	3,45	25,55	88,15
	3	4586,26	16500	55,2	0,4	55,2	0,4	3,33	24,94	83,05
	4	4456,46	16500	50,4	0,3	49,6	0,3	3,46	25,55	88,40
	5	4761,28	16300	57,2	0,4	55,5	0,4	3,31	25,16	83,28

Mixing Ratio	Specimen no.	Fmax	Et	σ_M	ε_M	σ_B	ε_B	h	b	A_0
		N	MPa	MPa	%	Mpa	%	mm	mm	mm^2
100:34	1	5235,98	16100	58,8	0,4	57,5	0,5	3,43	25,94	88,97
	2	5051,39	16400	57,0	0,4	56,6	0,4	3,42	25,91	88,61
	3	5030,43	16000	57,1	0,4	54,6	0,4	3,42	25,75	88,07
	4	4889,97	15500	55,0	0,4	52,9	0,4	3,45	25,76	88,87
	5	4750,99	15700	54,7	0,4	53,7	0,4	3,41	25,49	86,92

Appendix

The curve graph and Statistics table of 100:28 mixing ratio of UD:

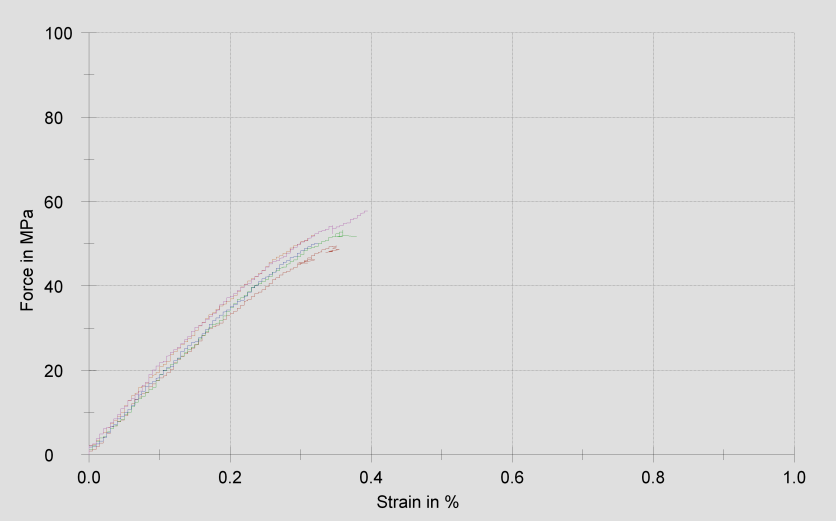

Table 12-1. Statistics of mixing ratio 100:28 of UD laminate.

Airstone 100:28 UD	Fmax	E_t	σ_M	ε_M	σ_B	ε_B	h	b	A_0
n = 5	N	MPa	MPa	%	MPa	%	mm	mm	mm^2
min	4217,07	15500	49,5	0,3	48,0	0,3	3,37	25,14	84,72
max	4894,48	16700	57,8	0,4	57,8	0,4	3,38	25,21	85,21
x	4461,77	16200	52,5	0,3	51,9	0,4	3,374	25,17	84,93
s	268,48	485	3,27	0,0	3,64	0,0	0,005477	0,02588	0,21
ν	6,02	2,98	6,23	9,04	7,02	9,73	0,16	0,10	0,25

The curve graph and Statistic table of 100:29 mixing ratio of UD:

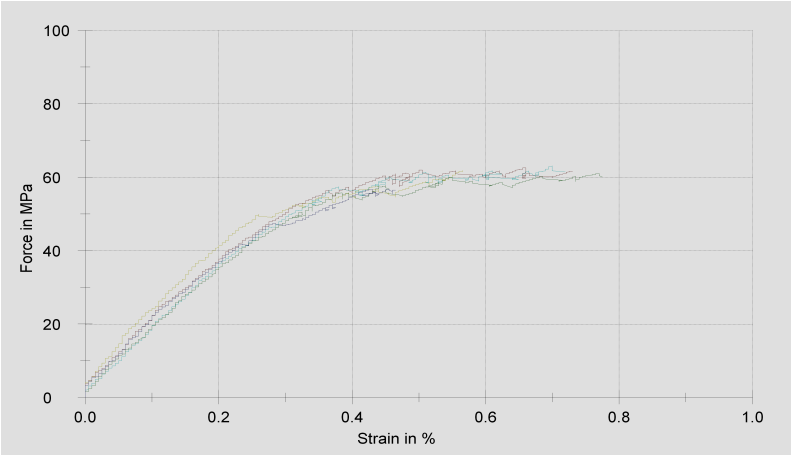

Table 12-2. Statistics of mixing ratio 100:29 of UD laminate.

Airstone 100:29 UD	Fmax	E_t	σ_M	ε_M	σ_B	ε_B	h	b	A_0
n = 5	N	MPa	MPa	%	MPa	%	mm	mm	mm^2
min	4856,74	15800	56,8	0,5	56,5	0,5	3,4	24,79	84,53
max	5344,14	17100	63,1	0,8	61,6	0,8	3,43	25,19	86,40
x	5201,89	16300	61,1	0,6	60,2	0,7	3,414	24,96	85,21
s	204,01	572	2,51	0,1	2,15	0,1	0,0114	0,1947	0,77
ν	3,92	3,50	4,11	19,45	3,57	20,06	0,33	0,78	0,90

Curve graph and Statistics table of Airstone 100:30 UD:

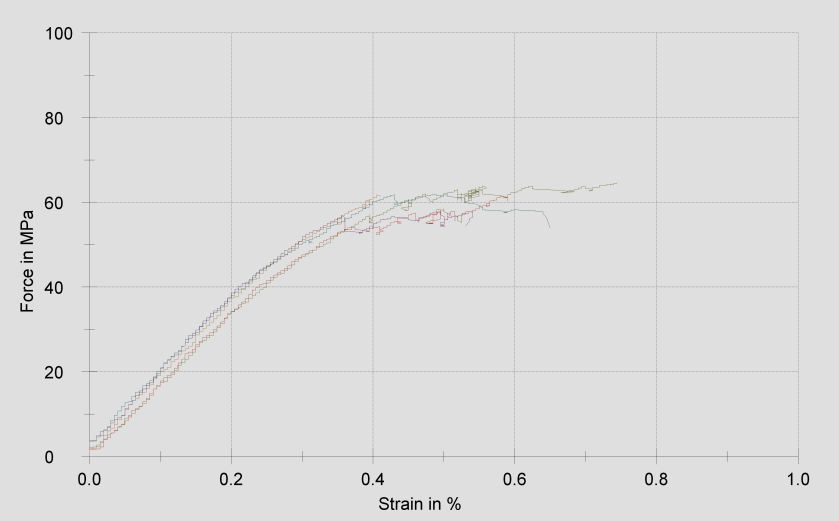

Table 12-3. Statistics of mixing ratio 100:30 of UD laminate.

Airstone 100:30 UD	Fmax	E_t	σ_M	ε_M	σ_B	ε_B	h	b	A_0
n = 5	N	MPa	MPa	%	MPa	%	mm	mm	mm^2
min	4775,14	16200	57,9	0,4	53,9	0,4	3,28	25	82,51
max	5464,70	17700	64,6	0,7	64,6	0,7	3,37	25,31	84,82
x	5151,38	16900	61,5	0,5	58,9	0,6	3,326	25,17	83,71
s	247,51	537	2,41	0,1	4,63	0,1	0,03912	0,1332	0,99
ν	4,80	3,17	3,92	25,19	7,86	21,49	1,18	0,53	1,18

Curve graph and Statistics table of Airstone 100:31 UD:

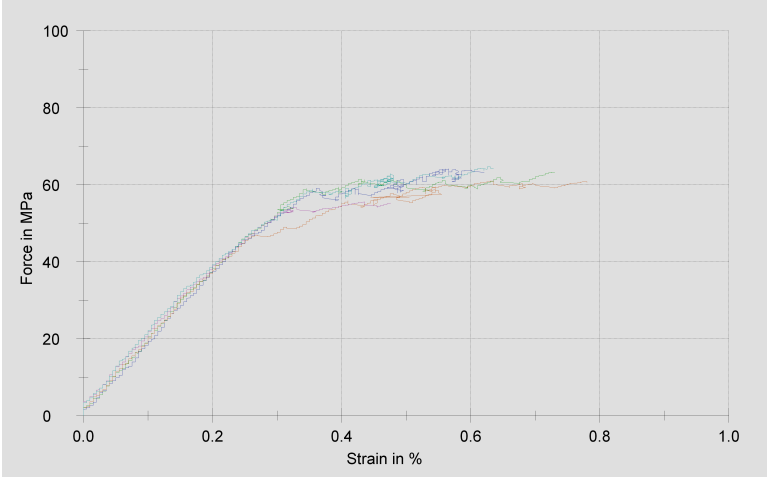

Table 12-4. Statistics of mixing ratio 100:31 of UD laminate.

Airstone 100:31 UD	Fmax	E_t	σ_M	ε_M	σ_B	ε_B	h	b	A_0
n = 5	N	MPa	MPa	%	MPa	%	mm	mm	mm^2
min	4403,15	17100	55,6	0,4	55,3	0,5	3,22	24,45	79,22
max	5219,90	18400	64,6	0,7	64,2	0,8	3,24	25,03	80,81
x	4964,14	17600	61,7	0,6	61,3	0,6	3,228	24,9	80,39
s	335,82	590	3,71	0,1	3,61	0,1	0,008367	0,2539	0,67
ν	6,76	3,35	6,01	18,17	5,88	18,06	0,26	1,02	0,83

Curve graph and Statistics Airstone 100:32 UD:

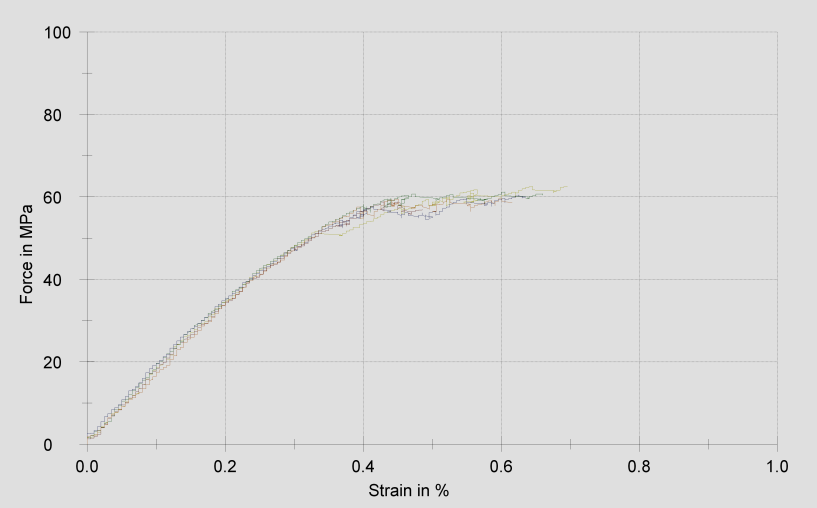

Table 12-5. Statistics of mixing ratio 100:32 of UD laminate.

Airstone 100:32 UD	Fmax	E_t	σ_M	ε_M	σ_B	ε_B	h	b	A_0
n = 5	N	MPa	MPa	%	MPa	%	mm	mm	mm^2
min	4963,51	15900	58,8	0,4	57,0	0,5	3,35	24,69	82,71
max	5258,77	16800	62,6	0,6	62,6	0,7	3,49	25,08	86,94
x	5150,96	16400	60,6	0,6	59,7	0,6	3,416	24,91	85,08
s	110,56	346	1,46	0,1	2,09	0,1	0,05771	0,1429	1,78
ν	2,15	2,11	2,41	14,85	3,49	12,94	1,69	0,57	2,09

Curve graph and Statistic table of Airstone 100:33 UD:

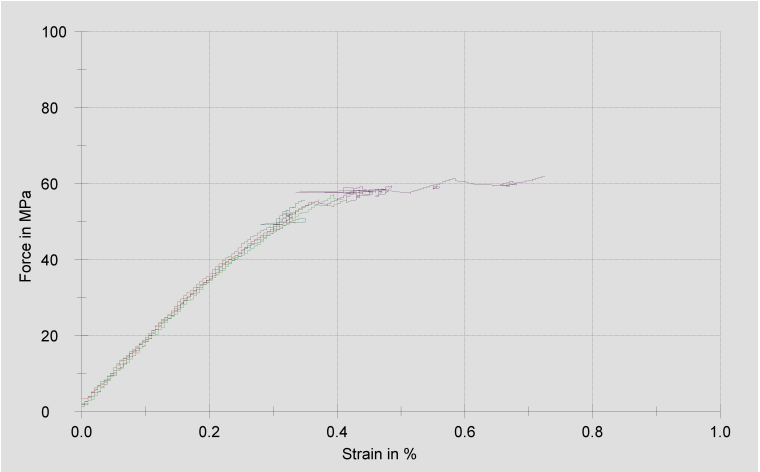

Table 12-6. Statistics of mixing ratio 100:33 of UD laminate.

Airstone 100:33 UD	Fmax	E_t	σ_M	ε_M	σ_B	ε_B	h	b	A_0
n = 5	N	MPa	MPa	%	MPa	%	mm	mm	mm^2
min	4456,46	15500	50,4	0,3	49,6	0,3	3,31	24,94	83,05
max	5178,25	16600	61,7	0,7	61,7	0,7	3,46	25,55	88,40
x	4777,46	16300	56,0	0,4	55,5	0,4	3,374	25,29	85,35
s	281,41	430	4,07	0,2	4,30	0,2	0,07436	0,2624	2,69
ν	5,89	2,64	7,27	36,68	7,74	35,68	2,20	1,04	3,15

Curve graph and Statistic table of Airstone 100:34 UD:

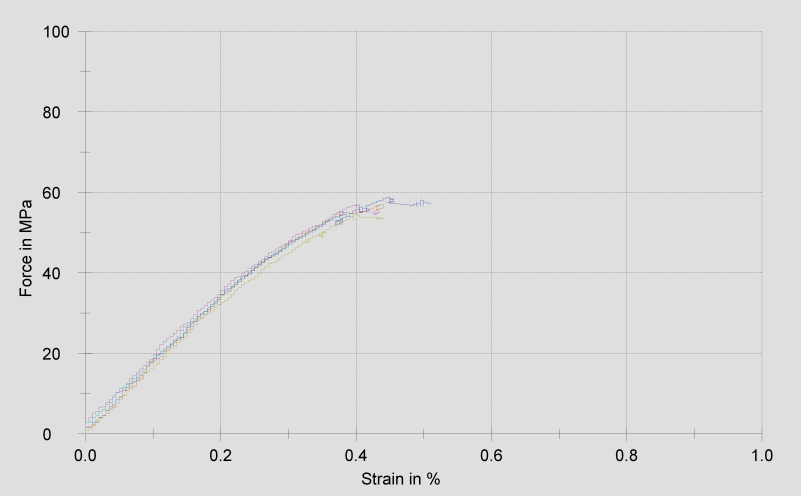

Table 12-7. Statistics of mixing ratio 100:34 of UD laminate.

Airstone 100:34 UD	Fmax	E_t	σ_M	ε_M	σ_B	ε_B	h	b	A_0
n = 5	N	MPa	MPa	%	MPa	%	mm	mm	mm^2
min	4750,99	15500	54,7	0,4	52,9	0,4	3,41	25,49	86,92
max	5235,98	16400	58,8	0,4	57,5	0,5	3,45	25,94	88,97
x	4991,75	15900	56,5	0,4	55,1	0,4	3,426	25,77	88,29
s	182,36	359	1,71	0,0	1,91	0,0	0,01517	0,1785	0,84
ν	3,65	2,25	3,03	6,58	3,48	9,45	0,44	0,69	0,95

The failure of the different mixing ratios laminates samples of tensile test are shown below:

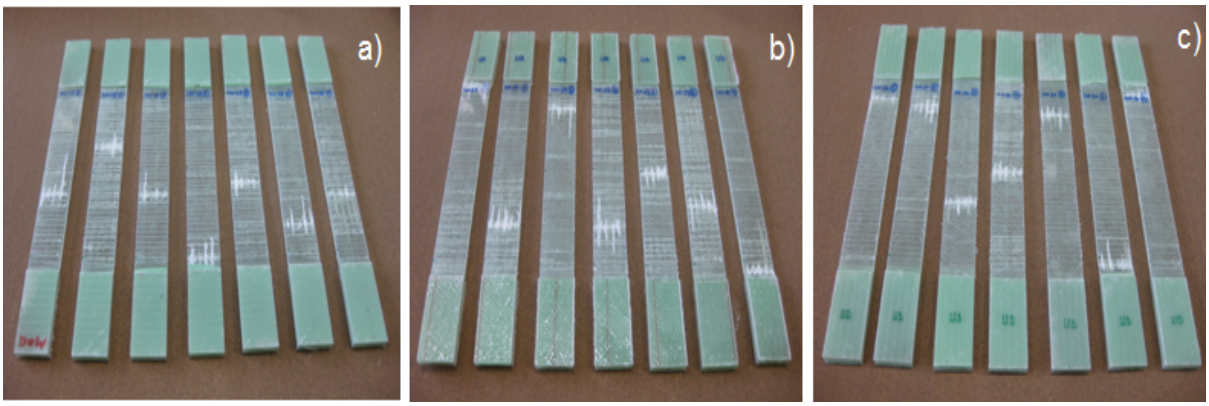

Figure 12-2. a) Failure mixing ratio 100:28UD. b) Failure mixing ratio 100:29UD. c) Failure mixing ratio 100:30UD.

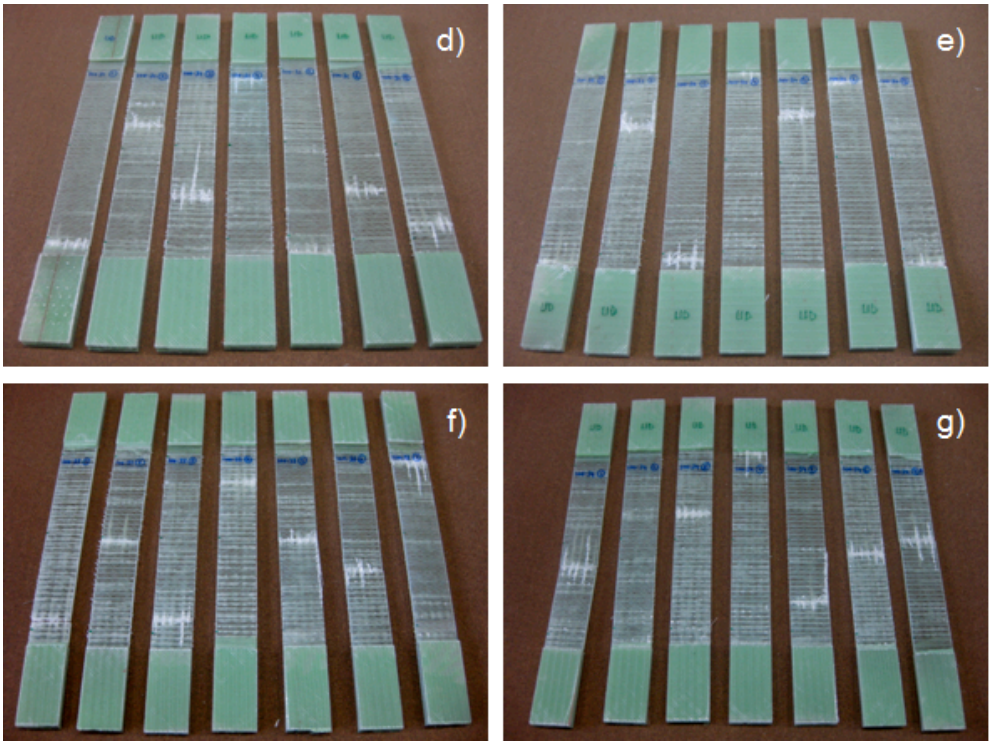

Figure 12-3. d) Failure mixing ratio 100:31UD e) Failure mixing ratio 100:32UD f) Failure mixing ratio 100:33UD g) Failure mixing ratio 100:34UD.

The ways of the coupons were failure were quite homogenous.

The results of the tensile tests of the other seven infused laminates of Biax with different resin mixing ratio are shown below:

12.2. Parameters of report for Biax laminates:

Test standard	:	ISO 14129
Material	:	Dow Airstone & Kush Biax
Specimen type	:	B
Machine data	:	AGW & OCV

Curve graph of all the datas (Figure 12-4):

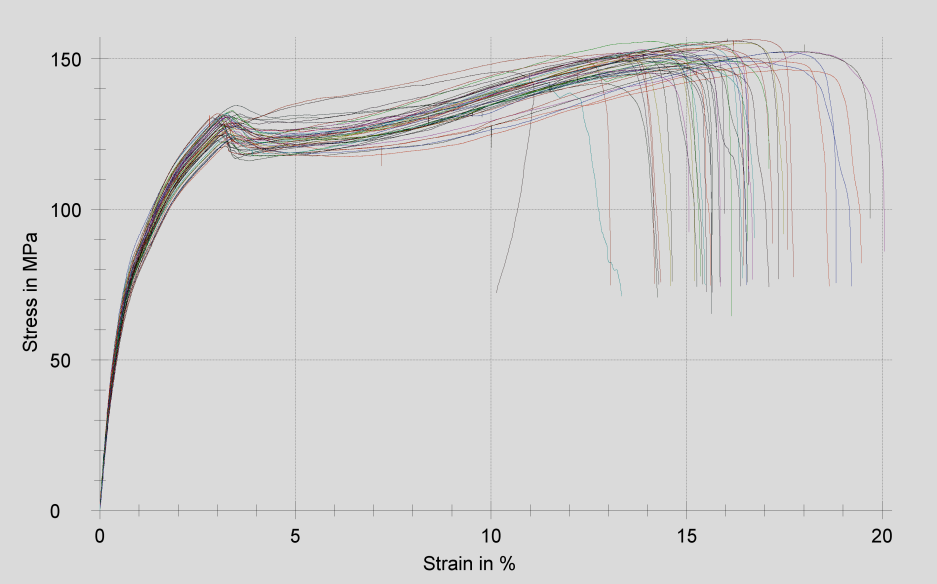

Figure 12-4 Curve graph of Biax laminates.

Making a zoom to amplified the interested zone (interfibre zone):

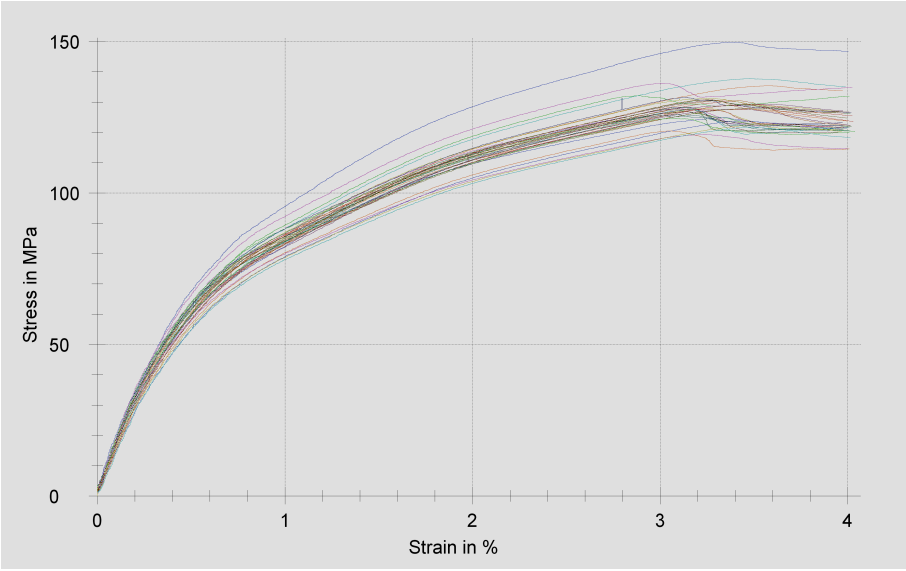

Mixing Ratio	Specimen no.	Fmax	E_t	σ_Y	ε_Y	σ_M	ε_M	σ_B	ε_B	h	b	A_0
		N	MPa	MPa	%	MPa	%	MPa	%	mm	mm	mm^2
100:28	1	7707,61	14900	130	3,4	130	3,4	124	4,0	2,35	25,18	59,17
	2	7535,19	14800	127	3,1	127	3,1	120	4,0	2,36	25,17	59,40
	3	7424,54	13500	125	3,3	125	3,3	122	4,0	2,36	25,2	59,47
	4	7583,35	14000	128	3,4	128	3,4	124	4,0	2,36	25,18	59,42
	5	7567,37	15300	128	3,1	128	3,1	122	4,0	2,35	25,19	59,20

Mixing Ratio	Specimen no.	Fmax	E_t	σ_Y	ε_Y	σ_M	ε_M	σ_B	ε_B	h	b	A_0
		N	MPa	MPa	%	MPa	%	MPa	%	mm	mm	mm^2
100:29	1	7513,69	14500	127	3,2	127	3,2	122	4,0	2,33	25,3	58,95
	2	7461,11	14600	128	3,2	128	3,2	121	4,0	2,33	25,05	58,37
	3	7621,87	14300	127	3,1	127	3,1	120	4,0	2,41	24,94	60,11
	4	7663,05	15100	128	3,1	128	3,1	122	4,0	2,4	24,92	59,81
	5	7563,78	15500	128	3,2	128	3,2	123	4,0	2,37	24,86	58,92

Mixing Ratio	Specimen no.	Fmax	E_t	σ_Y	ε_Y	σ_M	ε_M	σ_B	ε_B	h	b	A_0
		N	MPa	MPa	%	MPa	%	MPa	%	mm	mm	mm^2
100:30	1	7600,91	15400	131	3,3	131	3,3	122	4,0	2,33	24,96	58,16
	2	7522,23	14300	128	3,4	128	3,4	122	4,0	2,35	25,06	58,89
	3	7360,09	15200	126	3,1	126	3,1	121	4,0	2,32	25,21	58,49
	4	7274,79	15700	128	3,2	128	3,2	122	4,0	2,29	24,89	57,00
	5	7389,13	14500	128	3,2	128	3,2	122	4,0	2,32	24,96	57,91

Mixing Ratio	Specimen no.	Fmax	E_t	σ_Y	ε_Y	σ_M	ε_M	σ_B	ε_B	h	b	A_0
		N	MPa	MPa	%	MPa	%	MPa	%	mm	mm	mm^2
100:31	1	7852,86	16300	132	2,9	132	2,9	132	4,0	2,35	25,3	59,46
	2	7766,11	14200	150	3,4	150	3,4	147	4,0	2,09	24,81	51,85
	3	7786,70	14400	-	-	135	3,6	134	4,0	2,29	25,11	57,50
	4	7687,82	16300	136	3,0	136	3,0	135	4,0	2,25	25,1	56,48
	5	7726,05	14600	138	3,5	138	3,5	135	4,0	2,26	24,82	56,09

Mixing Ratio	Specimen no.	Fmax	E_t	σ_Y	ε_Y	σ_M	ε_M	σ_B	ε_B	h	b	A_0
		N	MPa	MPa	%	MPa	%	MPa	%	mm	mm	mm^2
100:32	1	7535,64	14500	131	3,2	131	3,2	127	4,0	2,29	25,08	57,43
	2	7546,67	14200	131	3,3	131	3,3	127	4,0	2,32	24,87	57,70
	3	7527,56	14400	131	3,3	131	3,3	126	4,0	2,31	24,93	57,59
	4	7543,36	14000	132	3,1	132	3,1	127	4,0	2,29	25,04	57,34
	5	7464,70	14300	131	3,3	131	3,3	126	4,0	2,28	25,03	57,07

Mixing Ratio	Specimen no.	Fmax	E_t	σ_Y	ε_Y	σ_M	ε_M	σ_B	ε_B	h	b	A_0
		N	MPa	MPa	%	MPa	%	MPa	%	mm	mm	mm^2
100:33	1	7703,99	13300	-	-	129	3,6	127	4,0	2,38	25,03	59,57
	2	7514,69	13500	126	3,0	126	3,0	122	4,0	2,39	25,01	59,77
	3	7516,90	13300	128	3,5	128	3,5	125	4,0	2,36	24,89	58,74
	4	7562,85	13300	129	3,5	129	3,5	126	4,0	2,35	24,91	58,54
	5	7565,05	13700	125	3,1	125	3,1	120	4,0	2,44	24,89	60,73

Mixing Ratio	Specimen no.	Fmax	E_t	σ_Y	ε_Y	σ_M	ε_M	σ_B	ε_B	h	b	A_0
		N	MPa	MPa	%	MPa	%	MPa	%	mm	mm	mm^2
100:34	1	7322,82	13000	124	3,4	124	3,4	121	4,0	2,37	24,96	59,16
	2	7436,40	13800	121	3,1	121	3,1	115	4,0	2,47	24,98	61,70
	3	7403,49	13600	119	3,2	119	3,2	115	4,0	2,45	25,33	62,06
	4	7418,93	13500	122	3,5	122	3,5	118	4,0	2,44	24,98	60,95
	5	7487,67	12900	-	-	123	3,6	120	4,0	2,42	25,23	61,06

The curve graph and Statistics table of 100:28 mixing ratio of Biax:

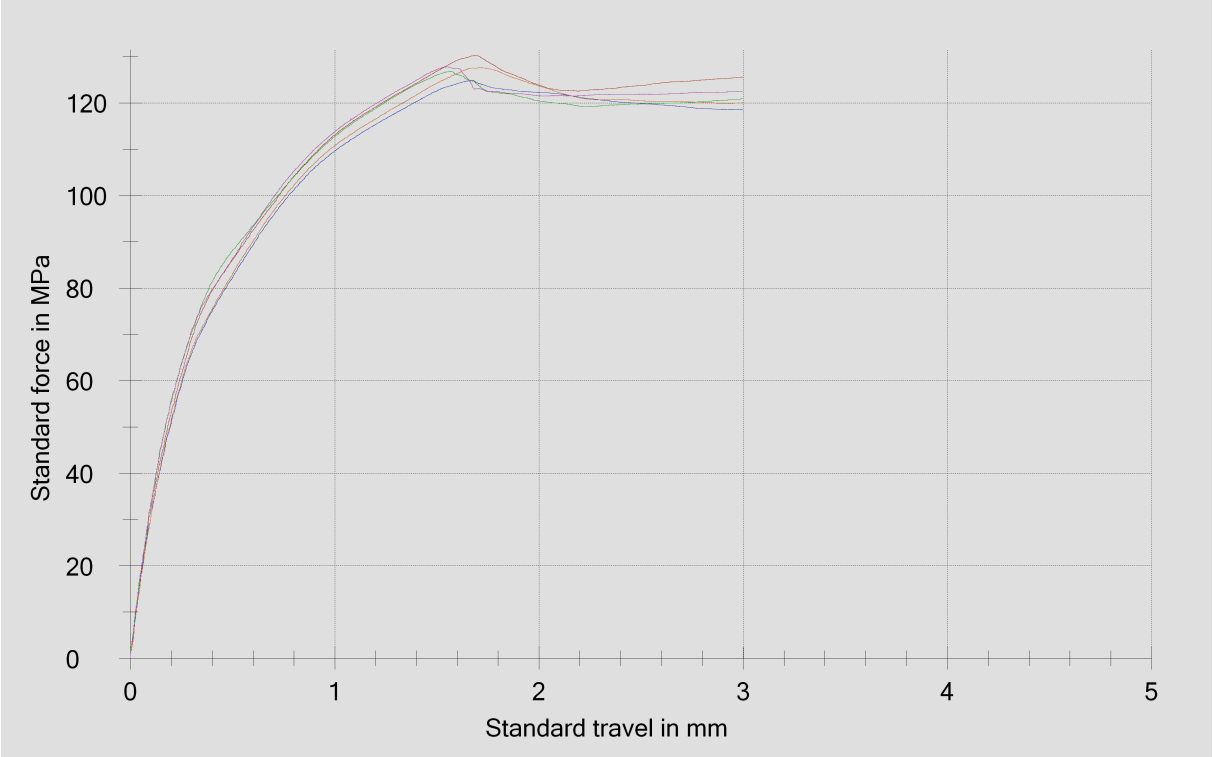

Table 12-8 Statistics of mixing ratio 100:28 of Biax laminate.

Airstone 100 28 Biax	Fmax	E_t	σ_Y	ε_Y	σ_M	ε_M	σ_B	ε_B	h	b	A_0
n = 7	N	MPa	MPa	%	MPa	%	MPa	%	mm	mm	mm^2
max	7707,61	15300	130	3,4	130	3,4	124	4,0	2,36	25,2	59,47
min	7424,54	13500	125	3,1	125	3,1	120	4,0	2,35	25,17	59,17
x	7563,61	14500	127	3,3	127	3,3	122	4,0	2,356	25,18	59,33
s	101,60	722	1,95	0,1	1,95	0,1	1,44	0,0	0,005477	0,0114	0,14
ν	1,34	4,98	1,53	4,47	1,53	4,47	1,17	0,66	0,23	0,05	0,23

The curve graph and Statistics table of 100:29 mixing ratio of Biax:

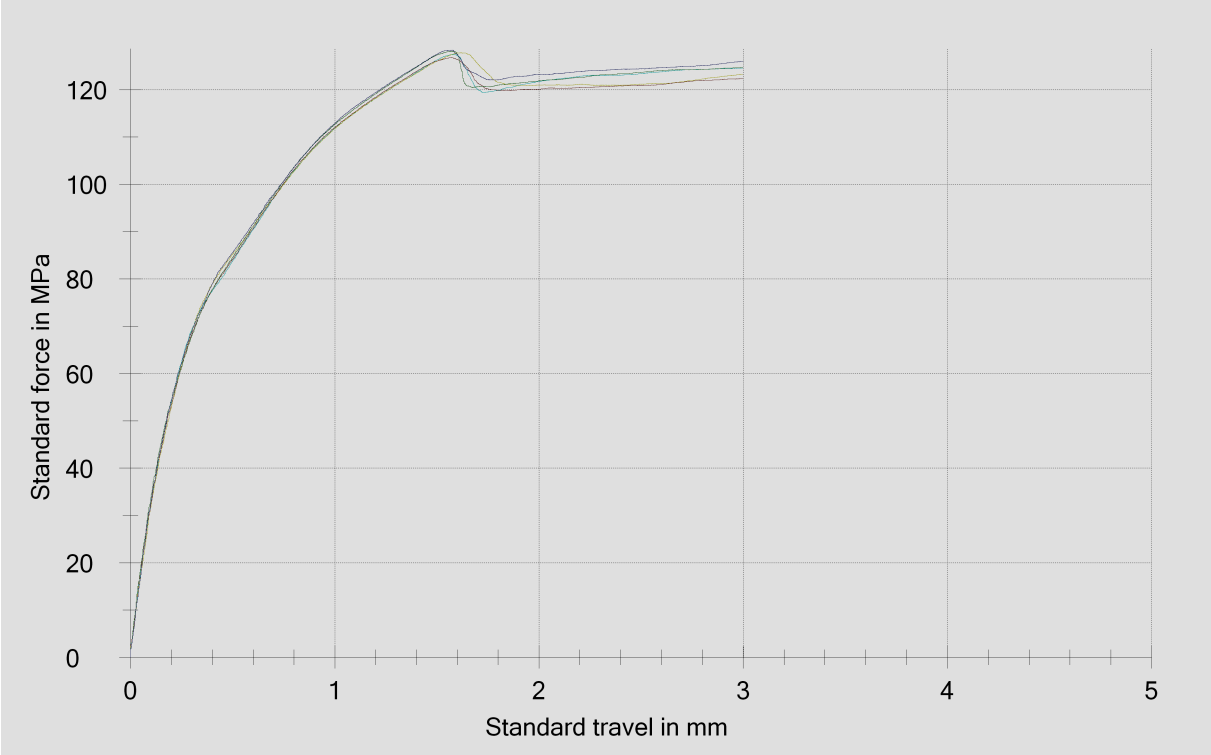

Table 12-9. Statistics of mixing ratio 100:29 of Biax laminate.

Airstone 100 29 Biax	Fmax	E_t	σ_Y	ε_Y	σ_M	ε_M	σ_B	ε_B	h	b	A_0
n = 5	N	MPa	MPa	%	MPa	%	MPa	%	mm	mm	mm^2
max	7663,05	15500	128	3,2	128	3,2	123	4,0	2,41	25,3	60,11
min	7461,11	14300	127	3,1	127	3,1	120	4,0	2,33	24,86	58,37
x	7564,70	14800	128	3,2	128	3,2	122	4,0	2,368	25,01	59,23
s	81,05	503	0,614	0,0	0,614	0,0	1,18	0,0	0,03768	0,174	0,71
ν	1,07	3,40	0,48	1,24	0,48	1,24	0,97	0,66	1,59	0,70	1,20

The curve graph and Statistics table of 100:30 mixing ratio of Biax:

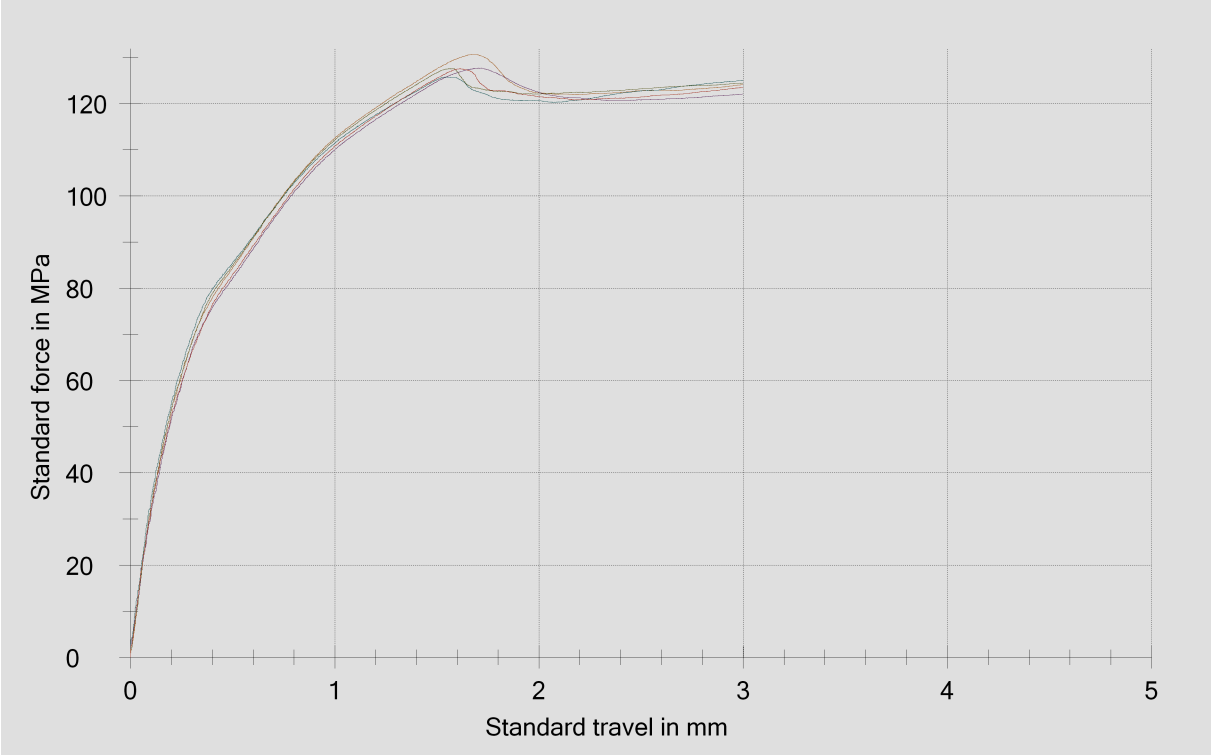

Table 12-10. Statistics of mixing ratio 100:30 of Biax laminate.

Airstone 100 30 Biax	Fmax	E_t	σ_Y	ε_Y	σ_M	ε_M	σ_B	ε_B	h	b	A_0
n = 5	N	MPa	MPa	%	MPa	%	MPa	%	mm	mm	mm^2
max	7600,91	15700	131	3,4	131	3,4	122	4,0	2,35	25,21	58,89
min	7274,79	14300	126	3,1	126	3,1	121	4,0	2,29	24,89	57,00
x	7429,43	15000	128	3,3	128	3,3	122	4,0	2,322	25,02	58,09
s	130,73	577	1,75	0,1	1,75	0,1	0,744	0,0	0,02168	0,1242	0,71
ν	1,76	3,84	1,37	4,32	1,37	4,32	0,61	0,43	0,93	0,50	1,23

The curve graph and Statistics table of 100:31 mixing ratio of Biax:

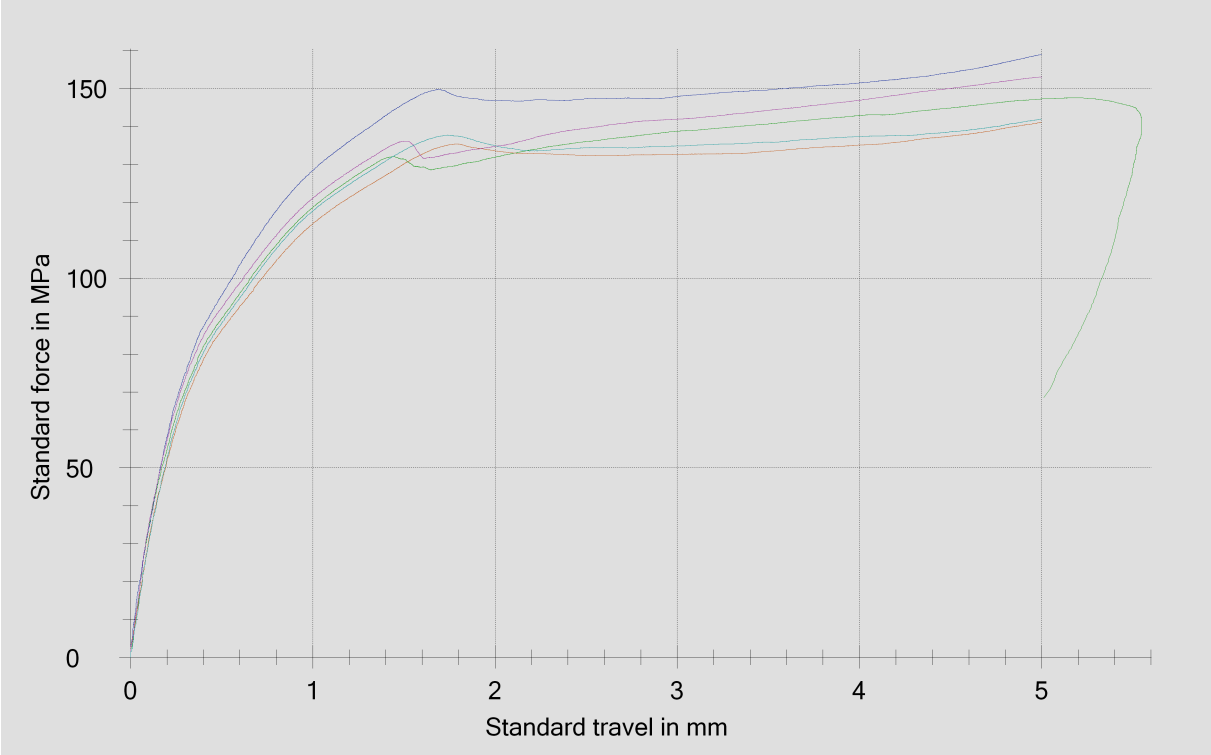

Table 12-11. Statistics of mixing ratio 100:31 of Biax laminate.

Airstone 100 31 Biax	Fmax	E_t	σ_Y	ε_Y	σ_M	ε_M	σ_B	ε_B	h	b	A_0
n = 5	N	MPa	MPa	%	MPa	%	MPa	%	mm	mm	mm^2
max	7852,86	16300	150	3,5	150	3,6	147	4,0	2,35	25,3	59,46
min	7687,82	14200	132	2,9	132	2,9	132	4,0	2,09	24,81	51,85
x	7763,91	15200	139	3,2	138	3,3	136	4,0	2,248	25,03	56,28
s	62,57	1050	7,61	0,3	6,78	0,3	5,90	0,0	0,09654	0,2102	2,79
ν	0,81	6,93	5,48	9,00	4,90	9,36	4,33	0,48	4,29	0,84	4,97

The curve graph and Statistics table of 100:32 mixing ratio of Biax:

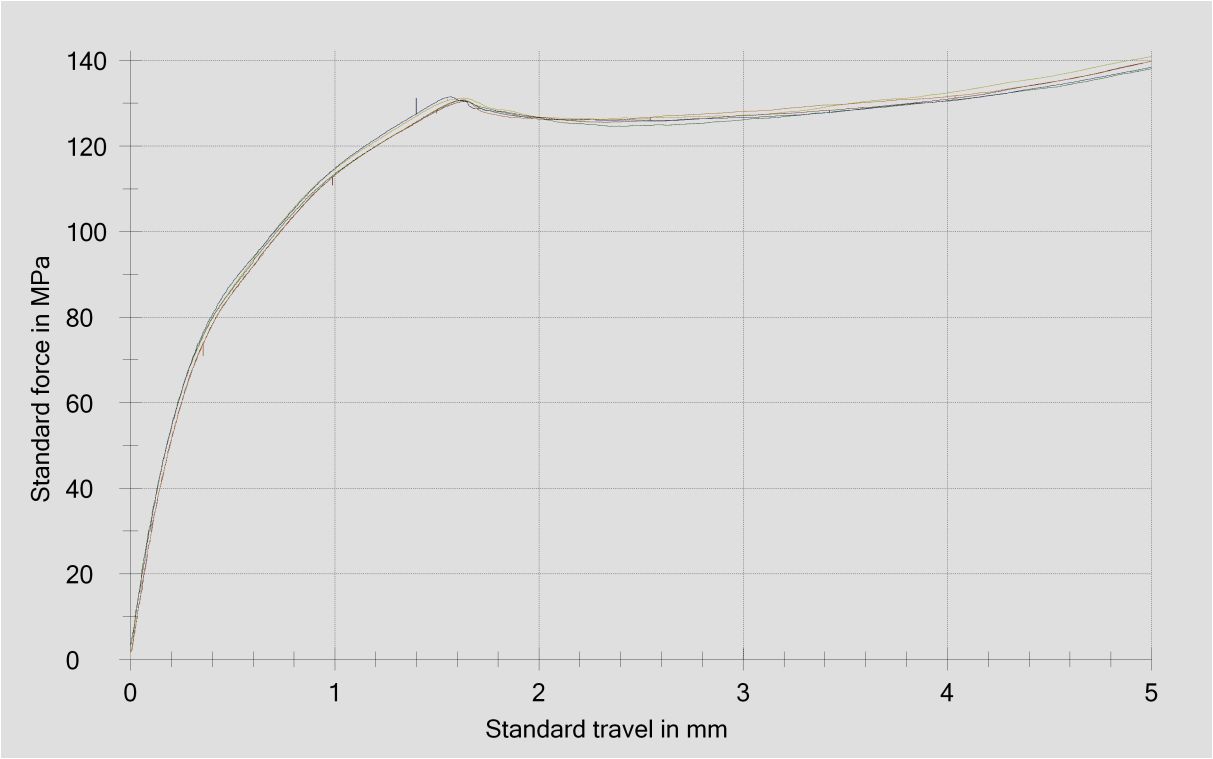

Table 12-12. Statistics of mixing ratio 100:32 of Biax laminate.

Airstone 100 32 Biax	Fmax	E_t	σ_Y	ε_Y	σ_M	ε_M	σ_B	ε_B	h	b	A_0
n = 5	N	MPa	MPa	%	MPa	%	MPa	%	mm	mm	mm^2
max	7546,67	14500	132	3,3	132	3,3	127	4,0	2,32	25,08	57,70
min	7464,70	14000	131	3,1	131	3,1	126	4,0	2,28	24,87	57,07
x	7523,59	14300	131	3,2	131	3,2	127	4,0	2,298	24,99	57,43
s	33,74	204	0,357	0,1	0,357	0,1	0,260	0,0	0,01643	0,08689	0,24
ν	0,45	1,43	0,27	1,68	0,27	1,68	0,21	0,69	0,72	0,35	0,42

The curve graph and Statistics table of 100:33 mixing ratio of Biax:

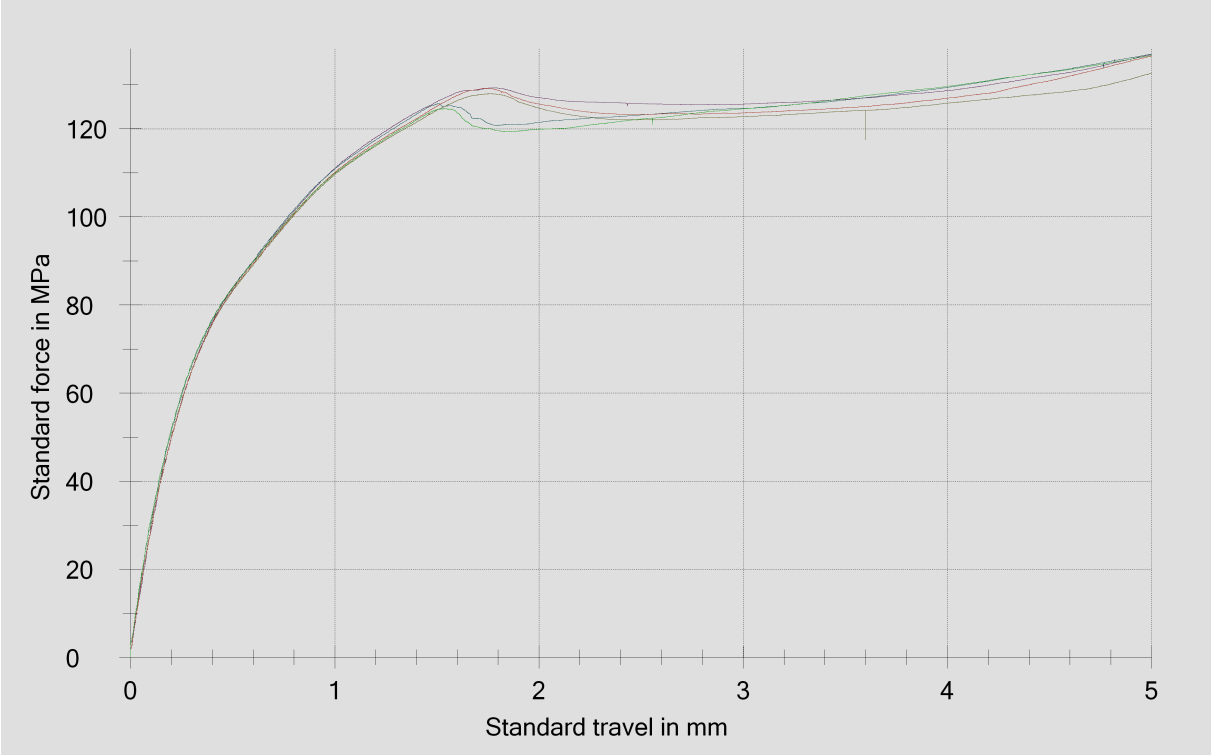

Table 12-13. Statistics of mixing ratio 100:33 of Biax laminate.

Airstone 100 33 Biax	Fmax	E_t	σ_Y	ε_Y	σ_M	ε_M	σ_B	ε_B	h	b	A_0
n = 5	N	MPa	MPa	%	MPa	%	MPa	%	mm	mm	mm^2
max	7703,99	13700	129	3,5	129	3,6	127	4,0	2,44	25,03	60,73
min	7514,69	13300	125	3,0	125	3,0	120	4,0	2,35	24,89	58,54
x	7572,70	13400	127	3,3	127	3,3	124	4,0	2,384	24,95	59,47
s	77,25	172	2,10	0,3	2,13	0,3	2,96	0,0	0,03507	0,06841	0,88
ν	1,02	1,28	1,66	7,84	1,67	7,76	2,39	0,46	1,47	0,27	1,48

The curve graph and Statistics table of 100:34 mixing ratio of Biax:

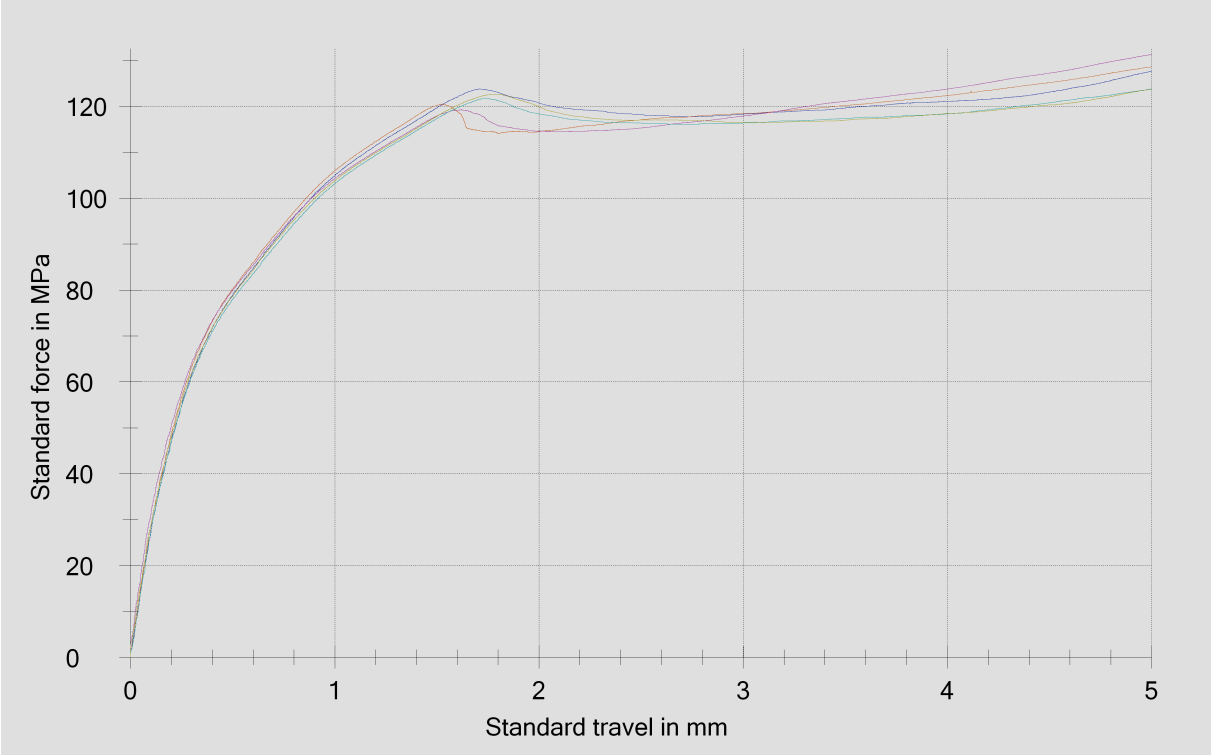

Table 12-14. Statistics of mixing ratio 100:34 of Biax laminate.

Airstone 100 34 Biax	Fmax	E_t	σ_Y	ε_Y	σ_M	ε_M	σ_B	ε_B	h	b	A_0
n = 5	N	MPa	MPa	%	MPa	%	MPa	%	mm	mm	mm^2
max	7487,67	13800	124	3,5	124	3,6	121	4,0	2,47	25,33	62,06
min	7322,82	12900	119	3,1	119	3,1	115	4,0	2,37	24,96	59,16
x	7413,86	13300	121	3,3	122	3,4	118	4,0	2,43	25,1	60,98
s	59,95	382	1,91	0,2	1,76	0,2	3,00	0,0	0,03808	0,1718	1,12
ν	0,81	2,86	1,58	5,70	1,44	6,25	2,55	0,51	1,57	0,68	1,84

The failures of all different mixing ratio coupons after tensile test are shown below:

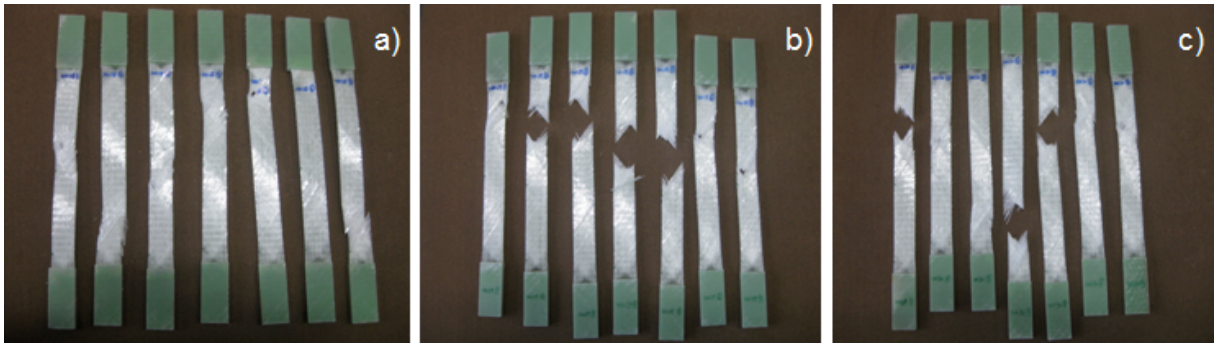

Figure 12-5. a) Failure mixing ratio 100:28Biax b) Failure mixing ratio 100:29Biax c) Failure mixing ratio 100:30Biax.

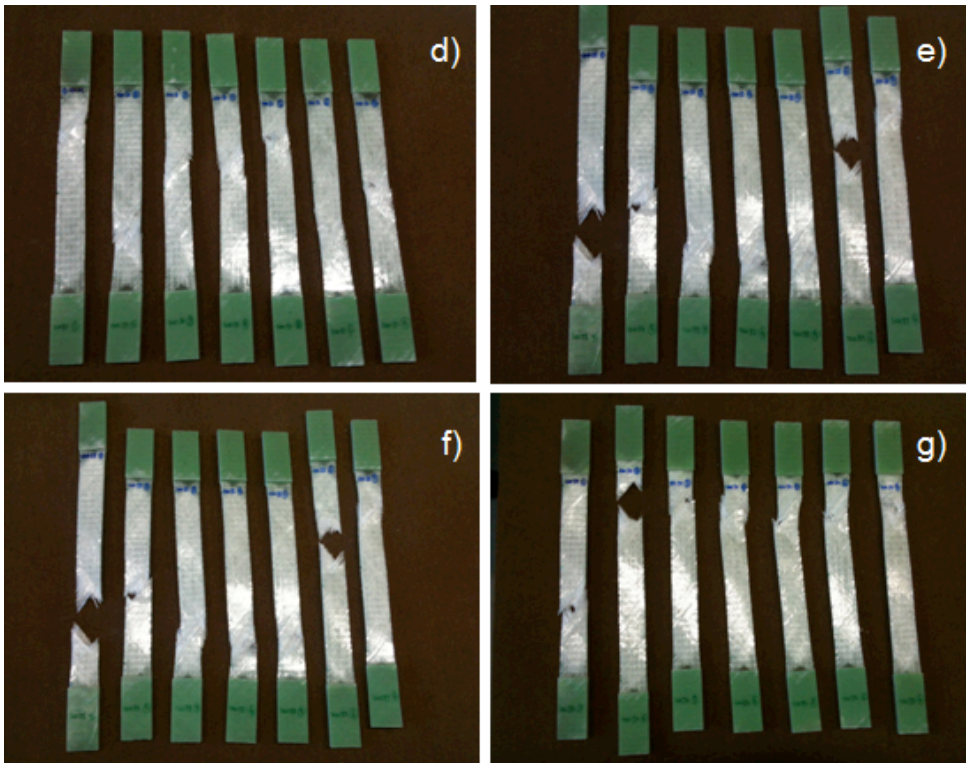

Figure 12-6. d) Failure mixing ratio 100:31Biax e) Failure mixing ratio 100:32Biax f) Failure mixing ratio 100:33Biax g) Failure mixing ratio 100:34Biax.

12.3. Parameters of report for DOW resin coupons:

DOW Resin	Fmax	E_t	σ_Y	ε_Y	σ_M	ε_M	σ_B	ε_B	h	b	A_0
Mixing ration	N	MPa	MPa	%	MPa	%	MPa	%	mm	mm	mm^2
100:28	1955,04	1910	-	-	48,9	3,2	48,9	3,2	3,95	10,12	39,97
	1516,29	1830	7,26	0,2	38,4	2,3	38,4	2,3	3,88	10,19	39,54
	3116,07	2400	10,4	0,2	67,7	5,1	57,5	6,4	4,54	10,14	46,04
	2459,24	1710	8,33	0,2	74,2	5,1	72,1	5,4	3,3	10,05	33,17
	2204,02	1950	8,93	0,2	76,4	4,3	76,1	4,5	2,85	10,12	28,84
100:29	2172,72	2860	72,3	5,6	72,3	5,6	70,8	6,2	2,98	10,09	30,07
	2926,86	1890	-	-	69,8	5,1	69,1	5,4	4	10,03	41,93
	2462,46	2430	-	-	61,3	3,9	61,3	3,9	3,93	9,89	40,14
	2731,25	2260	69,2	5,7	69,2	5,7	67,5	6,1	3,96	9,96	39,44
	2913,26	1640	-	-	69,1	4,4	68,6	4,5	4,25	9,92	42,16
100:30	2478,27	2010	-	-	70,7	5,0	70,1	5,4	3,55	9,88	35,07
	2702,57	2530	69,4	5,0	69,4	5,0	65,9	5,4	3,94	9,88	38,93
	3032,76	2790	68,2	5,0	68,2	5,0	64,8	5,1	4,48	9,92	44,44
	2857,37	2890	69,0	5,2	69,0	5,2	67,2	6,2	4,19	9,89	41,44
	2695,21	2190	7,78	0,2	70,7	5,5	69,7	6,1	3,83	9,95	38,11
100:31	2656,53	2950	-	-	72,1	5,0	71,8	5,3	3,71	9,93	36,84
	2597,70	2960	-	-	66,5	4,1	66,5	4,1	3,95	9,89	39,07
	2564,60	2650	73,0	5,6	73,0	5,6	68,0	6,1	3,58	9,82	35,16
	2796,25	2310	71,4	5,0	71,4	5,0	68,6	5,1	4,01	9,77	39,18
	2647,70	2960	-	-	73,9	5,2	73,8	5,3	3,61	9,92	35,81
100:32	2568,28	2410	8,20	0,2	67,9	5,6	61,5	7,5	3,88	9,75	37,83
	2718,30	2690	68,2	5,1	68,2	5,1	60,0	6,8	4,04	9,86	39,83
	2930,82	2690	66,6	5,3	66,6	5,3	62,6	7,1	4,46	9,86	43,98
	2769,04	2740	65,7	5,2	65,7	5,2	59,4	6,7	4,22	9,98	42,12
	2714,25	2370	68,9	5,5	68,9	5,5	65,8	6,4	4,06	9,71	39,42
100:33	2480,40	2290	-	-	70,0	5,2	70,0	5,2	3,61	9,81	35,41
	2758,74	2110	84,9	5,6	84,9	5,6	64,8	6,5	3,47	9,36	32,48
	2357,23	2500	-	-	69,6	5,5	69,4	5,6	3,42	9,9	33,86
	2488,86	2650	70,5	5,1	70,5	5,1	69,3	5,5	3,61	9,78	35,31
	2490,33	2400	74,5	5,3	74,5	5,3	63,9	5,9	3,48	9,61	33,44
100:34	2848,09	2130	66,3	4,9	66,3	4,9	62,1	5,8	4,36	9,86	42,99
	2812,06	2720	63,3	4,9	63,3	4,9	57,9	5,7	4,45	9,98	44,41
	2764,26	2490	-	-	63,2	4,5	63,0	4,7	4,38	9,98	43,71
	2146,17	2180	-	-	55,2	5,3	55,1	5,3	3,95	9,84	38,87
	2056,82	2340	8,04	0,2	70,5	5,3	69,8	5,7	2,95	9,89	29,18

Statistics table Dow resin 100:28

Table 12-15. Statistics of mixing ratio 100:28 of Dow resin.

Dow 100:28	Fmax	E_t	σ_Y	ε_Y	σ_M	ε_M	σ_B	ε_B	h	b	A_0
n = 5	N	MPa	MPa	%	MPa	%	MPa	%	mm	mm	mm^2
x	2250,13	1960	8,73	0,2	61,1	4,0	58,6	4,4	3,704	10,12	37,51
s	596,09	262	1,31	0,0	16,7	1,2	15,8	1,7	0,6486	0,0503	6,65
ν	26,49	13,37	14,96	6,99	27,32	30,72	26,89	38,00	17,51	0,50	17,73

Statistics table Dow resin 100:29

Table 12-16. Statistics of mixing ratio 100:29 of Dow resin.

Dow 100:28	Fmax	E_t	σ_Y	ε_Y	σ_M	ε_M	σ_B	ε_B	h	b	A_0
n = 5	N	MPa	MPa	%	MPa	%	MPa	%	mm	mm	mm^2
x	2641,31	2220	70,8	5,6	68,4	4,9	67,5	5,2	3,824	9,978	38,75
s	322,16	474	2,13	0,1	4,12	0,8	3,64	1,0	0,4885	0,08167	4,99
ν	12,20	21,37	3,01	1,15	6,02	15,76	5,39	19,13	12,77	0,82	12,87

Statistics table Dow resin 100:30

Table 12-17. Statistics of mixing ratio 100:30 of Dow resin.

Dow 100:28	Fmax	E_t	σ_Y	ε_Y	σ_M	ε_M	σ_B	ε_B	h	b	A_0
n = 5	N	MPa	MPa	%	MPa	%	MPa	%	mm	mm	mm^2
x	2753,24	2480	53,6	3,9	69,6	5,2	67,5	5,6	3,998	9,904	39,60
s	206,47	377	30,6	2,4	1,08	0,2	2,32	0,5	0,3541	0,0305	3,54
ν	7,50	15,20	57,00	62,94	1,55	4,53	3,43	8,60	8,86	0,31	8,93

Statistics table Dow resin 100:31

Table 12-18. Statistics of mixing ratio 100:31 of Dow resin.

Dow 100:28	Fmax	E_t	σ_Y	ε_Y	σ_M	ε_M	σ_B	ε_B	h	b	A_0
n = 5	N	MPa	MPa	%	MPa	%	MPa	%	mm	mm	mm^2
x	2652,55	2770	72,2	5,3	71,4	5,0	69,7	5,2	3,772	9,866	37,21
s	88,65	287	1,11	0,5	2,89	0,6	2,99	0,7	0,197	0,06877	1,85
ν	3,34	10,38	1,54	8,83	4,05	11,08	4,29	13,89	5,22	0,70	4,96

Statistics table Dow resin 100:32

Table 12-19. Statistics of mixing ratio 100:32 of Dow resin.

Dow 100:28	Fmax	E_t	σ_Y	ε_Y	σ_M	ε_M	σ_B	ε_B	h	b	A_0
n = 5	N	MPa	MPa	%	MPa	%	MPa	%	mm	mm	mm^2
x	2740,14	2580	55,5	4,2	67,5	5,3	61,9	6,9	4,132	9,832	40,64
s	130,27	175	26,5	2,3	1,26	0,2	2,55	0,4	0,2194	0,1062	2,42
ν	4,75	6,80	47,70	53,26	1,86	4,35	4,12	6,27	5,31	1,08	5,94

Statistics table Dow resin 100:33

Table 12-20. Statistics of mixing ratio 100:33 of Dow resin.

Dow 100:28	Fmax	E_t	σ_Y	ε_Y	σ_M	ε_M	σ_B	ε_B	h	b	A_0
n = 5	N	MPa	MPa	%	MPa	%	MPa	%	mm	mm	mm^2
x	2515,11	2390	76,6	5,3	73,9	5,3	67,5	5,7	3,518	9,692	34,10
s	147,30	204	7,46	0,2	6,46	0,2	2,89	0,5	0,08701	0,2132	1,25
ν	5,86	8,55	9,74	4,30	8,74	3,59	4,29	8,28	2,47	2,20	3,68

Statistics table Dow resin 100:34

Table 12-21. Statistics of mixing ratio 100:34 of Dow resin.

Dow 100:28	Fmax	E_t	σ_Y	ε_Y	σ_M	ε_M	σ_B	ε_B	h	b	A_0
n = 5	N	MPa	MPa	%	MPa	%	MPa	%	mm	mm	mm^2
x	2525,48	2370	45,9	3,3	63,7	5,0	61,6	5,4	4,018	9,91	39,83
s	389,46	239	32,8	2,7	5,59	0,3	5,58	0,4	0,6285	0,06633	6,33
ν	15,42	10,08	71,50	81,42	8,78	6,17	9,06	7,88	15,64	0,67	15,90

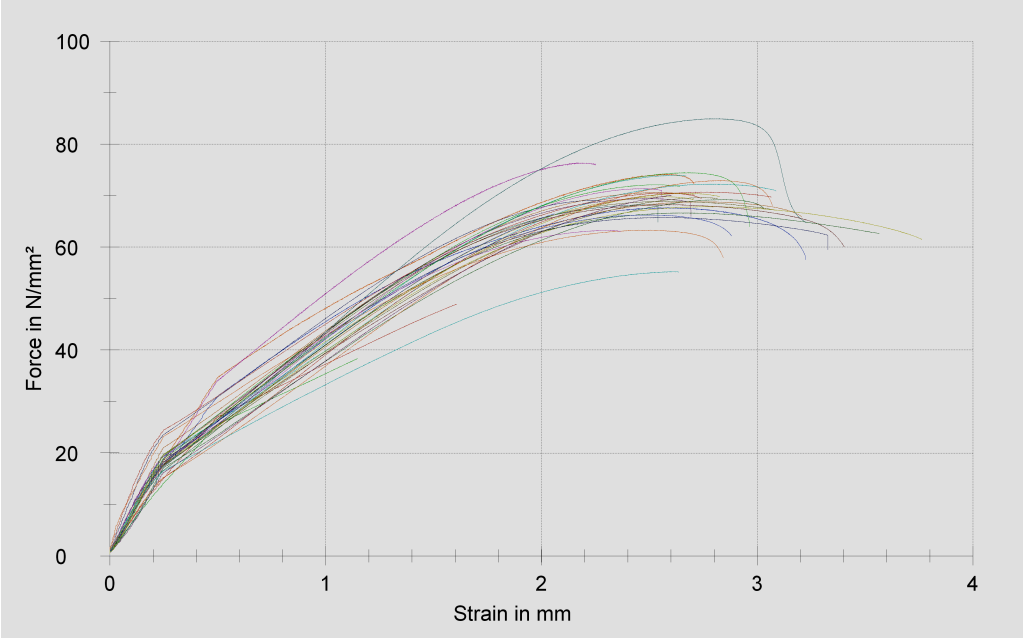

Figure 12-7. Curve graph of DOW resin coupons.

12.4. Analyse of DSC

Analyse of UD laminates on DSC:

Tg of 100:28 mixing ratio. Post cure:

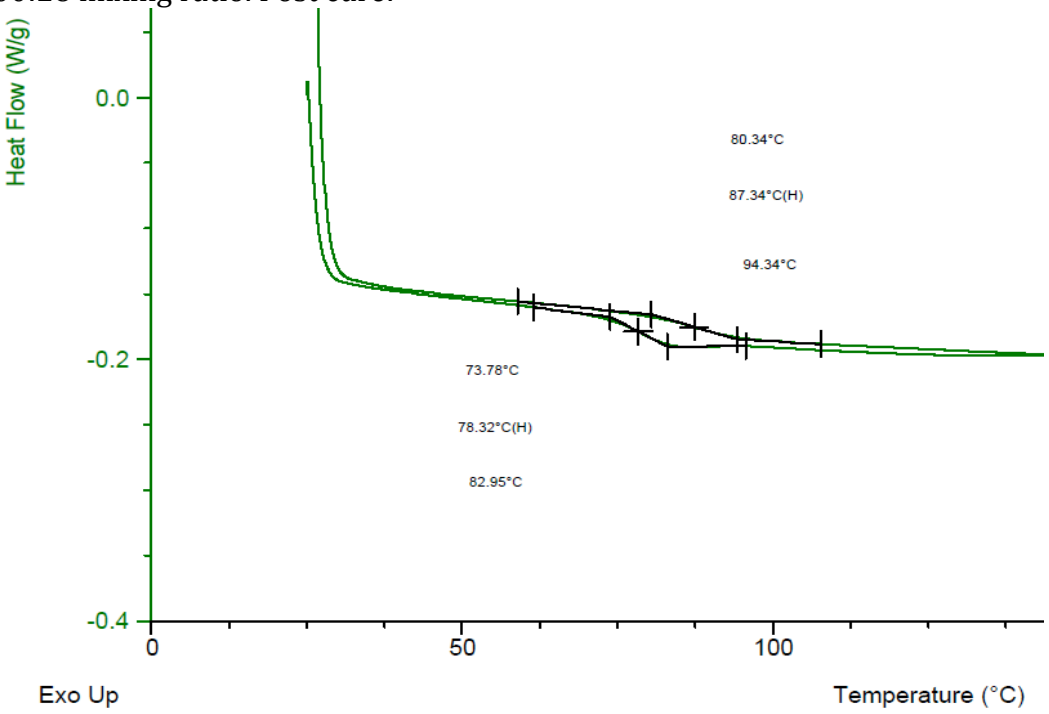

Figure 12-8. Tg of mixing ratio 100:28. UD Laminate. Post cure.

Tg of 100:29 mixing ratio. Post cure:

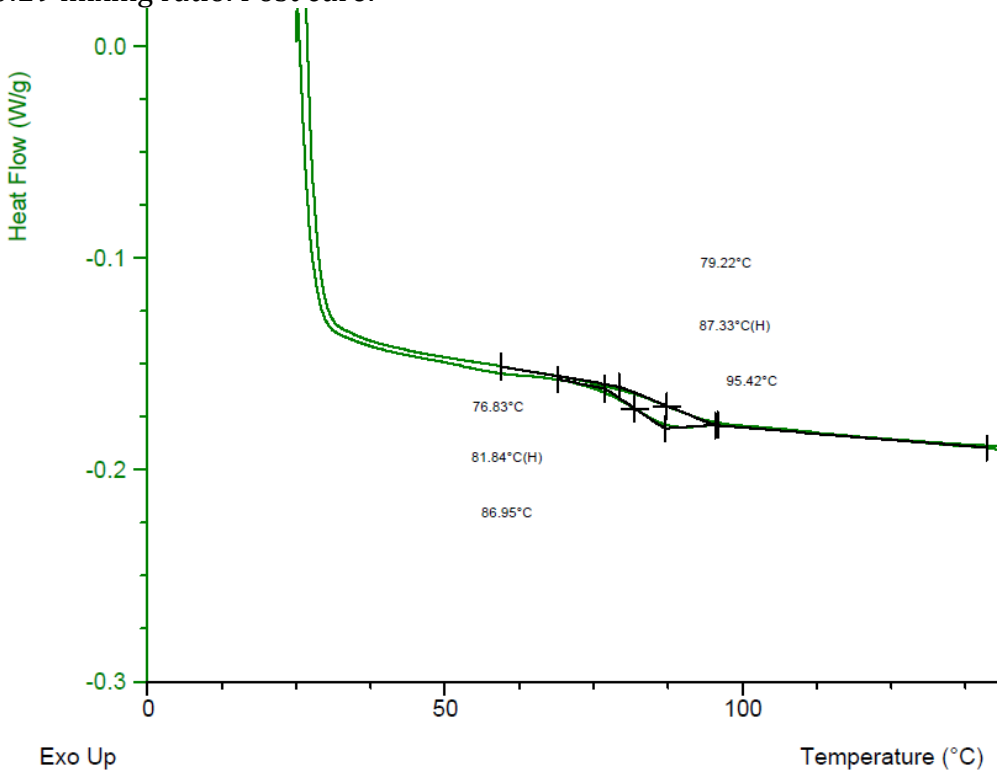

Figure 12-9. Tg of mixing ratio 100:29. UD Laminate. Post cure.

Tg of 100:30 mixing ratio. Post cure:

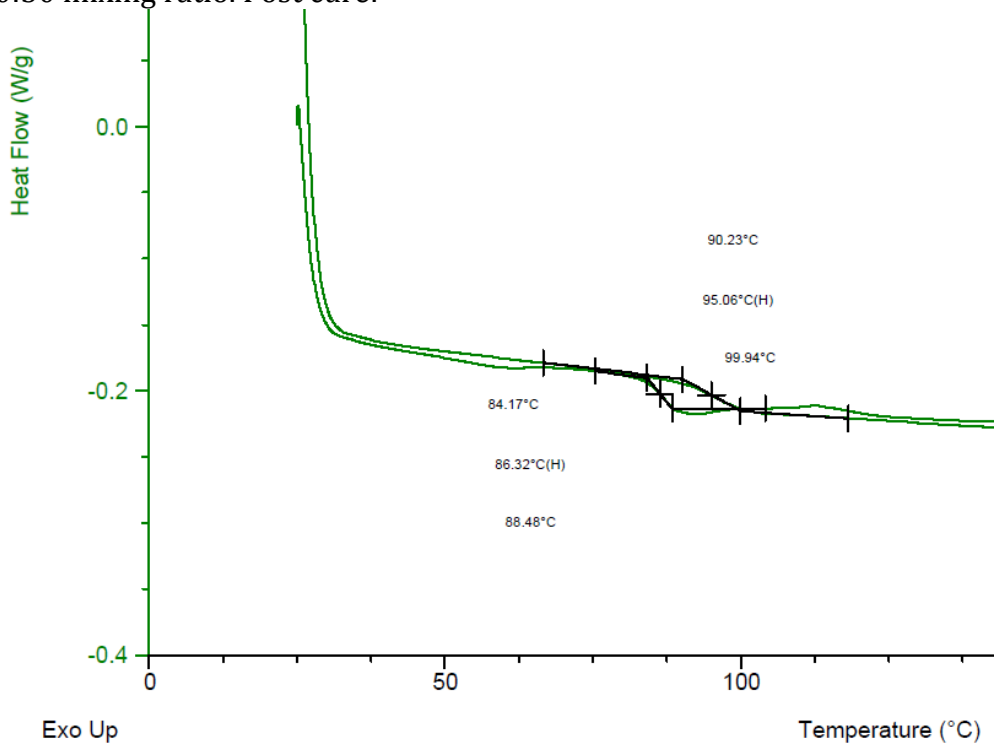

Figure 12-10. Tg of mixing ratio 100:30. UD Laminate. Post cure.

Tg of 100:31 mixing ratio. Post cure:

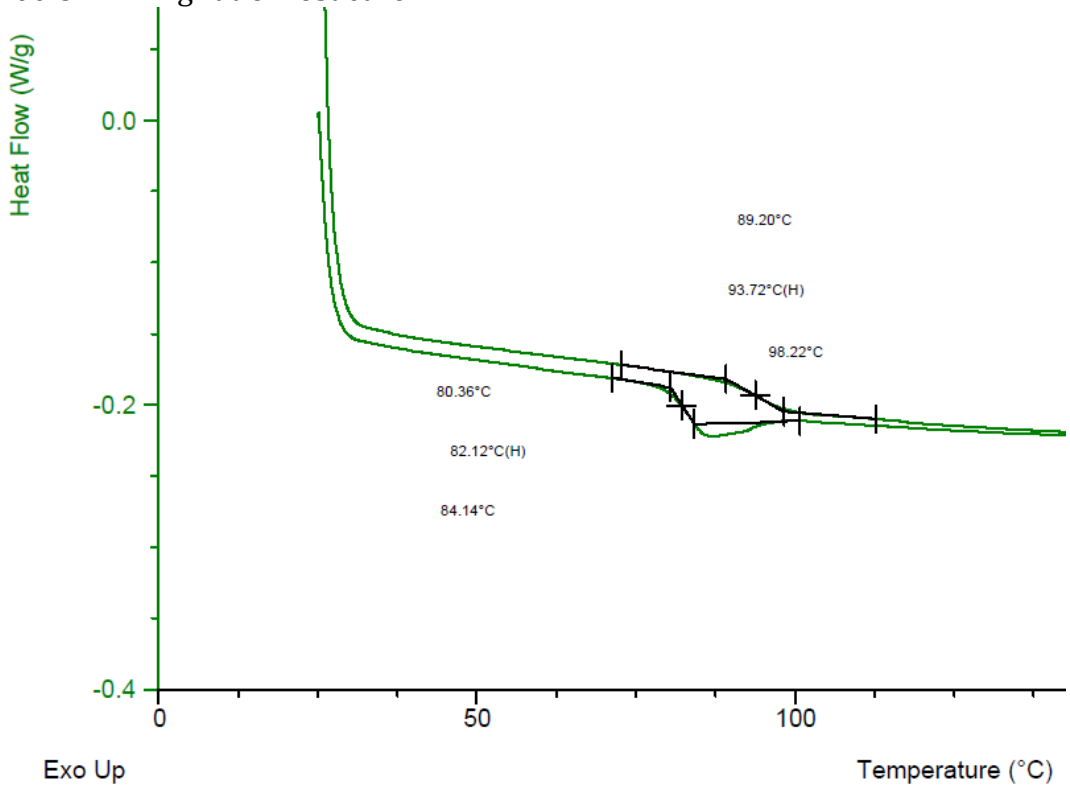

Figure 12-11. Tg of mixing ratio 100:31. UD Laminate. Post cure.

Tg of 100:32 mixing ratio. Post cure:

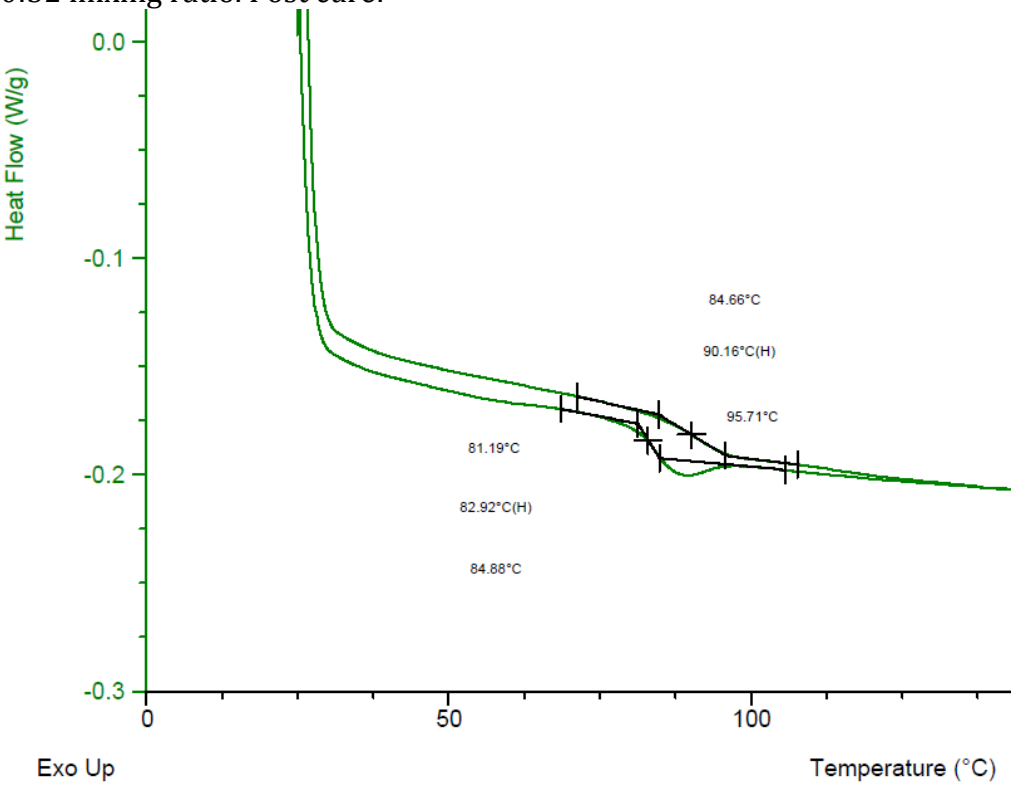

Figure 12-12. Tg of mixing ratio 100:32. UD Laminate. Post cure.

Tg of 100:33 mixing ratio. Post cure:

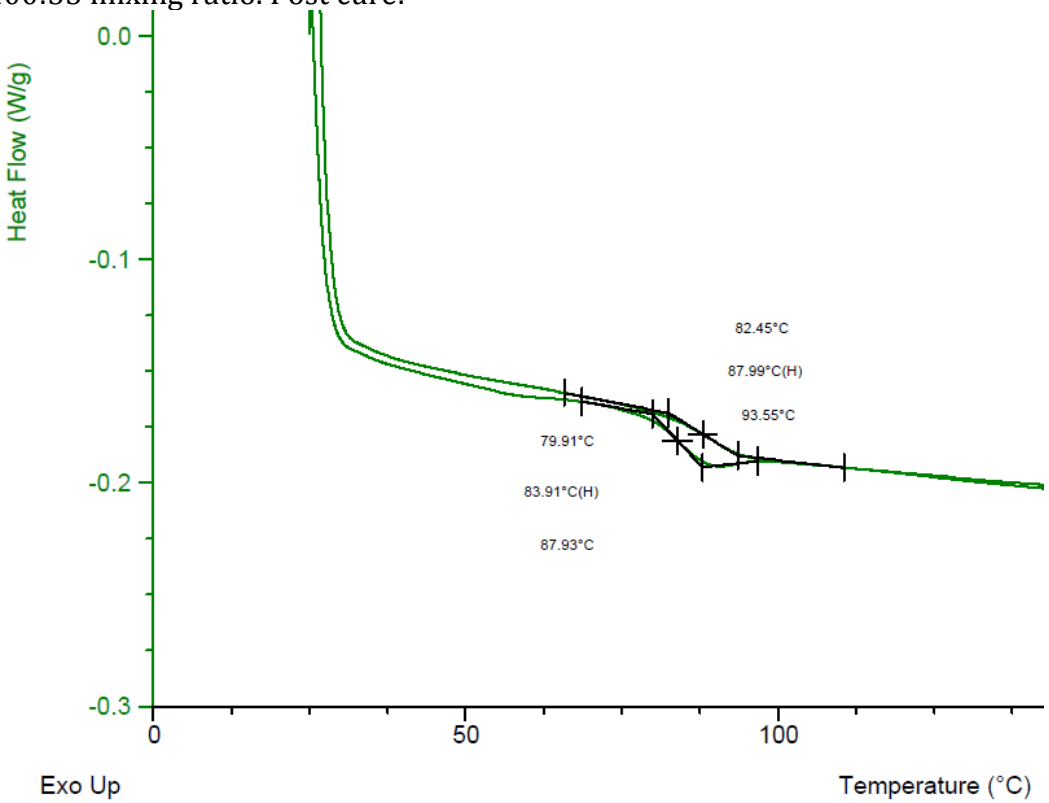

Figure 12-13. Tg of mixing ratio 100:33. UD Laminate. Post cure.

Tg of 100:34 mixing ratio. Post cure:

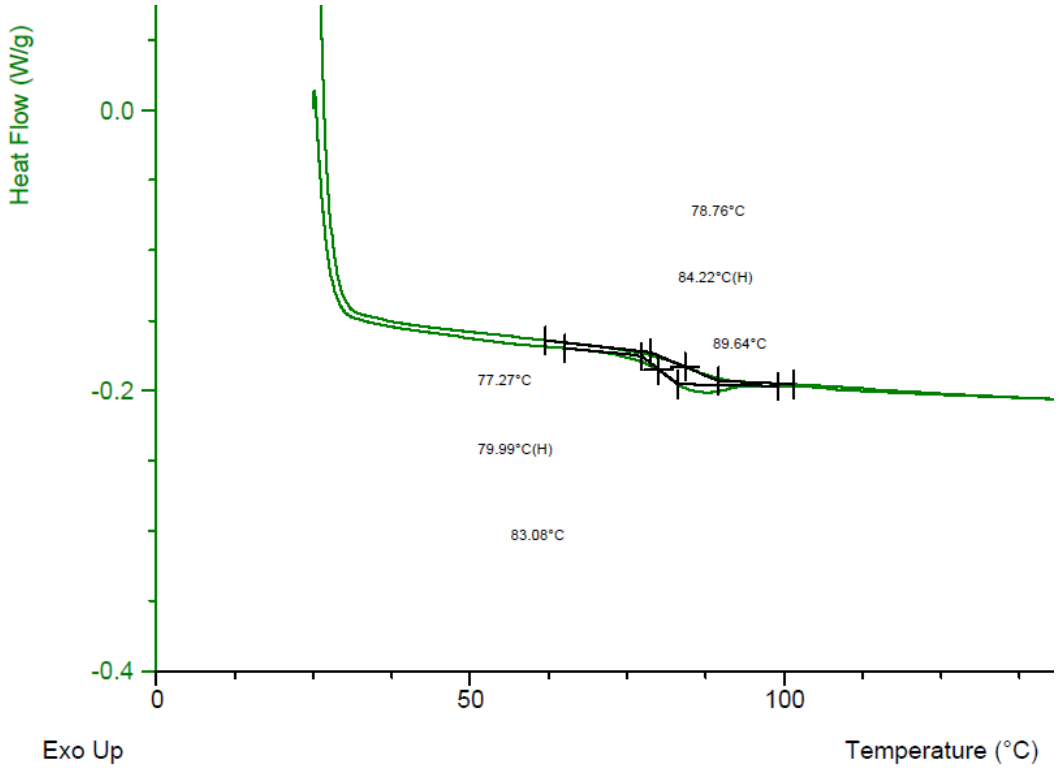

Figure 12-14. Tg of mixing ratio 100:34. UD Laminate. Post cure.

Analyse of Biax laminates on DSC:

Tg of 100:28 mixing ratio. Post cure:

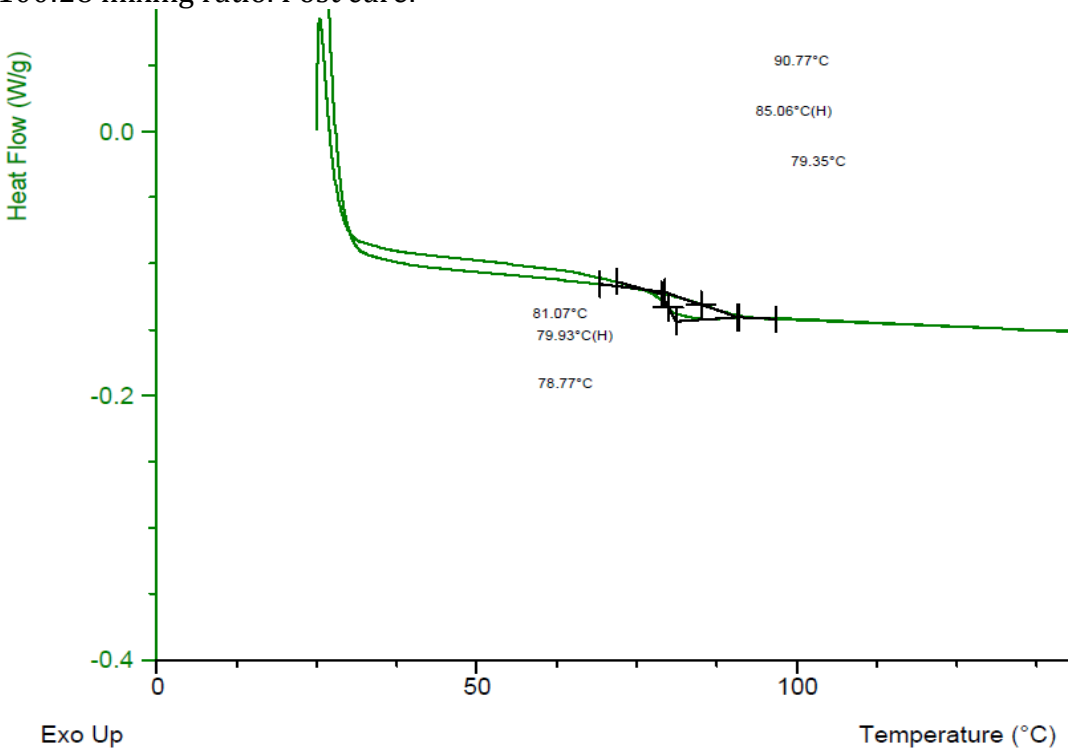

Figure 12-15. Tg of mixing ratio 100:28. Biax Laminate. Post cure.

Tg of 100:29 mixing ratio. Post cure:

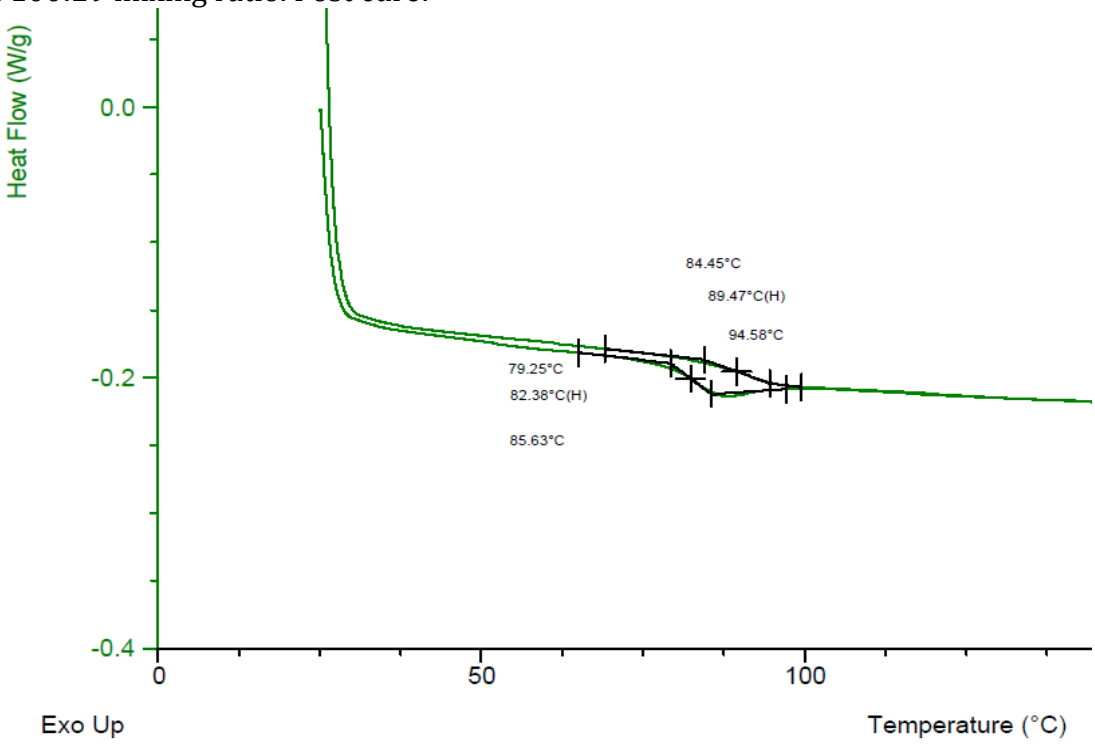

Figure 12-16. Tg of mixing ratio 100:29. Biax Laminate. Post cure.

Tg of 100:30 mixing ratio. Post cure:

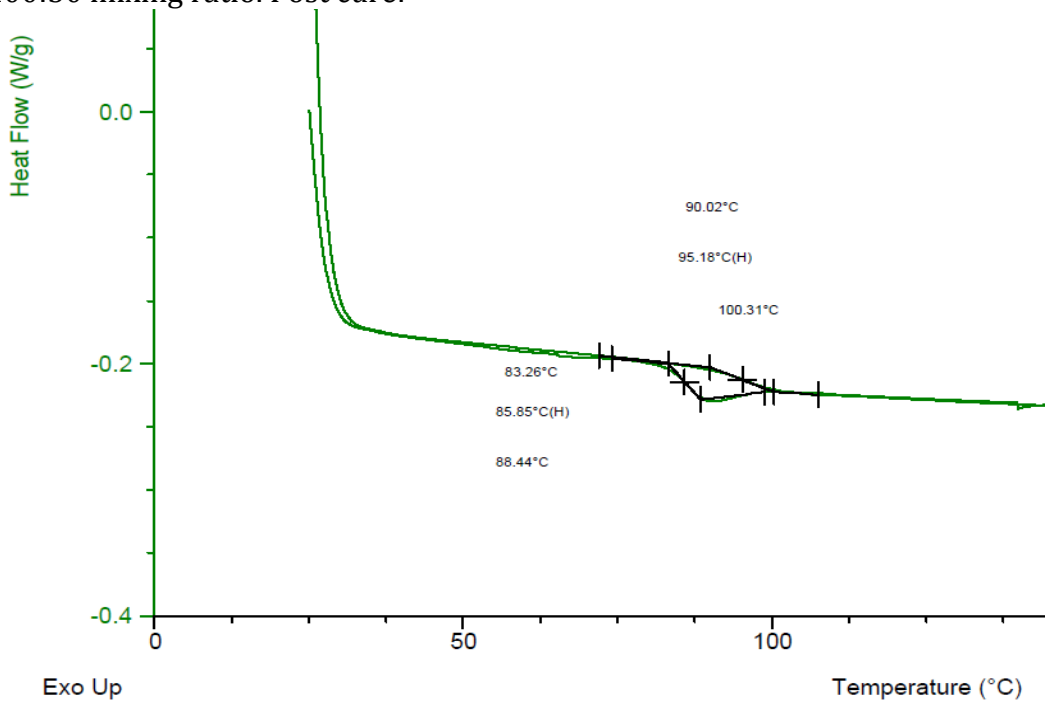

Figure 12-17. Tg of mixing ratio 100:30. Biax Laminate. Post cure.

Tg of 100:31 mixing ratio. Post cure:

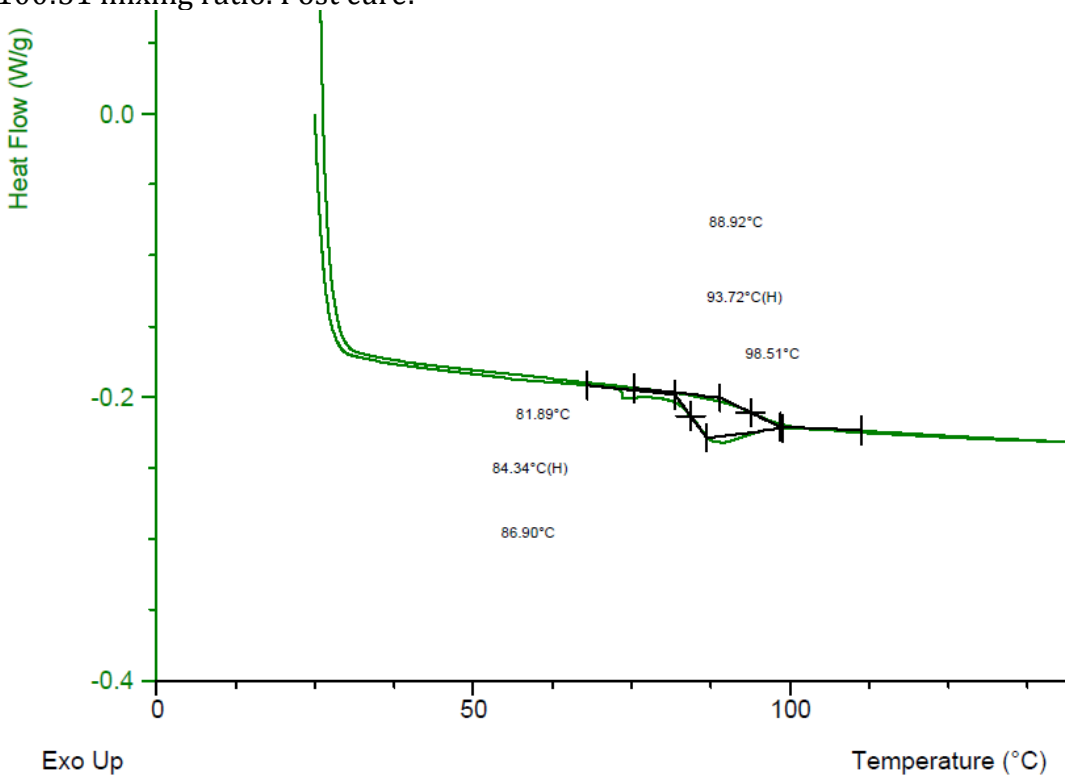

Figure 12-18. Tg of mixing ratio 100:31. Biax Laminate. Post cure.

Tg of 100:32 mixing ratio. Post cure:

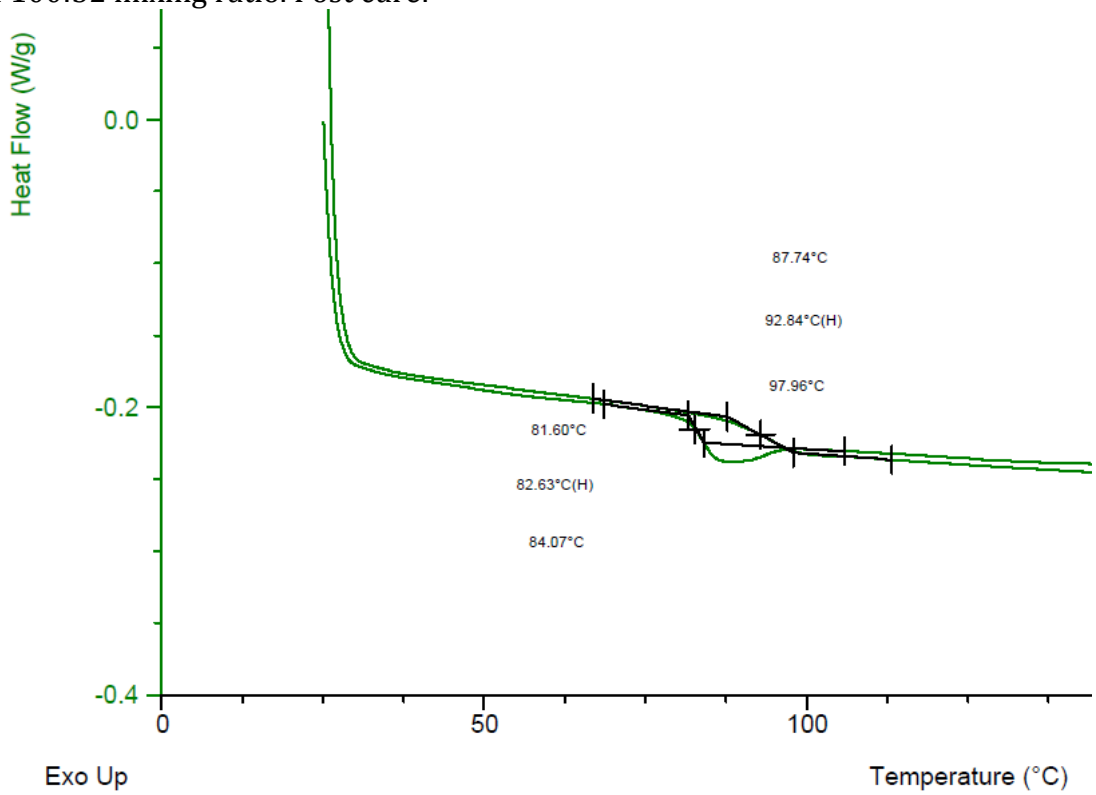

Figure 12-19. Tg of mixing ratio 100:32. Biax Laminate. Post cure.

Tg of 100:33 mixing ratio. Post cure:

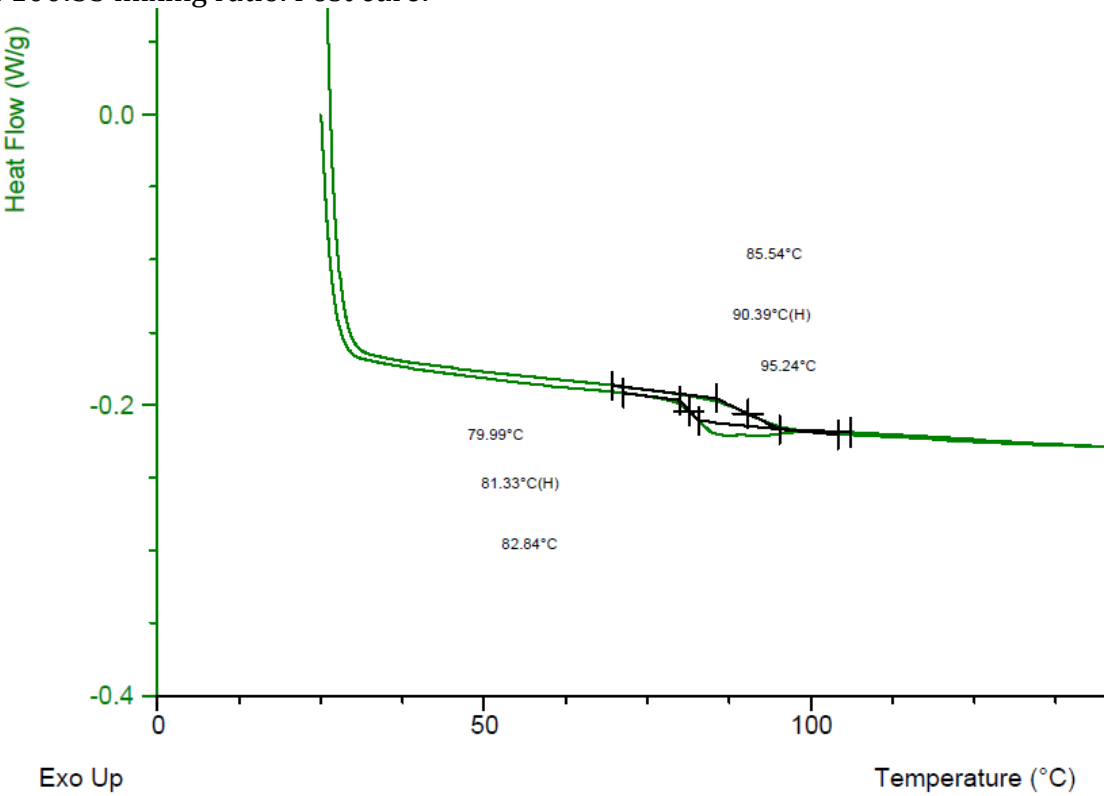

Figure 12-20. Tg of mixing ratio 100:33. Biax Laminate. Post cure.

Tg of 100:34 mixing ratio. Post cure:

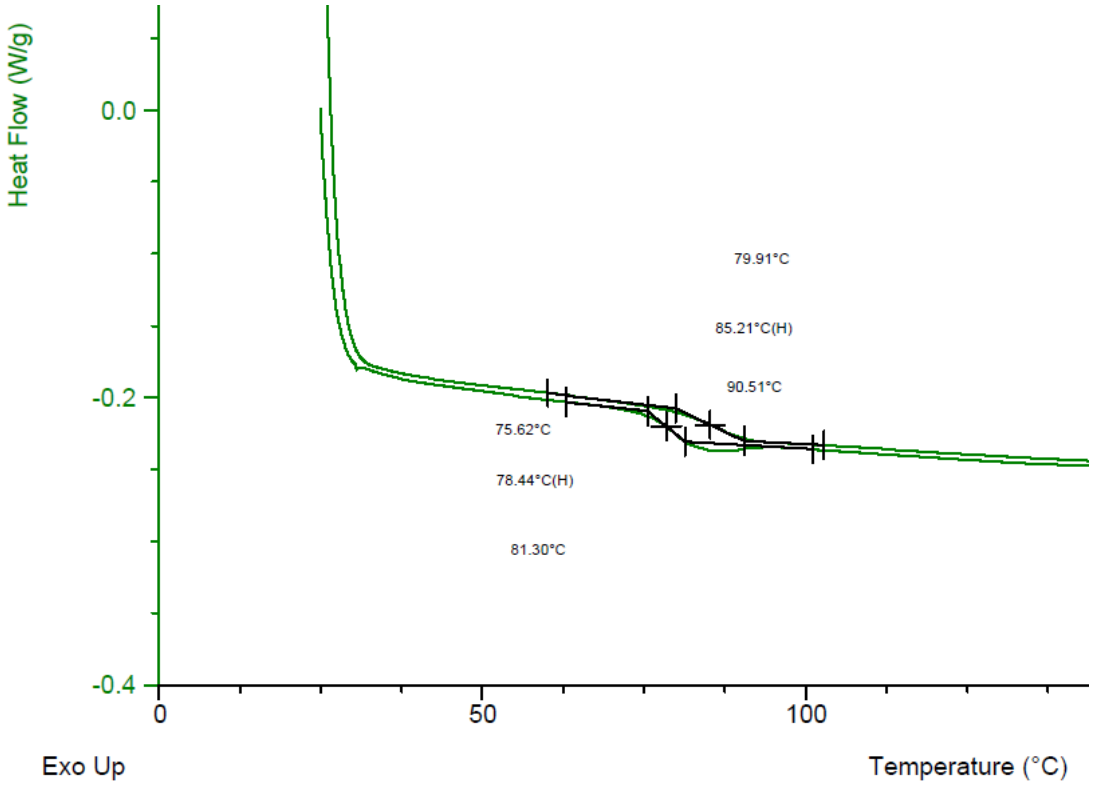

Figure 12-21. Tg of mixing ratio 100:34. Biax Laminate. Post cure.

13. ATTACHMENTS.

Data specifications of the material used on this investigation from different suppliers.

From KUSH company:

Physical properties

Comparison of *Advantex* glass fibers to E-glass

Property	Test method	Unit	*Advantex* glass	E-glass
Density	ASTM D1505[1]	g/cc	2.62	2.52 - 2.62

From DOW chemical company:

Property[1]	AIRSTONE 780E Epoxy Resin	AIRSTONE 785H Hardener
Viscosity @ 25°C (mPa•s) ASTM D-445	1400	16
Density @ 25°C (g/cc) ASTM D-4052	1.15	0.95

Ideal Mixing Ratio (PHR): 100 parts of Resin per 31 parts of Hardener.